

# Land-ice studies and glacial geology

## Variations of the west antarctic ice streams associated with sea-level and climatic changes during the Late Pleistocene

MIKHAIL VERBITSKY and BARRY SALTZMAN, *Department of Geology and Geophysics, Yale University, New Haven, Connecticut 06520*

Until now, the most comprehensive modeling studies of the antarctic ice sheet considered large-scale and mesoscale behavior as separate problems because the thermal features of coastal ice streams cannot be resolved in a large-scale model. It is not unlikely that the artificial horizontal diffusion inherent in numerical solutions of the three-dimensional (3-D) equations forces modelers to sacrifice mesoscale effects in favor of numerical stability. Nevertheless, our ultimate objective is to simulate the ice sheets with a 3-D model from which we can *produce* ice streams internally without prescribing them. With this goal, we have formulated an ice-sheet model using a simple formula for the basal temperature that is free from an artificial horizontal diffusivity. We have demonstrated that by applying our model to the late Pleistocene, ice streams switch to active or stagnant modes as a part of a single solution responding to external forcing.

The dynamics of the model are governed by an equation representing a mass balance of the nonlinear ice flow (Verbitsky and Saltzman 1995), and the above-mentioned simple formula (Verbitsky and Saltzman in press) has been used for the basal temperature. Solving the model equations on a high-resolution [40×40 kilometer (km)] grid for values of the climatic temperature, bedrock topography, and snowfall rate adopted from Huybrechts (1992), we find that the ice-sheet model reproduces reasonably well the ice topography and velocity distribution of the present-day antarctic ice sheet. The basal temperature also compares well with the shape and extent of the areas of melting and freezing temperature obtained by Huybrechts (1992) as a solution of the full 3-D thermodynamical equation (figure 1). This suggests that our simplified

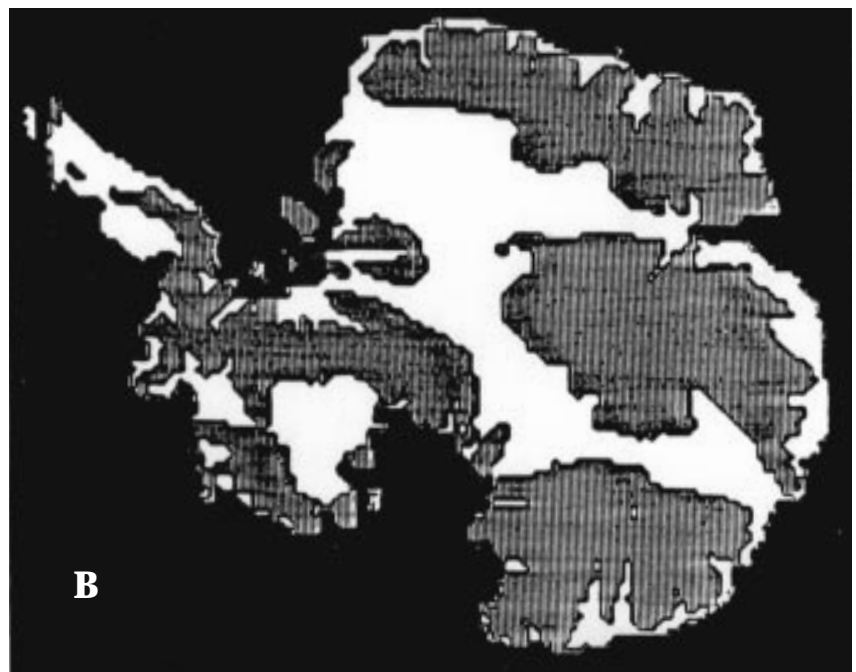


Figure 1. "Present-day," equilibrium, regime of the antarctic ice sheet: (A) the calculated basal temperature; (B) the same from Huybrechts (1992). White areas are at the pressure-melting point.

formula can represent the relevant thermodynamics. Our approach allowed us to simulate the fine temperature structure in coastal zones. For example, at the west antarctic Siple Coast, areas at the pressure-melting-point are separated by strips of frozen-to-bed ice, suggestive of ice streams A-E. Thus,

- ice streams A and B unite to form a single flow downstream,
- a structure similar to A and B is formed by streams D and E, and
- a narrow ice stream C occupies the central part of the coast.

Not only are the *shapes* of these structures similar to the ice streams found on the Siple Coast, but their behavior is also similar in the sense that their horizontal flow is dominated by the basal sliding and is much faster than the flow of the neighboring ice.

We next forced our model with the late Pleistocene temperature and the sea-level changes, invoking the Vostok tem-

perature and the SPECMAP isotopic oxygen-18 ( $\delta^{18}\text{O}$ ) records, respectively. The snow accumulation rate is taken as the sum of its present-day value and forced departures, assumed to be proportional to the temperature variations at the southern ocean core MD88-770 (supposing that these variations might be a good proxy for the moisture availability over the Antarctic).

The streamlike structure of the Siple Coast found in the steady-state solution appears to be robust, being observed during the whole glacial cycle under the wide range of external forcing conditions (figure 2). Interestingly, ice stream C switches to a slow mode during the penultimate interglacial 128,000 years ago when snowfall rates were high. We found that ice stream C is more vulnerable to increased snowfall rates because in the model it has the coldest “background” temperature (that is, values of temperature advected from the top of the ice sheet) and a low value of internal friction, both of which give ice stream C the weakest possibility to counteract the

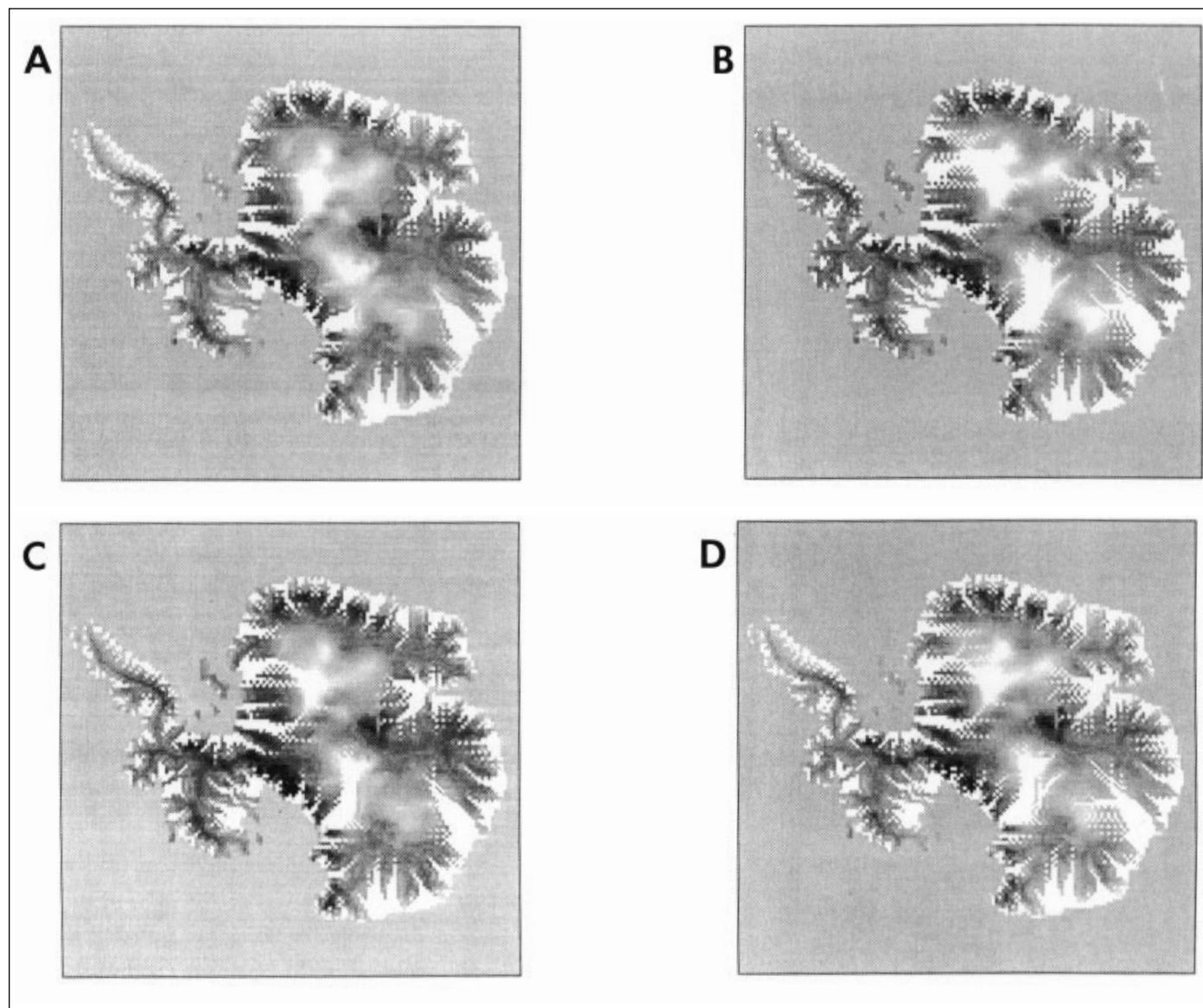


Figure 2. Calculated basal temperature at 128,000 (A), 50,000 (B), 10,000 (C), and 0 (D) years ago. White areas are at the pressure-melting point.

advective cooling. The differences between ice streams disappear when the real bedrock topography, and the shape of the coastline of the Siple Coast, are replaced by a flat plane and a straightline coast, respectively. We may conjecture, therefore, that peculiarities of local topography may create a situation in which an ice stream develops at a local divide and consequently has a lower surface temperature and reduced shear stresses and internal friction. It is possible that this situation is characteristic of ice stream C, a conclusion we regard as tentative because only the simplest form of a sliding law was used, and also, a higher resolution may be necessary to make definitive conclusions. We also excluded from consideration the transition zone between an ice sheet and ice shelf. Consequently, our study is not intended to challenge existing hypotheses concerning ice stream C stagnation, but we do suggest that some

distinctive features of the ice-stream structure found at the Siple Coast may have roots in its large-scale topography.

This work has been supported by National Science Foundation grant OPP 93-19674 and by National Aeronautics and Space Administration grant NAGW-4197.

## References

- Huybrechts, P. 1992. *The antarctic ice sheet and environmental change: A three-dimensional study* (Reports on Polar Research, Vol. 99). Bremerhaven: Alfred-Wegener-Institute.
- Verbitsky, M.Y., and B. Saltzman. 1995. Behavior of the east antarctic ice sheet as deduced from a coupled GCM/ice-sheet model. *Geophysical Research Letters*, 22, 2913-2916.
- Verbitsky, M.Y., and B. Saltzman. In press. Modeling the antarctic ice sheet. *Annals of Glaciology*.

# Ice-core glaciochemical reconnaissance in inland West Antarctica

KARL J. KREUTZ, PAUL A. MAYEWSKI, MARK S. TWICKLER, and SALLIE I. WHITLOW, *Climate Change Research Center, Institute for the Study of Earth, Oceans, and Space and Department of Earth Sciences, University of New Hampshire, Durham, New Hampshire 03824*

To date, the highest resolution ice cores have come from Greenland [the U.S. Greenland Ice Sheet Project 2 (GISP2) and European Greenland Ice Core Project (GRIP)]. The ability to determine annual layering in these cores over at least the past 50,000 years has allowed the reconstruction of a detailed environmental history covering major glacial and interglacial climatic events (e.g., Mayewski et al. 1994; O'Brien et al. 1995). Although these cores have significantly advanced our understanding of paleoclimatic change in the Northern Hemisphere, questions remain as to whether the two hemispheres have responded synchronously to climate forcing through time. Determining the existence, similarity, and phasing of climatic change in the Southern Hemisphere is crucial to understanding the importance of various climate-forcing factors.

Two sites in West Antarctica (Siple Dome and inland West Antarctica) have been identified by the U.S. ice-core community as potential deep-drilling locations where records similar in quality to the Greenland cores may be recovered. Siple Dome (Mayewski, Twickler, and Whitlow 1995) is an ideal location for deep ice-core drilling, because of the homogeneous spatial variability of surface snow chemistry and well-preserved annual signals in chemical species and physical properties. In this article, we describe the initial results of work done at the second location in inland West Antarctica.

The 1995 field season involved drilling three ice cores and collecting snowpit samples along a 158-kilometer (km) traverse trending 26° (relative to true north) from Byrd Surface Camp (figure 1). Visual stratigraphy revealed numerous depth

hoar and wind crust layers throughout the cores, but identifying distinct and consistent annual layering proved to be difficult. As a test, annual layer counting estimates were compared to the accumulation rate calculated from a beta profile. The prominent peak in radioactivity at 14.5 meters (m), corresponding to the height of bomb testing in 1964, suggests an

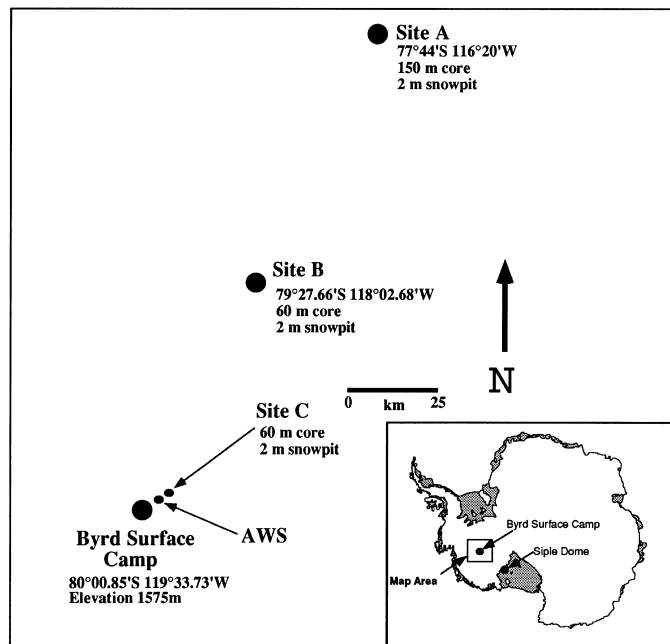


Figure 1. Location map. (AWS denotes automatic weather station.)

accumulation rate of 28.8 centimeters (cm) of ice per year at site A (Dibb personal communication; figure 2). An accumulation rate estimate based on annual layer counting is significantly lower (20 cm of ice per year), suggesting that more than one depth hoar layer forms during a year.

Glaciochemical concentrations of major anions, cations, and methanesulfonic acid (MSA) have been performed on snowpit samples. The most distinct annual signals are present in sulfate ( $\text{SO}_4^{=}$ ) and MSA profiles (figure 3). There appears to be more than one depth hoar layer corresponding to each summer peak in  $\text{SO}_4^{=}$  and MSA. Average values for all seasalt species are significantly lower than those found at more coastal sites and Siple Dome, suggesting that marine influence is greatly reduced on the west antarctic polar plateau (Mulvaney and

Wolff 1994). Species with gaseous precursors [nitrate ( $\text{NO}_3^-$ ),  $\text{SO}_4^{=}$ , and ammonium ( $\text{NH}_4^+$ )] have concentrations consistent with those found in other antarctic locations, suggesting that elevation and distance from the coast have little influence on their concentration (Mulvaney and Wolff 1994).

Snowpit data from the three sites in this study display significant spatial variability (figure 3). One possible explanation for this difference would be the existence of an ice divide between sites A and B. Atmospheric circulation in the area may be significantly altered by the presence of such a divide, thereby causing the observed changes in chemical concentrations. The spatial variability displayed in the snowpit data suggests that the region has complex atmospheric circulation patterns and highlights the need for increased sampling in West Antarctica.

From the cores collected in this study, we plan to develop an approximately 1,000-year ice core record for inland West Antarctica. We are examining the 1,150-year Siple Dome record for information on several aspects of the climate system in West Antarctica, including marine cyclogenesis, marine biogenic productivity, stratospheric denitrification, and mass balance. New continuous, high-resolution multi-variate ice-core records from inland West Antarctica are expected to provide insight into these same climate parameters. Ice-core records from Siple Dome and inland West Antarctica will be correlated with other cores within the Ross Ice Drainage System, one of the most climatologically and glaciologically dynamic areas of Antarctica. These cores are expected to be of the same quality as the Summit, Greenland, cores, allowing additional bipolar climate correlations to be attempted (Mayewski et al. 1996).

We thank Jeff Thomas and David Giles of the Polar Ice Coring Office and Geoffrey Hargreaves of the National Ice Core Laboratory for their work in recovering the three cores, and we appreciate the help we received from Antarctic Support Associates and Navy Squadron VXE-6. This work is supported by National Science Foundation grant OPP 93-16564.

## References

- Dibb, J. 1996. Personal communication.
- Mayewski, P.A., L.D. Meeker, S.I. Whitlow, M.S. Twickler, M.C. Morrison, P. Bloomfield, G.C. Bond, R.B. Alley, A.J. Gow, P.M. Grootes, D.A. Meese, M. Ram, K.C. Taylor, and W. Wumkes. 1994. Changes in atmospheric circulation and ocean ice cover over the North Atlantic during the last 41,000 years. *Science*, 263, 1747-1751.
- Mayewski, P.A., M.S. Twickler, and S.I. Whitlow. 1995. The Siple Dome ice core—Reconnaissance glaciochemistry. *Antarctic Journal of the U.S.*, 30(5), 85-87.
- Mayewski, P.A., M.S. Twickler, S.I. Whitlow, L.D. Meeker, Q. Yang, J. Thomas, K. Kreutz, P.M. Grootes, D.L. Morse, E.J. Steig, E.D. Waddington, E.S. Saltzman, P.-Y. Whung, and K.C. Taylor. 1996. Climate change during the last deglaciation in Antarctica. *Science*, 272, 1636-1638.
- Mulvaney, R., and E.W. Wolff. 1994. Spatial variability of the major chemistry of the antarctic ice sheet. *Annals of Glaciology*, 20, 440-447.
- O'Brien, S.R., P.A. Mayewski, L.D. Meeker, D.A. Meese, M.S. Twickler, and S.I. Whitlow. 1995. Complexity of Holocene climate as reconstructed from a Greenland Ice Core. *Science*, 270, 1962-1964.

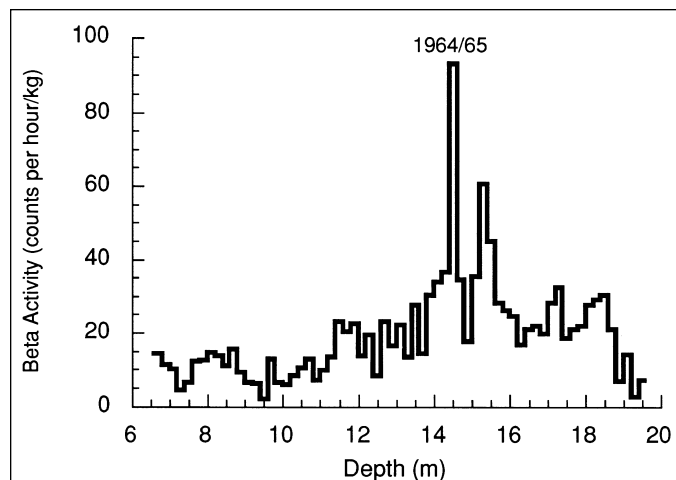


Figure 2. Radioactive bomb fallout peaks at site A. (kg denotes kilogram.)

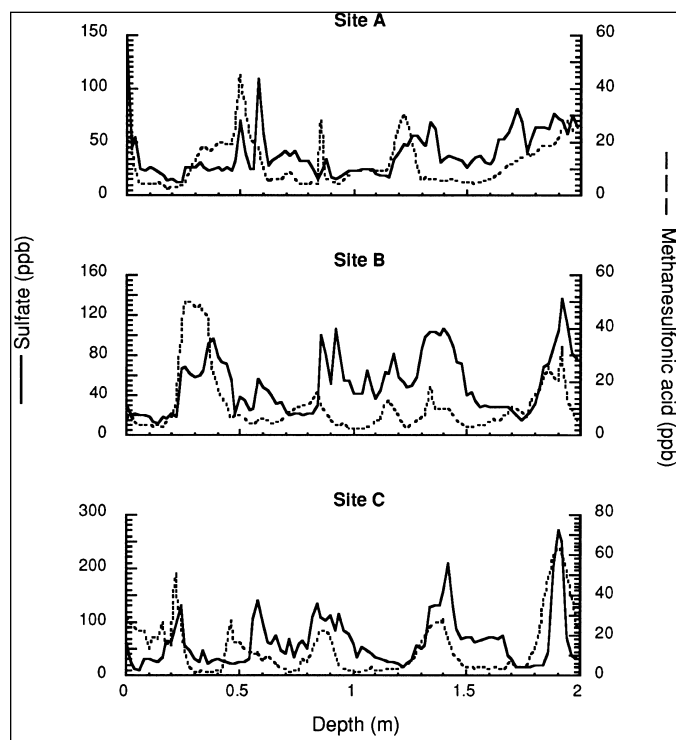


Figure 3. Sulfate and methanesulfonic acid concentrations in snowpits. (ppb denotes parts per billion.)

# Preliminary velocity field in the onset region of ice stream D, West Antarctica

ROBERT A. BINDSCHADLER, *Laboratory for Hydrospheric Processes, National Aeronautics and Space Administration, Goddard Space Flight Center, Greenbelt, Maryland 20771*

XIN CHEN and PATRICIA L. VORNBERGER, *General Sciences Corporation, Laurel, Maryland 20727-2929*

At the heads of the west antarctic ice streams, the ice experiences a transition from slow inland flow [typically a few meters per year (m/a)] where internal deformation is most important to speeds of over 100 m/a where basal sliding dominates. Although the reasons for this transition are not yet understood, being able to model this behavior from first principles is critical to modeling the temporal behavior of the west antarctic ice sheet.

The first step in researching this transition is to locate it. To that end, we established a large strain grid in the onset area of ice stream D during the 1995–1996 season (figure 1). The initial size and orientation of the grid was based on an interpretation of Landsat imagery. Refinements were made following the coregistration of this imagery with a grid of basal elevations based on radar-sounding flights conducted in the 1970s (Drewry 1983). These data show that ice stream D's course through this onset area is controlled by the bed topography (Bamber and Bindschadler in preparation).

The grid has a regular spacing of 5 kilometers (km) and stretches for 160 km from just upstream of Byrd Station near the north corner to just upstream of the first crevasses on the ice stream at the downstream end (figure 2). The width varies from 50 km to 30 km in accordance with the flow convergence in the area inferred from flowbands in the imagery. Previously determined velocities of 13 m/a at Byrd Station (Whillans 1979) and 130 m/a at the first crevasse just down-

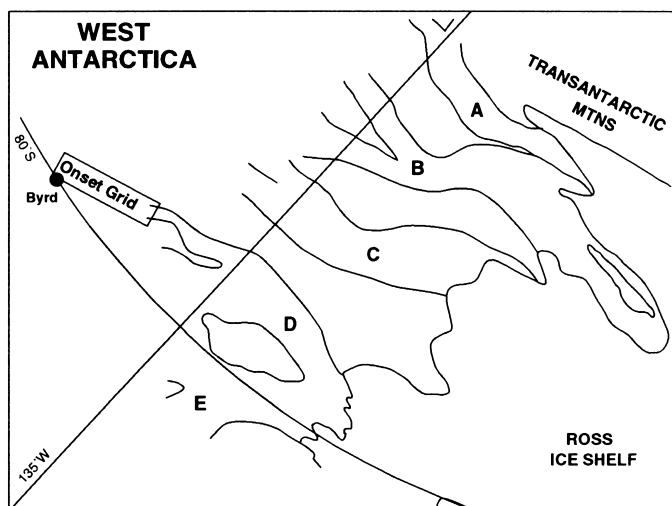


Figure 1. Map showing location of grid.

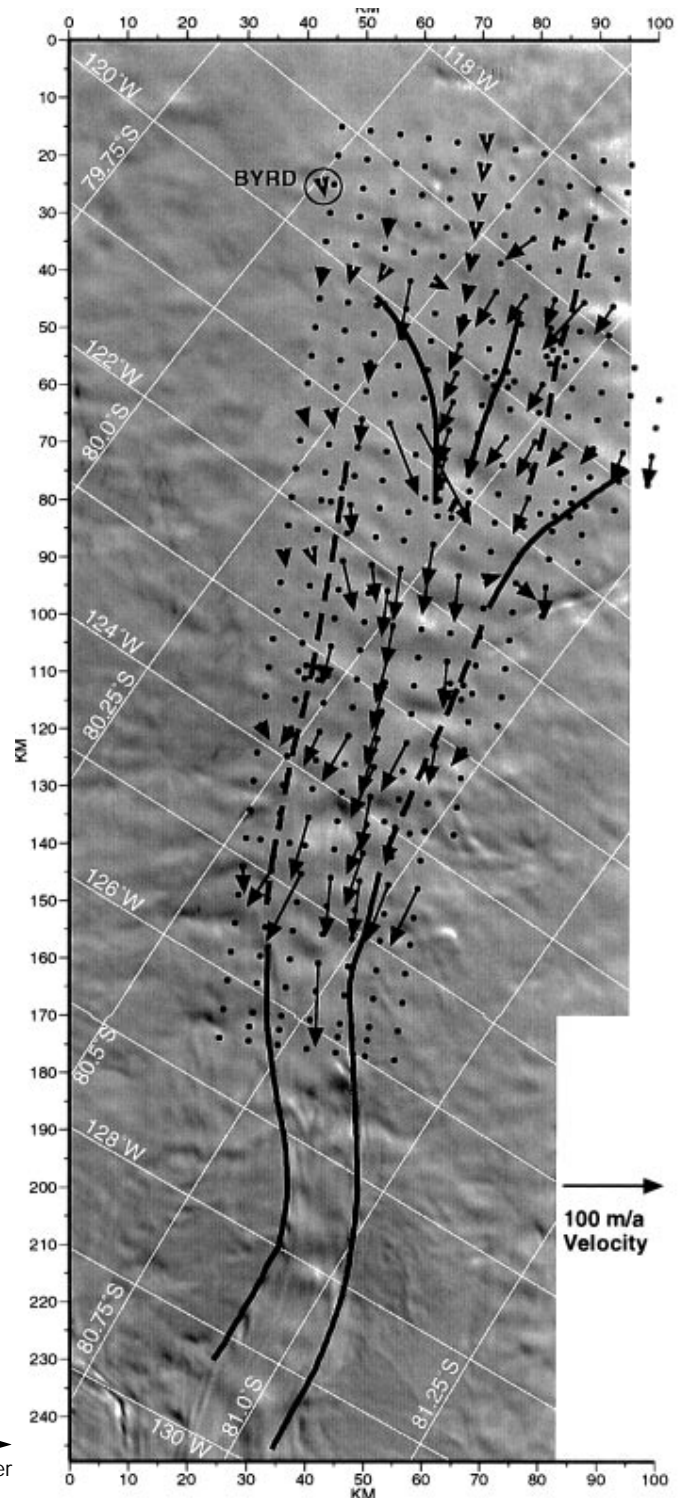


Figure 2. Gridpoint locations superimposed on Landsat thematic mapper imagery. Arrows indicate measured velocities. Velocity scale in lower right.

stream of the grid (Bindschadler and Vornberger, unpublished data) confirmed that the grid spanned the desired flow-transition area.

The initial survey consisted of setting a steel survey pole at each gridpoint and determining its position with Ashtech Z-12 global positioning system receivers. A base station, operated continuously for 1 month at Byrd Station by the Support Office for Aerogeophysical Research (SOAR), was intended to provide a tie to the global reference frame. Meanwhile, 11 sequential local surveys were conducted within the grid. Each local survey was performed in rapid-static mode; a local base station ran continuously for approximately 48 hours while roving receivers were transported via snowmobile to each gridpoint within a roughly  $25 \text{ km} \times 25 \text{ km}$  area. Occupation time at each gridpoint varied from 20 to 60 minutes depending on the baseline length. Data were checked at the end of each day to ensure baseline precisions of a few centimeters. Approximately 20 percent of the stations had to be resurveyed because of poor data quality.

The regional strain rate, based on the two velocities mentioned above is roughly  $10^{-3}$  per year. The desired noise level of 1 percent requires us to wait 1 year before the resurvey; however, we have discovered that the absolute position determinations, using fiducial orbits prepared at the Jet Propulsion Laboratory, permit the extraction of meaningful velocity data over our nominal survey period of 48 hours. The sites where this is possible are Byrd Station, the 11 local base stations, and the gridpoints around the perimeter of each survey block.

Data from each base station were descretized to 6-hour segments and independent absolute positions were determined using GIPSY software. Figure 3 shows that these positions give an accurate determination of velocity. Velocities for the perimeter gridpoints were determined by differential positions calculated from two independent base stations. Figure 2 shows the results of this preliminary velocity field. It clearly illustrates the convergence and acceleration of the ice as the ice stream develops.

The longer data set for Byrd Station allows us to make a particularly precise velocity measurement there. Our result of  $11.6 \pm 0.1 \text{ m/a}$  at an azimuth of  $220.8$  degrees true differs somewhat from the velocity ( $13 \text{ m/a}$  at  $209$  degrees true) measured by optical survey from 1963 to 1967 (data from

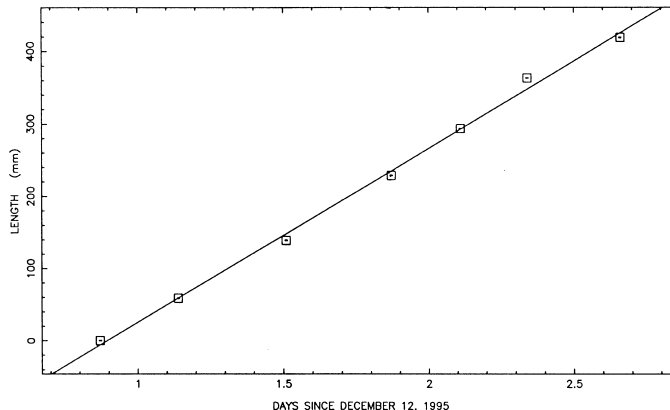


Figure 3. Motion of local base station C145 measured during approximately 2.5 days. Positions correspond to independent observation periods of approximately 6 hours each. Linear fit to positions yields velocity of  $88.0 \pm 2.1 \text{ m/a}$ . (mm denotes millimeter.)

Whillans, personal communication). This older survey lacked any fixed reference, relying instead on an assumed 0 horizontal velocity at the ice divide. We feel our velocity is more accurate and are not certain of the significance of the difference in azimuth of motion. To identify any possible changes in the strain field over this 30-year period, as might be associated with a change in the dynamics at the head of ice stream D, we have reestablished and intend to resurvey the lower 20 km of the Byrd Station Strain Network. A comparison of strain rates will be more meaningful because it is not dependent on the availability of a fixed reference.

This research was supported by National Science Foundation grant OPP 93-17627.

## References

- Bamber, J.L., and R.A. Bindschadler. In preparation. An improved elevation data set for climate and paleo-climatic modelling: Validation with satellite imagery. *Annals of Glaciology*.
- Drewry, D. 1983. *Antarctica: Glaciological and geophysical folio*. Cambridge, England: Scott Polar Research Institute, University of Cambridge.
- Whillans, I.M. 1979. Ice flow along the Byrd Station Strain Network, Antarctica. *Journal of Glaciology*, 24(90), 15–28.
- Whillans, I.M. 1995. Personal communication.

# Internal stratigraphy from ground-based radar studies at Siple Dome summit

ROBERT W. JACOBEL, ANDREW J. FISHER, and NANCY M. SUNDELL, *Department of Physics, St. Olaf College, Northfield, Minnesota 55057*

Today, the summit region of Siple Dome is a source area of slow-moving ice that contributes little to the mass flux into the Ross Ice Shelf. In the past, however, portions of the dome appear to have been overridden by inland ice draining the west antarctic ice sheet. Evidence in support of a relict ice stream traversing the flank of Siple Dome has resulted from a collaborative study of Siple Dome by St. Olaf College, the University of Washington, and the University of Colorado (Raymond et al. 1995; Jacobel et al. 1996).

In addition to our work on the relict ice stream, we carried out field studies in a region centered on the Siple Dome summit to characterize the ice dynamics and history of the area where a high-resolution climate core will be drilled. During the 1994–1995 field season, over 100 kilometers (km) of ground-based radar traverses were made in a 10-km-square grid centered on the topographic summit. Surface elevations were obtained for 45 points in the summit grid using stop-and-go kinematic global positioning system (GPS) and optical surveying. These data were augmented with continuous elevation measurements along the radar profiles obtained with a pressure transducer.

Ice thickness has been calculated from two-way travel times of the radar echoes, and together with the surface survey data, has been used to make a map of the bed topography (Fisher et al. 1995). Figure 1 shows that the bed beneath the summit region is generally smooth and slightly concave upward beneath approximately 1 km of overlying ice. Elevations in figure 1 are given with respect to the WGS-84 ellipsoid, and thus the bed is some 300 meters below mean sea level. The surface at the summit is largely two-dimensional, more of a ridge than a dome, with the ridge axis running approximately east-west. The greatest ice thickness is slightly south of this ridge, which has shallow surface slopes of 0.003 to 0.004.

Clear internal echoes down to approximately 60 percent of the ice thickness have also been measured from the radar profiles. Because they represent isochrones, they have the potential to reveal important information about ice history and dynamics. Figure 2 shows the topography of the ice surface and two of the more prominent internal layers at elevations of approximately 240 and 340 meters above the WGS-84 ellipsoid. The overall smooth variation in the internal layers shows that Siple Dome has been an area of generally stable accumulation throughout their history of deposition, about 10,000 years (Nereson et al. in press).

In addition to their general shape and smoothness, the internal layers also have two other common features:

- Although the current surface exhibits only slight asymmetry, dipping more steeply to the south, both internal layers dip substantially more toward the north.
- Both also show a slight “pinching” effect where the layers warp upward at the summit.

The latter may be understood as a consequence of iceflow at a stable, or nearly stable, ice divide (Raymond 1983). Mass deposited directly on the divide has no component of strain to either side, thus increasing the effective viscosity and creating the slight upwarp.

To quantify the slope information for the surface and internal layers, we have made least-squares fits with a first-order polynomial to the radar surface and internal echo-depth data. Fits were obtained for the surface and the two internal layers of each half of the five north-south profiles, 30 fits in all. Slopes from these fits were then averaged along the east-west dimension for the five profiles, and the results, together with standard deviations, are shown in the table. The

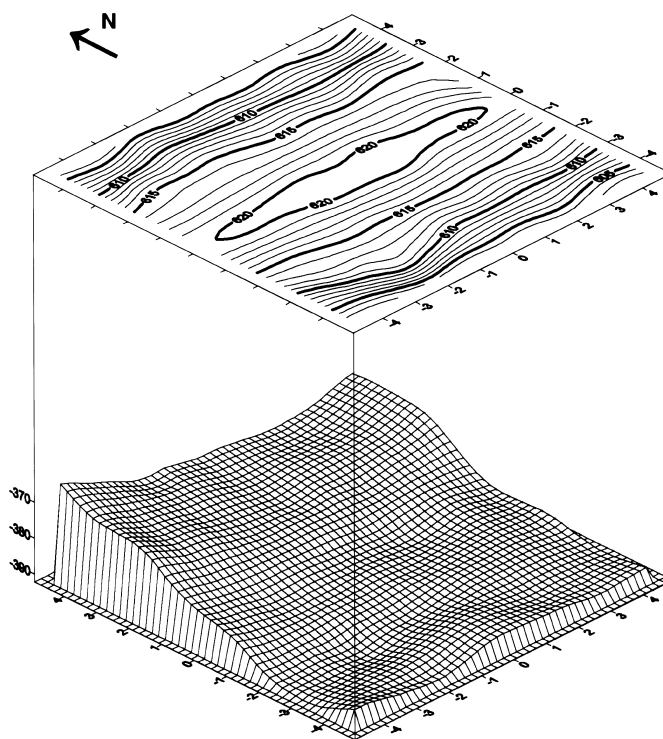


Figure 1. Siple Dome surface and bed topography obtained from over 100 km of surface-based radar traverses in a 10-km-square grid centered over the summit. Elevations are in meters with respect to the WGS-84 ellipsoid.

**Siple dome summit grid slopes. (Units are rise/run times  $10^{-5}$ .)**

Depth	South slope	North slope
Surface	399±06	348±16
Layer 1	378±45	1,281±43
Layer 2	316±19	1,053±27

table shows that both internal layers have slope patterns that differ substantially from the modern surface, quantifying what is depicted in figure 2. Also, although both internal layers have similar slopes, significant differences are evident.

Our analysis of the surface slopes and internal layers appears to rule out large changes in flow dynamics during the past 10,000 years, but some time-dependent behavior seems to be required to explain the pattern. Modeling work at the University of Washington is currently underway to test various mechanisms, such as ridge-migration and spatial accumulation rate gradients, which might account for the observations (Nereson and Raymond 1995; Nereson and Raymond, *Antarctic Journal*, in this issue).

We would like to acknowledge the efforts of our collaborators in the fieldwork: H. Conway, T. Gades, N. Nereson, C. Raymond, and T. Scambos. This work was supported by National Science Foundation grant OPP 93-16338 to St. Olaf College.

**References**

Fisher, A.M., R.W. Jacobel, N.M. Sundell, and T. Gades. 1995. Bedrock topography and internal stratigraphy of the Siple Dome summit. *EOS, Transactions of the American Geophysical Union*, 76(46), F194.

Jacobel, R.W., T.A. Scambos, C.R. Raymond, and A.M. Gades. 1996. Changes in the configuration of ice stream flow from the west antarctic ice sheet. *Journal of Geophysical Research*, 101(B3), 5499-5504.

Nereson, N.A., and C.F. Raymond. 1995. The geometry and stratigraphy of Siple Dome and implication for its history. *EOS, Transactions of the American Geophysical Union*, 76(46), F194.

Nereson, N.A., and C.F. Raymond. 1996. Recent migration of Siple Dome divide determined from 1994 radio-echo sounding measurements. *Antarctic Journal of the U.S.*, 31(2).

Nereson, N.A., E.D. Waddington, C.F. Raymond, and H.P. Jacobsen. In press. Predicted age-depth scales for Siple Dome and inland WAIS ice cores in West Antarctica. *Geophysical Research Letters*.

Raymond, C.F. 1983. Deformation in the vicinity of ice divides. *Journal of Glaciology*, 29(103), 357-373.

Raymond, C.F., N.A. Nereson, A.M. Gades, H. Conway, R.W. Jacobel, and T.A. Scambos. 1995. Geometry and stratigraphy of Siple Dome, Antarctica. *Antarctic Journal of the U.S.*, 30(5), 91-93.

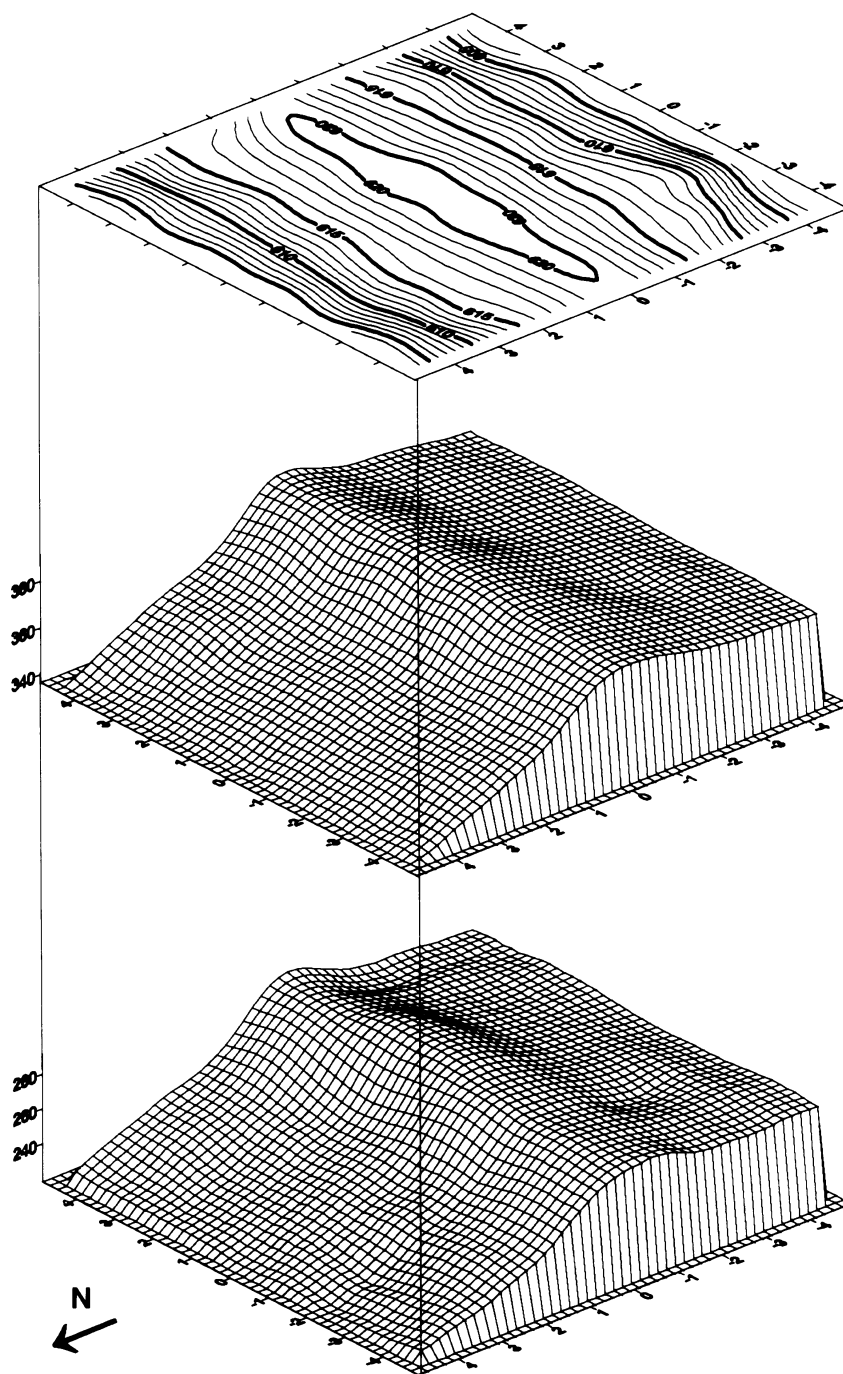


Figure 2. Comparison of the topography of the Siple Dome summit surface and two prominent internal layers. Elevations are in meters above the WGS-84 ellipsoid. Although iceflow near the summit has not changed dramatically throughout the history depicted by the layers (approximately 10,000 years), the difference in slope patterns of the surface and the internal layers requires some degree of non-steady-state behavior.

# Annual dust cycles measured in a short ice core from Siple Dome, West Antarctica

MICHAEL RAM and MICHAEL R. STOLZ, *Department of Physics, State University of New York, Buffalo, New York 14260-1500*

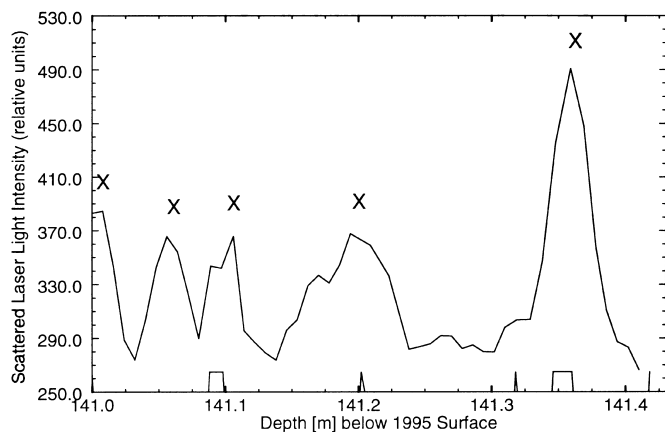
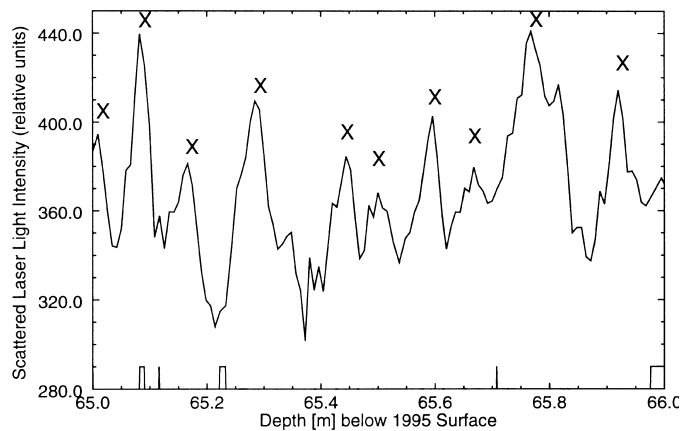
We have used laser-light scattering from ice meltwater to study variations in dust concentration along sections of an approximately 150-meter ice core retrieved by Paul Mayewski and Mark Twickler at Siple Dome, West Antarctica (81.65°S 148.81°W, 600 meters above sea level). The apparatus used for the measurements was the one Ram and Illing (1994) developed for measuring variations in dust concentration along the Greenland Ice Sheet Project 2 ice core from central Greenland.

We measured a total of 13.5 meters of ice from the Siple Dome ice core from depths of approximately 60 meters, approximately 105 meters, and approximately 140 meters. All sections measured exhibited distinct dust peaks, which we interpreted as corresponding to annual dust maxima (Hamilton and Langway 1967; Thompson 1977, pp. 351–364). The figure shows the results of two representative sets of measurements. The Xs indicate the positions of our dust maxima picks. The thickness of the annual dust layers measured were all in the range 9.5–10.5 centimeters, a range consistent with the measurements of Mayewski and Twickler (personal communication).

We would like to thank Paul Mayewski for making the Siple Dome ice available to us.

## References

- Hamilton, W.L., and C.C. Langway, Jr. 1967. A correlation of microparticle concentrations with oxygen isotope ratios in 700 year old Greenland ice. *Earth and Planetary Science Letters*, 3, 363–366.
- Mayewski, P.A., and M.S. Twickler. 1996. Personal communication.
- Ram, M., and M. Illing. 1994. Polar ice stratigraphy from laser-light scattering: Scattering from meltwater. *Journal of Glaciology*, 40(136), 504–508.
- Thompson, L.G. 1977. Variations in microparticle concentration, size distribution and elemental composition found in Camp Century, Greenland, and Byrd Station, Antarctica, deep ice cores. *International Symposium on Isotopes and Impurities in Snow and Ice* (IAHS Publication No. 118). United Kingdom: International Association of Hydrological Sciences.



Laser-light scattering measurements on two sections of the Siple Dome ice core. The Xs indicate the locations of the annual dust maxima. The markings on the horizontal axis show the positions and extent of core breaks.

# Recent migration of Siple Dome divide determined from 1994 radio-echo sounding measurements

NADINE A. NERESON and CHARLES F. RAYMOND, *Geophysics Program, University of Washington, Seattle, Washington 98195-1650*

Radio-echo sounding measurements made in 1994 across the divide of Siple Dome, West Antarctica (Raymond et al. 1995; Scambos and Nereson 1995), reveal internal reflecting horizons to about 70 percent of total depth [1,009±6 meters (m) at the summit]. These layers are asymmetric about the divide; layers to the north are deeper than layers to the south. Within 2 kilometers (km) of the divide, the internal layers are warped convex up along the divide with maximum displacement of about 50 m (figure). The variation in the shape of these layers along the divide ridge is minimal, so that the layer shapes are largely two-dimensional (Jacobel, Fisher, and Sundell, *Antarctic Journal*, in this issue). Examination of these layers shows that the axis of maximum warping is not vertical but tilted to the north toward ice stream D by about 60° (figure).

The warped layers beneath the divide may arise from a local low in accumulation over the divide and/or the special ice-flow field associated with the presence of a divide (Raymond 1983; Hvidberg 1996). Regardless of what causes layer warping observed at Siple Dome, it is likely an effect associated with the presence of the divide, and therefore, the tilted axis of the up-warping is suggestive of recent divide migration northward toward ice stream D.

We have used a two-dimensional finite element model (FEM) (Raymond 1983) to predict the shapes of isochrones under steady-state conditions at Siple Dome. The model assumes

- a nonlinear flow rheology ( $n=3$ ),
- a frozen bed,
- a constant accumulation rate of 10 centimeters per year ( $\text{cm a}^{-1}$ ) ice-equivalent, and
- a steady-state temperature profile following Firestone, Waddington, and Cunningham (1990) (see Nereson et al. 1996).

We find that the predicted warping of isochrones by the FEM is larger than the observed warping by a maximum of 50 m. We suspect that this difference is at least partially due to migration of the divide zone.

To simulate the effect of divide migration on isochrone layer shapes, we construct a kinematic flow model from the FEM flow field and move this flow field through a grid of ice particles in time. We track the path of these particles as they flow through the migrating flow field and map the shape of the resulting isochrones. We also simulate the effect of spatial accumulation gradients by assuming constant ice thickness and by scaling the FEM flow field to the surface accumulation rates, so that continuity is satisfied.

To compare the predicted layer shapes to the observed layer shapes, we define a mismatch parameter,  $J$ ,

$$J = \frac{1}{N-1} \sum \frac{\omega_i (m_i - d_i)^2}{\sigma^2} \quad (1)$$

- where
- $N$  is the number of points,
  - $m_i$  are the depth positions of points along the modeled layers and
  - $d_i$  are depth positions of points along the observed layers,
  - $\sigma_i$  is the expected combined error from the model and the data, and
  - $\omega_i$  is a weighting factor that depends on depth.

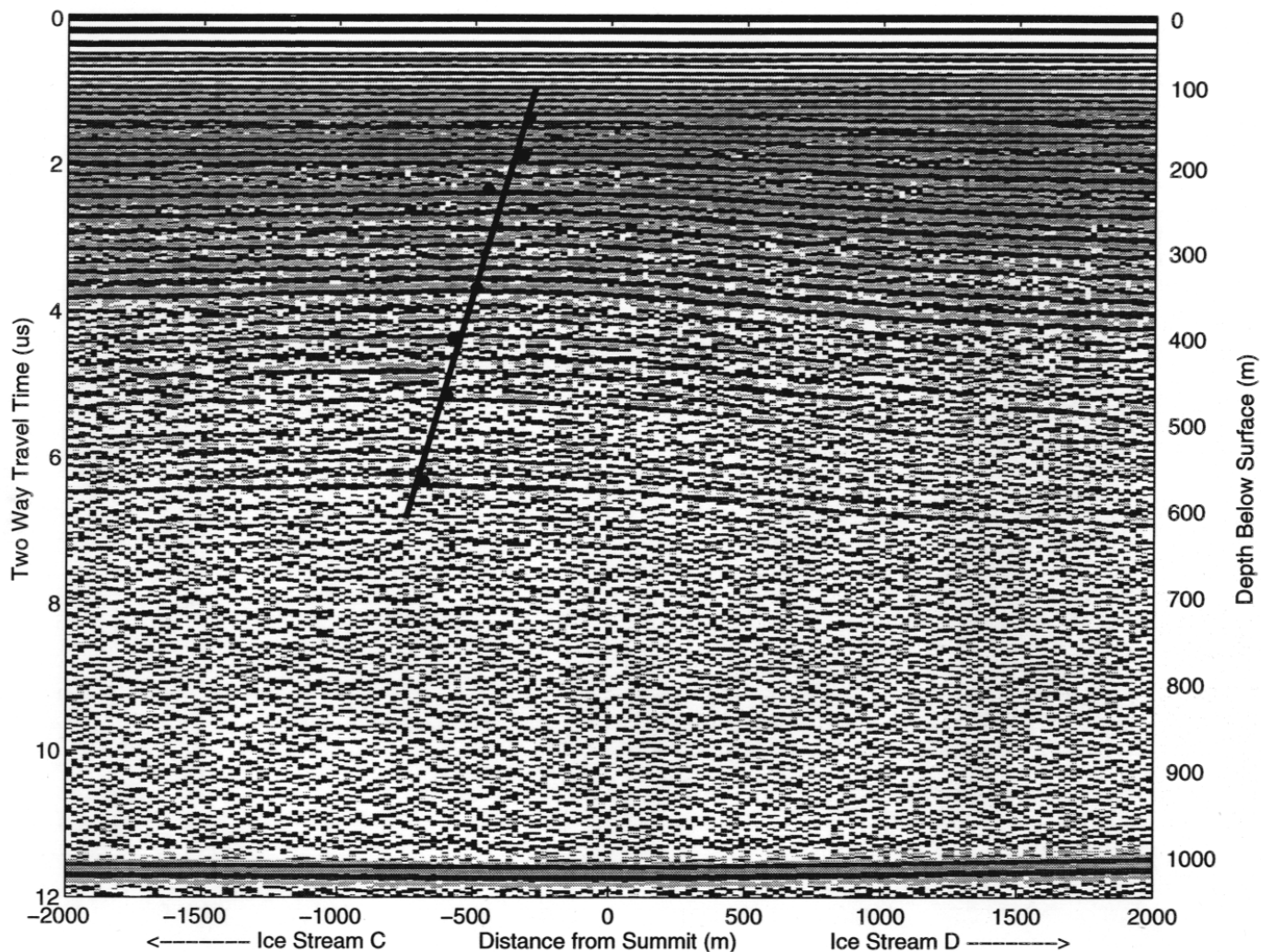
We define a set of parameters to represent divide migration and a simple spatial accumulation rate pattern, and find the set of parameters that minimize  $J$ . We consider two cases:

- case 1 includes the special flow field associated with an ice divide so that the isochrone warping is caused by a combination of this flow field and a local spatial accumulation pattern and
- case 2 assumes no special divide flow field so that the warped layers are caused solely by accumulation scouring on the divide with redeposition to the north.

For the first case, we assume a linear accumulation gradient on either side of the divide defined by two slopes. The spatial pattern looks like a hinge, centered at the divide. This pattern is divide-specific and moves as the divide migrates. We find the combination of three parameters, migration rate, and the two accumulation rate slopes, which minimizes  $J$ . This minimization gives a migration rate of  $3\pm 1$  times the reference accumulation rate, or about  $30 \text{ cm a}^{-1}$ .

For the second case, we define the accumulation scouring and redeposition as one cycle of a sinusoid superimposed on the "hinge" pattern given by the above minimization. We position the low of the sinusoid over the divide (scouring) with the rest of the cycle north of the divide (deposition). In this case, the migration rate, the amplitude of the sinusoid, and its wavelength are adjusted. The resulting minimization gives a migration rate of  $2\pm 1$  times the reference accumulation rate, or about  $20 \text{ cm a}^{-1}$ .

In both cases, the modeled layers match the observed layers to within 0.10 of the amplitude of the up-warping. It appears as though the migration rate inferred from this minimization scheme is only slightly sensitive to the prescribed cause of isochrone warping. Based on the regularity of the layer shapes, we expect that the divide has been migrating toward ice stream D for at least the past 5,000 years. Migration of the divide is important to the selection of the deep ice core at Siple Dome. It indicates effects from non-steady processes possibly including changing activity of ice streams C and D and evolution of the accumulation pattern.



A 5-megahertz radio-echo sounding profile extending 4 km across the Siple Dome summit. This profile is along the same line shown in figure 2 of Raymond et al. (1995). The apex (minimum depth) of observed internal reflecting horizons are marked with black dots. The black line shows the trend of the apex axis. (us denotes microseconds.)

Continuing investigations with the aid of new radio-echo sounding data from the south flank of Siple Dome to be collected in 1996 aim to place constraints on the time evolution of the spatial accumulation pattern, divide migration, and adjacent ice stream activity.

This work was supported by a National Science Foundation grant OPP 93-16807. We also gratefully acknowledge other members of the 1994 field team: H. Conway, A. Gades, R. Jacobel, and T. Scambos.

#### References

Firestone, J., E. Waddington, and J. Cunningham. 1990. The potential for basal melting under Summit, Greenland. *Journal of Glaciology*, 36(123), 163–168.

Hvidberg, C.S. 1996. Steady state thermo-mechanical modelling of ice flow near the centre of large ice sheets with the finite element technique. *Annals of Glaciology*, 23, 116–123.

Jacobel, R.W., A.J. Fisher, and N.M. Sundell. 1996. Internal stratigraphy from ground-based radar studies at Siple Dome summit. *Antarctic Journal of the U.S.*, 31(2).

Nereson, N.A., E.D. Waddington, C.F. Raymond, and H.P. Jacobsen. 1996. Predicted age-depth scales for Siple Dome and inland WAIS ice cores in West Antarctica. *Geophysical Research Letters*, 23(22), 3163–3166.

Raymond, C., N. Nereson, A. Gades, H. Conway, R. Jacobel, and T. Scambos. 1995. Geometry and stratigraphy of Siple Dome, Antarctica. *Antarctic Journal of the U.S.*, 30(5), 91–93.

Raymond, C.F. 1983. Deformation in the vicinity of ice divides. *Journal of Glaciology*, 29(103), 357–373.

Scambos, T., and N. Nereson. 1995. Satellite image and global positioning system study of the morphology of Siple Dome, Antarctica. *Antarctic Journal of the U.S.*, 30(5), 87–89.

# Analysis of ground-based geophysical fieldwork in West Antarctica

C.R. BENTLEY, T.S. CLARKE, C. LIU, N.E. LORD, and S. SHABTAIE, *Geophysical and Polar Research Center, University of Wisconsin, Madison, Wisconsin 53706-1692*

In this article, we summarize recent analyses of data collected from surface experiments carried out during previous field seasons.

## Seismic crustal studies

A densely recorded crustal-scale seismic refraction/wide-angle-reflection profile 235 kilometers (km) long was completed near the southern edge of the Byrd Subglacial Basin during the 1994–1995 field season (Clarke 1996; Clarke et al. in press). Recent work on the data has shown that the bottom third of the crust (22–30 km) contains many reflecting horizons. Clearly identified forward and reverse refractions through the mantle indicate a true wave speed of about 8.0 km per second. The relative thinness of the crust and the reflective character of the lower crust together strongly suggest crustal extension, although the normal wave speed in the mantle implies that extension is not currently active, at least in the area of the profile.

## Abandoned shear margin

SPOT satellite imagery of the ridge of nearly stationary ice between ice streams B1 and B2, known as the Unicorn, shows a curving lineation on the surface of the ice sheet of uncertain origin (Merry and Whillans 1993), which we refer to as the “Fishhook” (Bentley et al. 1994) (figure 1). A survey of a large section of the Unicorn with an 80-megahertz (MHz) impulse radar system during the 1993–1994 field season (Bentley et al. 1994; Clarke and Bentley 1995) showed that the Fishhook is associated with a likely abandoned shear margin—buried crevasses that characterize most of the Unicorn end abruptly along a boundary that is parallel to the Fishhook but 2.5 km grid northeast of it. Between that boundary and ice stream B1, the ice is essentially undisturbed. Detailed measurements revealed buried marginal crevasses that trend about grid N80°E where the boundary trends grid S50°E, which strongly suggests left-lateral shear, as at present in the B2 margin (the “Dragon”; figure 1). Calculations based on the local accumulation rates (Whillans personal communication) and the depths of crevasse burial imply that the shear margin abandoned its position about 180 years ago and migrated toward the Dragon at a rate of about 100 m per year.

## Bottom crevasse

Profiling with a 50-MHz radar system on the Unicorn (Bentley et al. 1994) produced evidence for a bottom crevasse extending upward to 200–300 m above the bed and at least 20 km long (figure 2), closely associated geographically

ly with the Fishhook. It is likely that this bottom crevasse is the cause of the slight topographic irregularity that produces the Fishhook.

## Ice-stream anisotropy

Several grids near the Upstream B camp on ice stream B were profiled during the 1991–1992 field season with the 50-MHz sounding radar system (Bentley et al. 1992). The combined histogram of differences in calculated ice thickness at 328 crossover points (value from the longitudinal profile minus value from the transverse profile) on three grids (figure 3) shows an approximately Gaussian distribution with a mean value of 2.8 m and a standard deviation of 0.9 m; all the differences are positive. We interpret this difference as due to anisotropy of the electromagnetic-wave speed; it accords quantitatively with calculations for a model in which ice-crystal *c* axes are randomly distributed in the plane perpendicular to the ice flow. These results support earlier conclusions based on radar-polarization studies (Liu, Bentley, and Lord 1994), seismic soundings (Blankenship 1989), and theoretical analysis (Alley 1988).

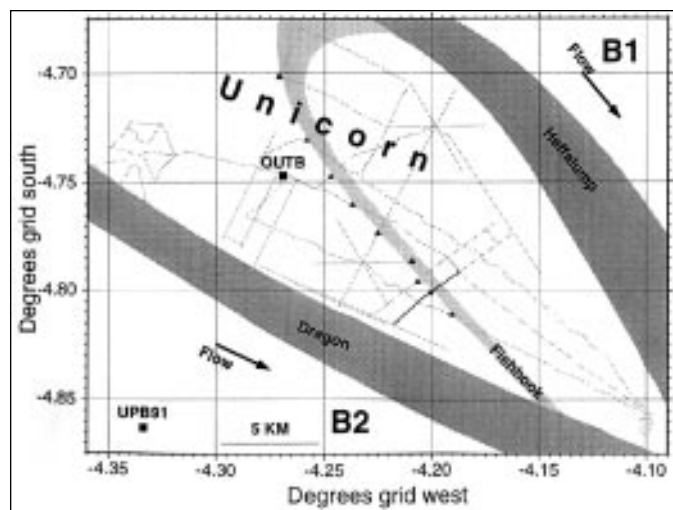


Figure 1. Sketch map of portions of ice streams B1 and B2 and the Unicorn. The dashed lines indicate radar-profiling tracks; the darker line marks the section of figure 2. The marginal shear zones (Dragon and Heffalump) of active ice streams B1 and B2 (Shabtaie and Bentley 1987) are heavily shaded. The light shading shows the Fishhook, as revealed by satellite imagery (Merry and Whillans 1993). The triangles mark crossings of the bottom crevasse shown in figure 2. The coordinates give distances on a grid centered on the South Pole with grid north toward Greenwich. True north is toward the lower left.

## Electrical conductivity of polar ice

The high conductivity of polar polycrystalline ice is due to the presence of ionic impurities, but the location of these impurities in the ice is largely unknown. We have compared *in situ* conductivity measurements with chemical data from ice cores at several arctic and antarctic field locations. Although we find no correlation between the measured conductivities and sea salts, the conductivities do show a close linear dependence on the concentrations of the three major acids: sulfuric ( $\text{H}_2\text{SO}_4$ ), nitric ( $\text{HNO}_3$ ), and hydrochloric ( $\text{HCl}$ ). Several theoretical models based on dielectric theory and the electrical and thermal properties of the acids show, when compared with the data, that

- the linear conductivity-acidity relationship is associated with the polycrystalline nature of polar ice;
- acid impurities are distributed in shells surrounding the ice grains, not just at the three-grain boundaries;
- a small fraction of the acid is present as isolated droplets within the polar ice and does not contribute to the electrical transport; and
- another small fraction of the acid lies within the ice-crystal lattice.

This is contribution number 572 of the Geophysical and Polar Research Center. This work was supported by National Science Foundation grants OPP 92-22092, OPP 92-20678, and OPP 90-18530.

## References

- Alley, R.B. 1988. Fabrics in polar ice sheets: Development and prediction. *Science*, 240(4851), 493-495.
- Bentley, C.R., P.D. Burkholder, T.S. Clarke, C. Liu, and N. Lord. 1994. Geophysical experiments on Ridge B1/B2, Siple Coast. *Antarctic Journal of the U.S.*, 29(5), 57-59.
- Bentley, C.R., A.N. Novick, N. Lord, T.S. Clark, C. Liu, Y.Y. Macheret, and A.N. Babenko. 1992. Radar experiments on ice stream B. *Antarctic Journal of the U.S.*, 27(5), 43-44.
- Blankenship, D.D. 1989. Seismological investigations of a west antarctic ice stream. (Ph.D. thesis, University of Wisconsin, Madison, Wisconsin.)
- Clarke, T.S. 1996. A crustal-scale seismic study of the Byrd Subglacial Basin, Antarctica. (Ph.D. thesis, University of Wisconsin, Madison, Wisconsin.)
- Clarke, T.S., and C.R. Bentley. 1995. Evidence for a recently abandoned ice stream shear margin. *EOS, Transactions of the American Geophysical Union*, 76(46), F194.
- Clarke, T.S., P.D. Burkholder, S.B. Smithson, and C.R. Bentley. In press. Optimum seismic shooting and recording parameters and a preliminary crustal model for the Byrd Subglacial Basin, Antarctica. *Terra Antarctica*.

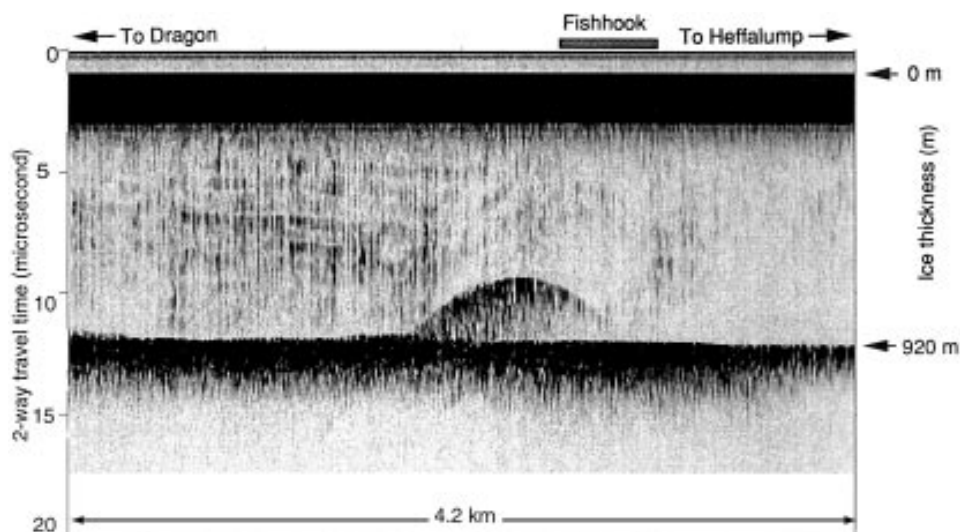


Figure 2. Radar-sounding section across the Fishhook on the Unicorn (see figure 1). The pronounced hyperbola with its apex about 2.5 microseconds above the bed is the presumed bottom crevasse.

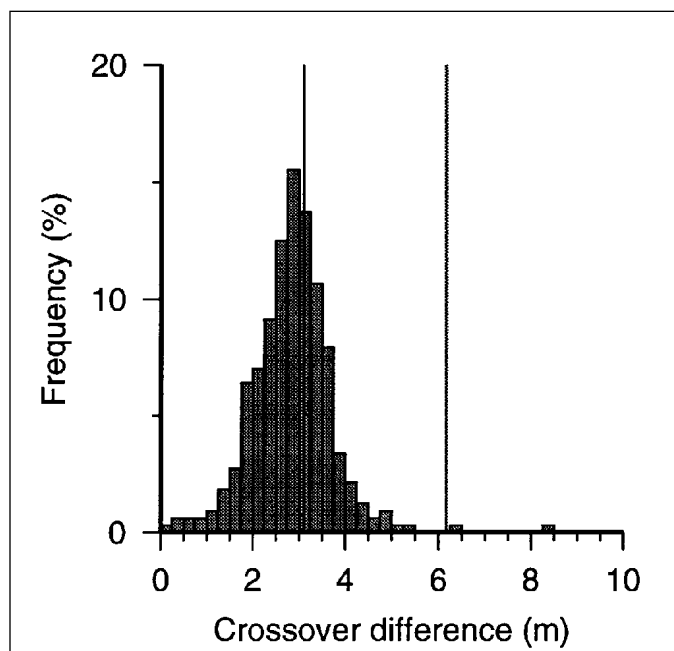


Figure 3. Histogram of differences in calculated ice thickness at 328 radar-sounding crossover points near Upstream B camp on ice stream B. The vertical line at 6.2 m shows the maximum theoretical difference for an ice sheet with all *c* axes perfectly aligned horizontally in the transverse direction; at 3.1 m, the line indicates the theoretical difference for *c* axes oriented randomly in a plane normal to the flow (longitudinal) direction.

- Liu, C., C.R. Bentley, and N.E. Lord. 1994. *C*-axes from radar depolarization experiments at Upstream B camp, Antarctica, in 1991-92. *Annals of Glaciology*, 20, 169-176
- Merry, C.J., and I.M. Whillans. 1993. Ice-flow features on ice stream B, Antarctica, revealed by SPOT high resolution visual imagery. *Journal of Glaciology*, 39(133), 515-527.
- Shabtaie, S., and C.R. Bentley. 1987. West antarctic ice streams draining into the Ross Ice Shelf: Configuration and mass balance. *Journal of Geophysical Research*, 92(B2), 1311-1336.
- Whillans, I.M. 1995. Personal communication.

# Airborne radar sounding over west antarctic ice streams

CHARLES R. BENTLEY, CHEN LIU, and NEAL E. LORD, *Geophysical and Polar Research Center, University of Wisconsin, Madison, Wisconsin 53706-1692*

In this article, we report on two aspects of our airborne radar sounding work: recent flights over the upstream end of ice stream D and recent analysis of older work over the downstream ends of ice streams B and C.

## Ice stream D

During January 1996, the Support Office for Aerogeophysical Research (SOAR) collected airborne-radar, laser-altimeter, barometric-pressure, dual-frequency global positioning system (GPS), and inertial-navigation data over the upstream section of ice stream D in support of a University of Wisconsin project to study the ice stream. Each of the 26 Twin Otter flights made over the University of Wisconsin research area typically included four flight lines 142 kilometers (km) long. Flight lines were spaced 5.3 km apart both across and along the ice-flow direction. The field data were delivered to us in June 1996.

- *Kinematic GPS.* Kinematic GPS receivers on the aircraft and at the base station were used for positioning the aircraft. Positions on all flights will be recoverable, despite a few GPS failures, because the Twin Otter had two GPS systems. The accuracy of the GPS positioning, after postprocessing is complete, is expected to be about  $\pm 0.5$  meters (m).
- *Laser altimetry.* The laser altimeter gives the distance between the aircraft and the ice surface with a typical precision of 10–20 centimeters. Clouds were the main source of interference. Six flights had cloud-caused “dropouts” that obscured the surface over less than 10 km; four flights had “dropouts” over larger regions. In those places, the surface height will be determined from the radar surface reflections. The radar reflection times should be accurate to about 10 nanoseconds, equivalent to 1.5–2.0 m in surface height.
- *Radar sounding.* The SOAR 60-megahertz (MHz) sounding radar was used to map the ice thickness. Penetration to the bed was not a problem except for places with a high density of crevasses, which produce the long-lasting, incoherent returns known as “clutter.” On the interstream ridges, where clutter was limited, the bottom echo was mostly strong, but it was obliterated by clutter over the ice-stream margins and weak compared to the clutter over the ice stream.

In figure 1, we show the radar-sounding data along the transverse profiles farthest upstream and farthest downstream within the University of Wisconsin area; the locations of the profiles are shown on a satellite-image map. Strong clutter clearly shows the location of the ice stream and its margins. The radargrams contain no evidence for the more northerly mapped branch of ice stream D, whereas the agreement between the radar evidence and the location of the more southerly branch of the ice stream

is excellent. This accords with the work of Rose (1979), whose first delineation of ice stream D, also based on clutter, showed the more northerly branch only west of around 138°W, i.e., only outside the area of figure 1.

- *Calibrator.* The University of Wisconsin designed and built a 60-MHz radar calibrator to test quickly and accurately the amplitude response of the radar system from the pre-amplifier to the digital converter. The University of Wisconsin calibrator has the advantage over manual calibrations in that a 120-decibel (dB) range of input values is taken in 1-dB rather than 10-dB steps; calibrations can be done without operator intervention. The calibration shows that the radar has a 70-dB usable input range and that the clipping point of the receiver is very abrupt.

## Ice streams B and C

During the 1987–1988 field season, the University of Wisconsin 50-MHz radar system, mounted in a Twin Otter, was flown over the downstream ends of ice streams B and C (Bentley, Blankenship, and Moline 1988). Grids with equal spacings in both directions were flown in both areas—the spacing was 5 km over ice stream B and 10 km over ice stream C. The largest source of navigational error was the drift of the inertial navigation system; residual errors after closure corrections are on the order of 1 km.

- *Ice thickness.* The detailed map of ice thickness that results from these high-density surveys (figure 2) is remarkably similar to the reconnaissance map previously produced (Shabtaie and Bentley 1988). Our analysis so far has not revealed any significant differences between the two.
- *Basal-reflection strength.* Basal reflection strengths corrected for propagation losses, mapped in figure 3, are determined principally by the reflection coefficient of the bed and by scattering from crevasses within the ice. Bands with losses greater than 30 dB are closely associated with the margin of ice stream B. Surprisingly, there is not nearly as close an association of weak reflections with the margins of ice stream C. The fact that reflections are at least 10 dB weaker on crevasse-free Ridge BC than on ice streams B and C suggests that the ice on the ridge is frozen to its bed. Ice stream C exhibits substantially stronger basal reflections than ice stream B. Although this is probably due in part to less scattering by buried crevasses on ice stream C than on ice stream B, it nevertheless implies that the bed of ice stream C is everywhere unfrozen and wet. Apparently, the cause of its stagnancy is not a lack of water at its bed.

This is contribution number 573 of the Geophysical and Polar Research Center. This work was supported by National Science Foundation grants OPP 93-19043 and OPP 90-18530.

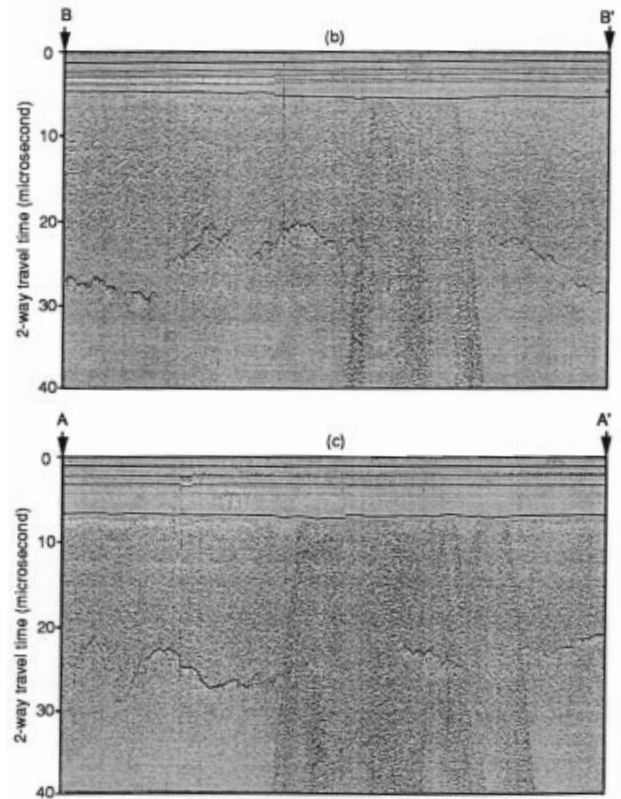
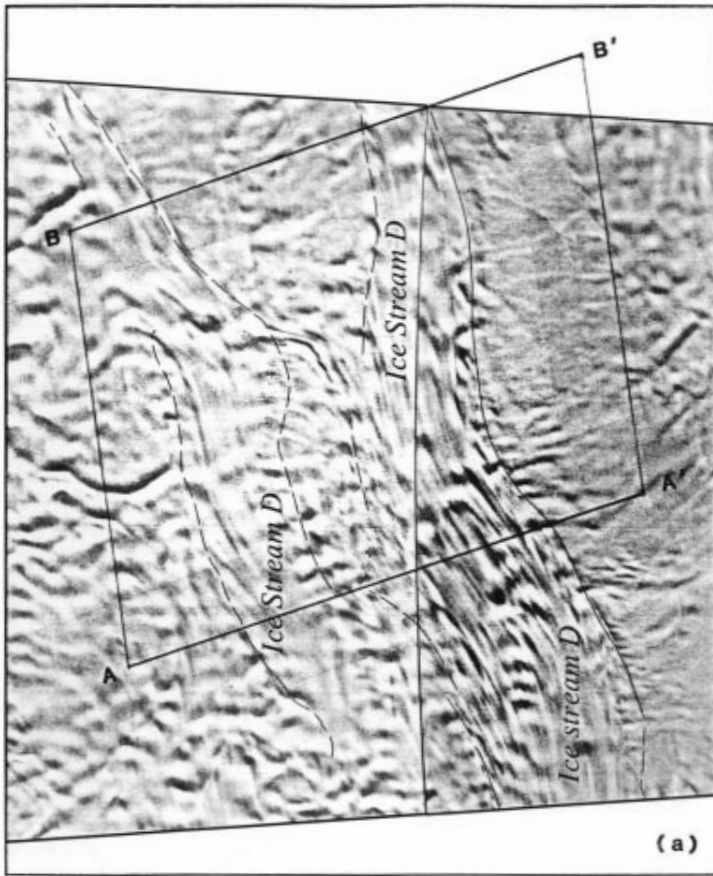


Figure 1. A. Composite of "Glaciological Features," taken from the USGS satellite image maps of the Ross ice streams (U.S. Geological Survey 1992). The ice-stream labeling is from those maps. AA' and BB' indicate the locations of the radargrams shown in B and C; each section is 110 km long. True north is toward the top; ice flow in the ice stream is approximately from right to left. Box AA'B'B' marks the boundaries of our survey. The lateral boundaries of the map are along 127°30'W and 135°W; the north and south boundaries are approximately along 80°20'S and 81°30'S, respectively. B-C. Radargrams along line AA' and BB', respectively. In each, the surface appears at about 8 microseconds and the bed between 20 and 30 microseconds. Scattering from near-surface crevasses produces "clutter," the incoherent signal that in places extends downward from the surface reflection and mostly obscures the bottom reflection.

## Ice Thickness (m)

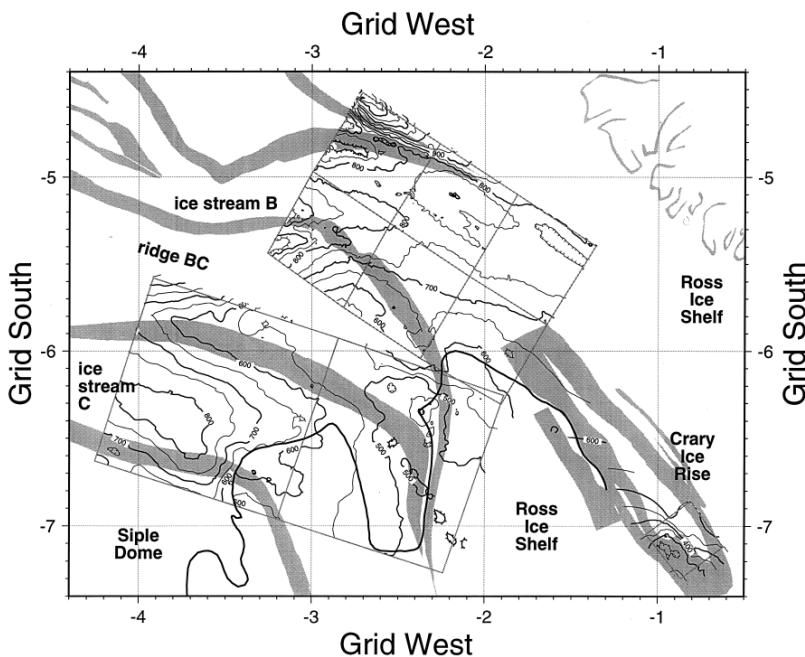


Figure 2. Map of ice thickness beneath the downstream portions of ice streams B and C. The heavy line marks the grounding line as mapped by Shabtaie and Bentley (1987). The contour interval is 50 m.

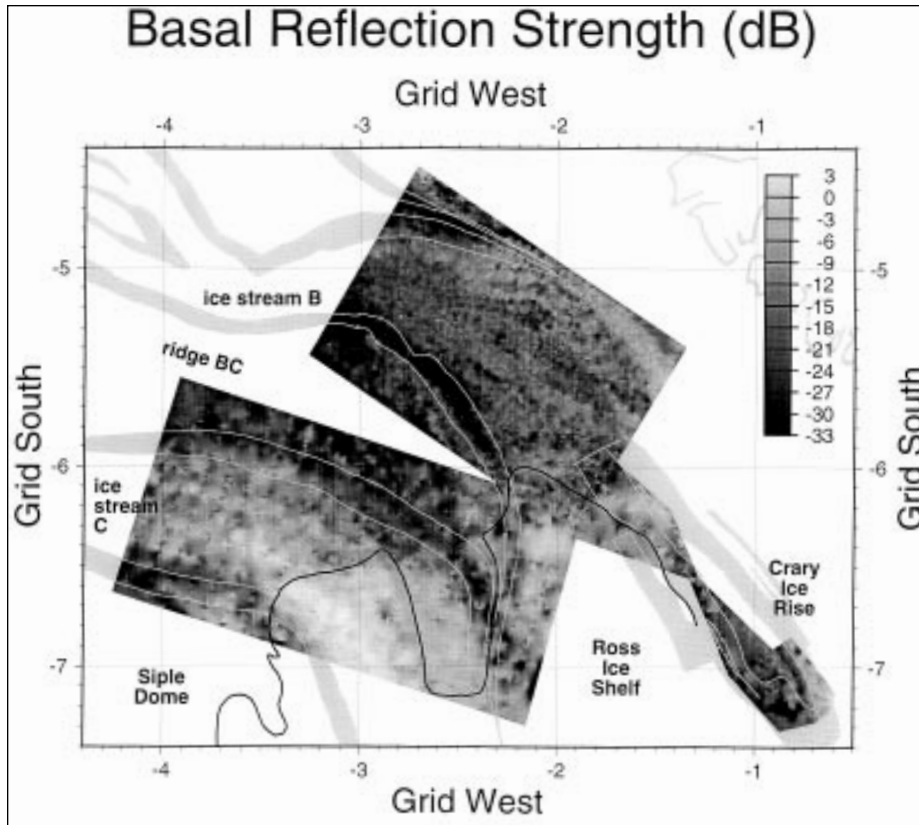


Figure 3. Map of basal-reflection strength (in dB—see scale) beneath the downstream portions of ice streams B and C. The heavy line marks the grounding line as mapped by Shabtaie and Bentley (1987).

- Bentley, C.R., D.D. Blankenship, and G. Moline. 1988. Electromagnetic studies on the Siple Coast, 1987–1988. *Antarctic Journal of the U.S.*, 23(5), 56–58.
- Rose, K.E. 1979. Characteristics of ice flow in Marie Byrd Land, Antarctica. *Journal of Glaciology*, 24(90), 63–75.
- Shabtaie, S., and C.R. Bentley. 1987. West antarctic ice streams draining into the Ross Ice Shelf: Configuration and mass balance. *Journal of Geophysical Research*, 92(B2), 1311–1336.
- Shabtaie, S., and C.R. Bentley. 1988. Ice-thickness map of the west antarctic ice streams by radar sounding. *Annals of Glaciology*, 11, 126–136.
- U.S. Geological Survey. 1992. Antarctica, Satellite Image Maps SU6-10/3 and SU6-10/7-11\*, Experimental Edition. Reston, Virginia: U.S. Geological Survey.

## Monitoring of basal seismicity rates of ice stream C, West Antarctica: Preliminary results of the Antarctic Microearthquake Project, 1994–1995 and 1995–1996

SRIDHAR ANANDAKRISHNAN, *Earth System Science Center and Department of Geosciences, Pennsylvania State University, University Park, Pennsylvania 16802-2711*

Because of their large ice flux, the ice streams of the Siple Coast have been and continue to be the focus of much research. One of them, ice stream C, largely stagnated about two centuries ago (Rose 1979; Retzlaff and Bentley 1993). Understanding the reasons for this shutdown is crucial to understanding the dynamics of the west antarctic ice sheet and its response to climate change. The speed of ice-streaming appears to be inversely related to the rates of basal seismicity (Anandakrishnan and Bentley 1993), and to quantify this relationship, an intensive program of seismic monitoring was initiated on ice stream C. Alley et al. (1994) hypothesized that ongoing drawdown of the ice sheet caused ice stream C to migrate into a region that caused a diversion of basal water from the lower parts of ice stream C. The Antarctic Microearthquake

Project (AMP) was designed to test that hypothesis because one consequence of the lack of basal water is high seismicity (under the right conditions; see Anandakrishnan and Alley [1994]).

Over the past two field seasons a series of seismic arrays has been deployed along the length of the ice stream from the grounding line to the head of the ice stream at a nominal spacing of 75 kilometers. The arrays consisted of four or five short-period seismometers deployed in a diamond pattern 6 kilometers wide by 8 kilometers long. During the first season (1994–1995), CWA, SH, and CC sites were occupied. During the second season (1995–1996), STC, WB, EF, and BC were occupied, and SH and CC re-occupied (see table). In addition to the seismic work, we surveyed the position of a steel pole at the center of each array at the beginning of the austral summer and then resurveyed the

sites at the end of the summer when we retrieved the instruments. We have determined iceflow velocities for each site. Because of the short time between occupations, our measurements of the velocities are not precise, but we hope to return to the sites and resurvey them at a later time.

The work was mainly carried out from a base camp at CWA during 1994–1995 and a base camp at STC during 1995–1996. The instruments were successfully installed at all the sites, and most (40 out of 44) ran for the whole period. The seismometers were configured to begin recording when an event was detected. Most triggers were due to earthquakes; very few wind-noise, crevassing, or firnquake events were recorded. The arrival times of the events were picked, and their hypocenters were located.

Preliminary analysis shows that most are basal events and the rates of those events (in number per day) are listed in the table. The pattern along ice stream C is one of low seismicity at the sites that have relatively high velocity and vice-versa. The ice stream is divided into two regions and the boundary between the high- and low-seismicity and between the low- and high-velocity regions is centered on site CC, about 350 kilometers from the grounding line. This boundary corresponds closely with a basal-water diversion zone (Alley et al. 1994; Anandakrishnan and Alley 1994) that was hypothesized to have caused the stagnation of ice stream C. We confirm that the data are consistent with that hypothesis.

Ice stream C has stagnated in its lower part because of the loss of basal lubricating water, and this stagnation has had two consequences: the ice has coupled to localized hard spots at the bed, causing microearthquakes, and has slowed to less than 10 meters per year because of the friction from those “sticky spots.” The region between the sticky spots is relatively soft and deformable and supports little of the basal shear stress resulting in a concentration of the shear stress on the sticky spots. Ice

stream C stagnated because of an accident of topography which has withdrawn water from the lower part of ice stream C and has probably increased the water supply to ice stream B.

I thank the members of my field team, Peter Burkholder, Paul Friberg, Anton Wopereis, and John Witzel, for their dedication and hard work. I thank Bjorn Johns, Antarctic Support Associates, and VXE-6 for their professional and efficient support. I thank the Incorporated Research Institutions for Seismology and University Navstar Consortium (UNAVCO) for their equipment support.

## References

- Alley, R.B., S. Anandakrishnan, C.R. Bentley, and N. Lord. 1994. A water-piracy hypothesis for the stagnation of ice stream C, Antarctica. *Annals of Glaciology*, 20, 187–194.
- Anandakrishnan, S., and R.B. Alley. 1994. Ice stream C, Antarctica, sticky-spots detected by microearthquake monitoring. *Annals of Glaciology*, 20, 183–186.
- Anandakrishnan, S., and C.R. Bentley. 1993. Microearthquakes beneath ice streams B and C, West Antarctica: Observations and implication. *Journal of Glaciology*, 39(133), 455–462.
- Retzlaff, R., and C.R. Bentley. 1993. Timing of stagnation of ice stream C, West Antarctica, from short-pulse-radar studies of buried surface crevasses. *Journal of Glaciology*, 39(133), 553–561.
- Rose, K. 1979. Characteristics of ice flow in Marie Byrd Land, Antarctica. *Journal of Glaciology*, 24(90), 63–74.

### **Summary of ice-flow velocities and basal seismicity rates at the sites occupied during the AMP experiment**

Site	Distance from grounding line (in kilometers)	Velocity (in meters per year)	Seismic events per day	Latitude	Longitude	Elevation (in meters)
BC	10	0.3	35	82°48'41"S	152°35'52"W	94.2
EF	86	0.6	43	82°41'31"S	147°22'50"W	138.6
WB	162	0.5	24	82°24'40"S	142°08'52"W	256.2
STC	252	7	15	82°20'49"S	136°04'52"W	508.6
CC	354	52	271	82°03'51"S	129°37'30"W	690.2
SH	432	62	0	81°48'14"S	124°59'13"W	807.6
CWA	482	11	0	82°07'37"S	118°08'18"W	1,067.0

# Surface exposure dating of glacial landscapes and deposits in the Transantarctic Mountains using *in situ* induced cosmogenic helium-3 and neon-21

L.A. BRUNO, H. BAUR, P. SIGNER, and R. WIELER, *Isotope Geology, ETH-Zentrum, Zürich, Switzerland*  
C. SCHLÜCHTER, *Institute of Geology, University of Bern, Bern, Switzerland*

In this study, tillites and glaciated surfaces in the Transantarctic Mountains were dated by cosmic-ray-produced noble gas nuclides, with a goal of improving knowledge on the Pliocene stability of the east antarctic ice sheet. These glacial surfaces and the tillites of the Sirius Group have apparently been formed during a maximum extension of the east antarctic ice sheet.

Cosmogenic nuclides are produced within the uppermost decimeters of an exposed rock surface as a result of cosmic-ray bombardment. The concentrations of nuclides such as helium-3 ( $^3\text{He}$ ) and neon-21 ( $^{21}\text{Ne}$ ) can be used to determine the age of the geological surface on timescales of thousands to millions of years. Therefore, exposure dating now offers a direct method of determining the time of exposures of geomorphological features such as glacial polish or clasts in a moraine. Such exposure ages are usually minimum ages for the formation or deposition of these features. The construction of an absolute timescale for terrestrial ice-age deposits has been hindered both by limitations in the dating methods and by a lack of datable material.

The samples dated in this study were quartz and clinopyroxene fractions separated from granites, dolerites, and sandstones collected at Table Mountain and Mount Fleming in the western dry valleys region of the Transantarctic Mountains. In addition, whole-rock samples have been analyzed from some dolerites from these sites. Until now, few or no age determinations have been based on cosmogenic noble gases in pyroxene and whole-rock samples of dolerite. All 53 samples analyzed in our study revealed mixtures of cosmogenic and atmospheric noble gases, without detectable amounts of other trapped components and also with at most minor contributions from nucleogenic noble gases. The pyroxenes show identical  $^3\text{He}$  and  $^{21}\text{Ne}$  ages, indicating complete retention of both these nuclides. Quartz ages are based on the cosmogenic  $^{21}\text{Ne}$  content only, because  $^3\text{He}$  is incompletely retained in quartz. Loss of  $^3\text{He}$  and even partial loss of  $^{21}\text{Ne}$  occurred from plagioclase in the dolerites. The cosmogenic  $^{21}\text{Ne}$ -based dolerite ages are thus minimum values.

Calculated exposure ages of our samples range from 0.2 to 7.0 million years. Some of these values are the oldest ages measured so far in any terrestrial samples. An age of 7.0 million years was determined for a dolerite clast on the Sirius tillite at Mount Fleming. This value affords a minimum age for the formation of this Sirius tillite deposit and perhaps others like it in the Transantarctic Mountains. An age of 6.1 million years at Table Mountain has been measured on a sample from the bedrock plateau surface just slightly higher in eleva-

tion than the nearby Sirius deposit. In comparison, an age of only 2.6 million years was determined for the surface of the Sirius tillite at Table Mountain. The relatively young age indicated for this tillite is probably due to erosion.

Constraints on the uplift rates of the Transantarctic Mountains have been estimated from the concentrations of cosmogenic nuclides in our samples from Mount Fleming and Table Mountain. If it is postulated that the samples were located at sea level at the beginning of exposure and were subsequently uplifted at a constant rate, then the maximum uplift for Mount Fleming is 160 meters per million years and for Table Mountain, 180 meters per million years. Different uplift rates would affect the altitude correction of the production rates and thus the exposure ages. For example, uplift of 100 meters per million years as reported by some authors would change the minimum ages for the deposition of the Mount Fleming tillite from more than 7 million years to more than 11 million years and the minimum age for the cutting of the Table Mountain plateau from 6 million years to prior to 8 million years. Uplift rates of 300 meters per million years or even 1,000 meters per million years suggested by other workers seem to be very unlikely, even if they occurred episodically.

The data presented here imply a stable behavior of the east antarctic ice sheet since exposure of the sampled Sirius tillite at Mount Fleming. The exposure ages of 6.1 and more than 7.0 million years for glacial surfaces and deposits, respectively, contradict the postulate of Pliocene ice sheet overriding of Transantarctic Mountains between 2.5 and 3.1 million years. The age difference between the Table Mountain and the Mount Fleming tillites is most likely due to partial erosion of the Table Mountain deposit. If the key samples were eroded since they were exposed to cosmic rays, the limiting ages for the maximum extension of antarctic ice sheet would be even older, and the maximum uplift rates would have been smaller than those reported here.

This research was supported by the National Science Foundation grant OPP 90-20975, ETH-Zürich research grant 0-20-624-92, and Swiss National Science Foundation grant 2118-28971.90.

## Reference

- Bruno, L.A. 1995. Dating of moraines and glacially overridden surface areas in Antarctica using *in situ* induced cosmogenic noble gases. [Datierung von Moränen und glazial überprägten Oberflächen in der Antarktis mit *in situ*-produzierten kosmogenen Edelgasen.] (Ph.D. Dissertation No. 11,256, ETH-Zürich, Abt. Xc; Aug. 11, 1995.) [In German]

# Basal processes at subfreezing temperatures: Meserve Glacier revisited

H. CONWAY, K. CUFFEY, A.M. GADES, B. HALLET, C.F. RAYMOND and R. SLETTEN, *Geophysics Program and Department of Geological Sciences, University of Washington, Seattle, Washington 98195*

**B**asal layers whose composition and mechanical properties differ markedly from that of overlying ice exist beneath many cold-based ice sheets and glaciers. Such layers have been observed at the bottom of deep ice cores from the Arctic and Antarctic (Herron and Langway 1982; Fischer and Koerner 1986; Dahl-Jensen and Gundestrup 1987; Gow, Epstein, and Sheehy 1979; Souchez et al. 1995; Gow and Meese 1996) and at the margins and in tunnels beneath polar and subpolar glaciers (Holdsworth 1974; Echelmeyer and Zhongxiang 1987; Sugden et al. 1987; Knight 1989).

The origin and rheological properties of these basal layers are poorly understood, yet accurate ice-sheet flow modeling requires knowledge of the viscosity and spatial extent of these layers because deformations are strongest near the bed where shear stresses are highest. Further, understanding the origins of these layers could help in extracting paleoclimate records from ice cores (Gow, Meese, and Alley 1993). For example, entrainment processes are thought to be slow or nonexistent at subfreezing temperatures, and it is not clear how a debris-rich basal layer can form under these conditions. Formation of this basal layer raises the possibility that the layers form by regelation or freeze-on under temperate conditions, a process that implies radically different conditions at the bed in the past. Alternatively, if basal processes are active at subfreezing temperatures, this activity would place a limit on how close to the bed one could obtain an undisturbed stratigraphic sequence for paleoclimate analyses.

Analyses of basal layers revealed by ice cores are hindered by the small size of the sample—a cylinder never more than 20 centimeters in diameter—which reveals little information about spatial variability or spatial relationships and provides little material for analyses of composition and crystal fabric. One way to avoid this limitation is to tunnel through the basal layers inward from the margin (Holdsworth 1974; Echelmeyer and Zhongxiang 1987). We have just begun a study of basal processes at Meserve Glacier, one of the alpine glaciers in Wright Valley, using this approach.

Meserve Glacier has a silt-rich basal layer, which has a distinctive amber color (Holdsworth 1974). The basal temperature is approximately  $-17^{\circ}\text{C}$ . During the 1995–1996 field season, we excavated a 20-meter (m) long tunnel into the tongue of the lower glacier. The tunnel floor followed the ice/rock interface, and we mapped and sampled ice to obtain measurements of spatial variations of properties such as stable isotopes, ice texture and fabric, particle stratigraphy, and ionic chemistry. Inside the tunnel, we are measuring ice deformation at two strain grids, and also motion at the bed.

Although not a perfect analog for conditions under a large ice sheet, the Meserve basal layer provides an excellent natural laboratory for examining processes at subfreezing temperatures. For example, here we can examine how chemical impurities, solid impurities, and crystal fabrics together affect ice rheology. We can test theoretical predictions for glacier sliding at subfreezing temperatures. We hope to use measurements of ice chemical and particle composition, and their spatial variations, to understand the physical processes and environments responsible for the formation and diagenesis of the basal layer. A crucial part of our investigation is the analysis of stable isotope composition, which constitutes a powerful tool for investigating basal processes and establishing the origin of basal layers (Souchez and de Groot 1985; Souchez and Jouzel 1984).

Preliminary observations and measurements indicate the glacier is sliding (at least locally) at the bed. The existence of cavities in the lee of boulders suggests sliding is occurring. Further, some of the ice in the cavity roofs is striated and the wavelength of the striations appears to be related to the roughness of the surface of the boulder. Most convincingly, we measured sliding directly using linear displacement transducers and displacement markers and found the slip rate to be approximately 0.5 centimeter per year. This rate of sliding is considerably faster than that predicted by current sliding theory for ice at  $-17^{\circ}\text{C}$  (Shreve 1984; Dash 1989).

Measurements from the two strain grids installed in the tunnel walls show that the shear strain rate varies with height above the bed. Variations appear to be at least partly correlated with ice impurity content. The shear strain rate increases sharply from near zero to approximately 0.4 per year at a distance of 0.5 m above the bed. At one site, the increase occurs at a discontinuity in the (visual) particle distribution, but this is not the case at the other site. In addition, the shear strain rate increases significantly about 1.5 m above the bed, and this increase does not appear to correlate with impurity content. The strain rate may be more closely correlated with the strength of crystal fabrics. Analyses of ice composition and crystal fabric are currently in progress.

We also measured the ice thickness by radar along several transects on the lower glacier tongue and in the upper accumulation basin. In addition to providing an important constraint on ice-flow calculations, the ice-thickness measurements revealed an interesting bed morphology: the middle portion of the glacier rests in a U-shaped trough. This suggests that glacial erosion has played a significant role in modifying the bed of this cold-based glacier.

The research is supported by National Science Foundation grant OPP 94-18381. We thank R. Hawley, L. Nightingale, K. Whilden, and John Wright for assistance in the field. We also thank all those in the U.S. Antarctic Program who provided logistical and science support.

## References

- Dahl-Jensen, D., and N.S. Gundestrup. 1987. *Constitutive properties of ice at Dye III, Greenland* (IAHS Publication No. 170). United Kingdom: International Association of Hydrologic Sciences.
- Dash, J.G. 1989. Thermomolecular pressure in surface melting: Motivation for frost heave. *Science*, 246, 1591–1593.
- Echelmeyer, K., and W. Zhongxiang. 1987. Direct observations of basal sliding and deformation of basal drift at sub-freezing temperatures. *Journal of Glaciology*, 33(113), 83–98.
- Fisher, D.A., and R.M. Koerner. 1986. On the special rheological properties of an ancient microparticle-laden Northern Hemisphere ice as derived from borehole and core measurements. *Journal of Glaciology*, 32(112), 501–510.
- Gow, A.J., S. Epstein, and W. Sheehy. 1979. On the origin of stratified debris in ice cores from the bottom of the antarctic icesheet. *Journal of Glaciology*, 23(89), 185–192.
- Gow, A.J., and D.A. Meese. 1996. Nature of basal debris in the GISP2 and Byrd ice cores and its relevance to bed processes. *Annals of Glaciology*, 22, 134–140.
- Gow, A.J., D.A. Meese, and R.A. Alley. 1993. Discontinuities including possible distortion of the environmental record in cores of deep basal ice from central Greenland. *EOS, Transactions of the American Geophysical Union*, 74(43), 84.
- Herron, S.L., and C.C. Langway. 1982. A comparison of ice fabrics and textures at Camp Century, Greenland, and Byrd Station, Antarctica. *Annals of Glaciology*, 3, 118–124.
- Holdsworth, G. 1974. *Meserve Glacier, Wright Valley, Antarctica: Part 1, Basal processes* (Institute of Polar Studies Report No. 37). Columbus: Ohio State University Research Foundation.
- Knight, P.G. 1989. Stacking of basal debris layers without bulk freezing-on: Isotopic evidence from west Greenland. *Journal of Glaciology*, 35(120), 214–216.
- Shreve, R.L. 1984. Glacier sliding at subfreezing temperatures. *Journal of Glaciology*, 30(106), 341–347.
- Souchez, R.A., and J.M. de Groote. 1985.  $\delta D$ - $\delta^{18}O$  relationships in ice formed by subglacial freezing: Paleoclimatic implications. *Journal of Glaciology*, 31(109), 229–232.
- Souchez, R.A., L. Janssens, M. Lemmens, and B. Stauffer. 1995. Very low oxygen concentration in basal ice from Summit, central Greenland. *Geophysical Research Letters*, 22(15), 2001–2004.
- Souchez, R.A., and J. Jouzel. 1984. On the isotopic composition in  $dD$  and  $d^{18}O$  of water and ice during freezing. *Journal of Glaciology*, 30(106), 369–372.
- Sugden, D.E., C.M. Clapperton, J.C. Gemmell, and P.G. Knight. 1987. Stable isotopes and debris in basal glacier ice, South Georgia, southern ocean. *Journal of Glaciology*, 33(115), 324–329.

---

# Glacial/interglacial variations in the flux of atmospherically transported diatoms in Taylor Dome ice core

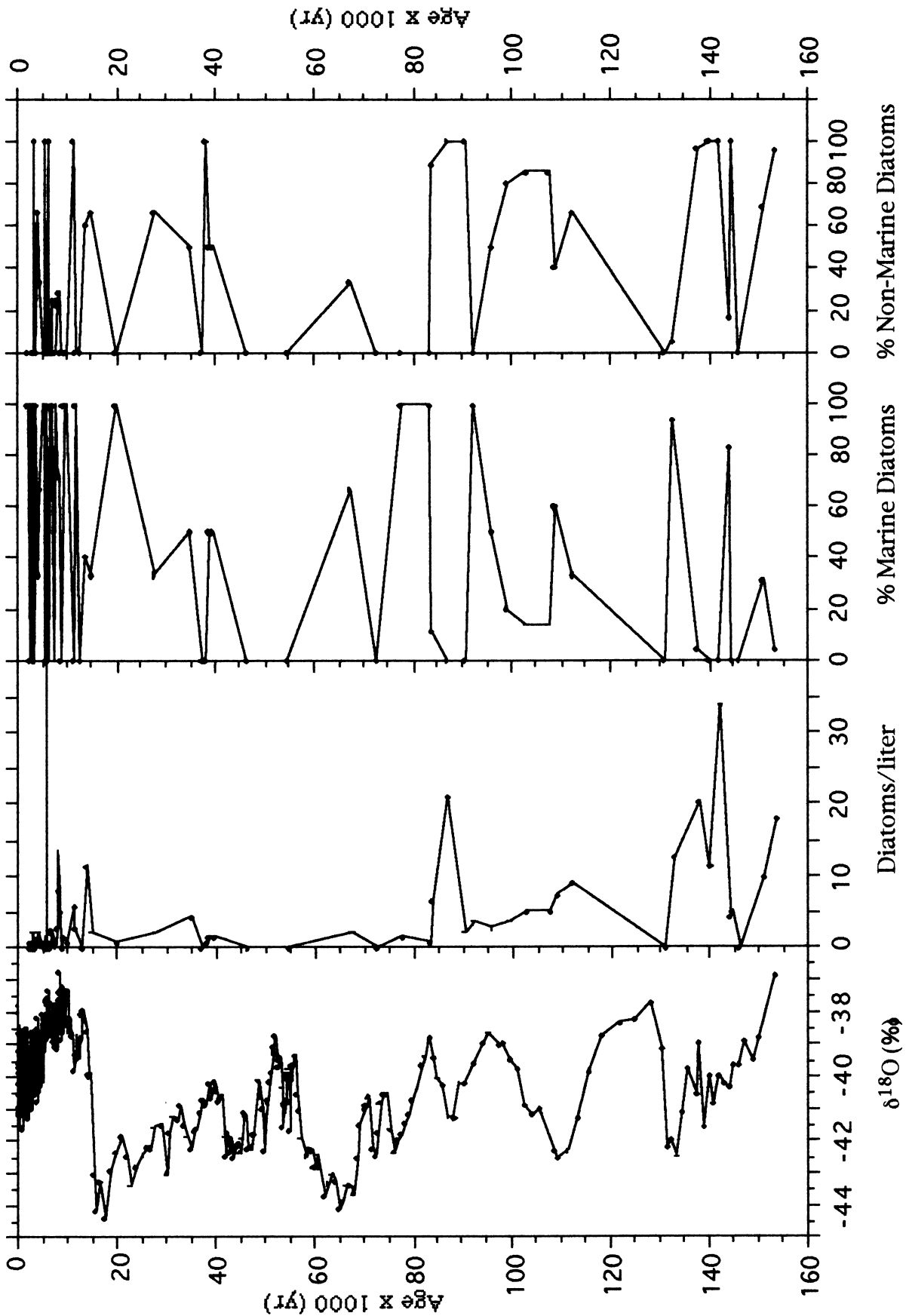
DAVIDA E. KELLOGG and THOMAS B. KELLOGG, *Institute for Quaternary Studies and Department of Geological Sciences, University of Maine, Orono, Maine 04469*

After finding eolian-deposited diatoms in an ice core drilled at South Pole (Kellogg and Kellogg 1996), we were anxious to determine whether wind-blown diatoms are routinely incorporated into ice at other remote antarctic locations. Specifically, we were interested in determining how widespread these diatoms are, how diatom assemblages and abundance patterns differ between the east and west antarctic ice sheets, and how diatom flux varies down long ice cores, especially across glacial/interglacial transitions. We hope to use this information as input into climate models to reconstruct past storm tracks over Antarctica and determine how atmospheric circulation changes across climatic transitions.

The availability of material from the 554-meter (m) Polar Ice Coring Office ice core drilled at the Taylor Dome (77°47.7'S 158°43.1'E, elevation 2,400±20 m) during the 1993–1994 field season (Groote, Steig, and Stuiver 1994) permitted us to address some of these questions. All samples were taken below the firn-to-glacial-ice transition, which occurs between 70 and 80 m. Ages given here are interpolated ages of the midpoint of each sample based on an age model derived from the isotopic oxygen-18 ( $\delta^{18}O$ ) data by Steig

(1996). The core spans approximately the last 155,000 years. Sample intervals vary because our material was mostly remnants from other studies. Melted samples, ranging in volume from 250 to 2,000 milliliters, were filtered through a Millipore system with 1.2-micron perforated “MF Nuclepore” filters at the National Ice Core Laboratory (NICL) in Denver, Colorado. Sections of dried filters were placed on glass cover slips, made transparent with acetic acid, and mounted on standard glass slides. Each slide was examined in its entirety at 1,000×. Some workers may wonder whether our samples are contaminated and therefore unreliable indicators of atmospheric diatom transport. If contamination occurred at NICL or in our laboratory, we would expect to see a significant extra-antarctic component in the diatom assemblage. Because our samples are all dominated by typical antarctic species, we conclude that our samples were not contaminated after collection.

Diatoms are a small and sporadic constituent of snow falling at Taylor Dome, in a patchy pattern through both space and time (figure). Six marine and 45 nonmarine taxa were recorded. Abundances range from nil to over 660 specimens in individual samples. Of the 78 samples, 26 (33.3 per-



Stratigraphy and diatom distributions in the Taylor Dome ice core: A.  $\delta^{18}\text{O}$  curve (Steig 1996); B. diatom abundance per liter of melted ice; C. percent marine diatoms; D. percent nonmarine diatoms.

cent) contain more than 75 percent marine specimens, 16 (20.5 percent) are more than 75 percent nonmarine, 15 (19.2 percent) have intermediate mixtures of marine and nonmarine taxa, and the remaining 21 (26.9 percent) are barren. Lowest abundances occur during glacial intervals (isotope stages 3–5), and higher abundances occur during interstadials (isotope stages 5b, 5d, and 6). Highest values occur at 256.2 m (5,615 years ago: 497.25 specimens per liter, which seems anomalously high) and 542 m (approximately 142,000 years ago: 33.75 specimens per liter). Most species reported were also present in the South Pole ice core and have also been reported by us and/or other workers from a variety of other antarctic sites (Kellogg and Kellogg 1996). No uniquely extra-antarctic taxa were recorded.

The antarctic surface wind field is dominated by katabatic flow, outward and down from the domes of East and West Antarctica toward the sea (Parish and Bromwich 1987). Storms tend to track around the continent. Occasionally, large storms break through the circumpolar flow and penetrate to the South Pole (Bromwich and Robasky 1993). Taylor Dome diatoms were probably deposited by these episodic events, which occur today a few times annually. Specific provenances for our diatoms cannot be identified because the individual species have been reported from a number of antarctic locations (Kellogg and Kellogg 1996). Marine diatom-bearing sediments are widespread in the dry valleys area, especially where Late Wisconsin Ross Sea Drift (Stuiver et al., 1981, pp. 319–436; Denton et al. 1989) is exposed. The marine taxa reported here are present in most samples of this drift that we have examined; similar diatomaceous sediments probably exist elsewhere around Antarctica. That most marine specimens have been reworked from subaerially exposed sediments is further suggested by the high degree of dissolution and breakage exhibited by the marine specimens. Nonmarine diatoms are also widespread in the dry valleys, in subaerially exposed deposits, and in most lakes, ponds, and seasonal melt pools. Many of these water bodies are ephemeral or display fluctuating water levels. Complete or partial desiccation exposes fossil material for transport by winds as described above.

The Taylor Dome diatom distribution pattern suggests that aeolian diatom transport depends on conditions in the

source region(s). During glacials, with an expanded west antarctic ice sheet covering most of the Ross Sea continental shelf (Stuiver et al. 1981, pp. 319–436; Kellogg, Hughes, and Kellogg 1996), the nearest open water source for marine diatoms would be far offshore. Extent of ice-free areas in the dry valleys also would have been limited by lobes of grounded ice pushing into the valleys from the sea and by large ice-covered lakes (e.g., Glacial Lake Washburn in Taylor Valley: Stuiver et al. 1981, pp. 319–436), greatly reducing possible sources for reworked marine diatoms.

We thank Eric Steig, Pieter Grootes, Ken Taylor, Joan Fitzpatrick, Ellen Moseley-Thompson, Jeff Hargreaves, and Todd Hinckley for assistance in ice core sampling. Eric Steig filtered some of the samples and provided the oxygen isotope data. Ben Carter of Corning-Costar supplied modified Nuclepore filters. Financial support was provided by National Science Foundation grant OPP 93-16306.

## References

- Bromwich, D.H., and F.M. Robasky. 1993. Recent precipitation trends over the polar ice sheets. *Meteorology and Atmospheric Physics*, 51, 259–274.
- Denton, G.H., J.G. Bockheim, S.C. Wilson, and M. Stuiver. 1989. Late Wisconsin and early Holocene glacial history, inner Ross embayment, Antarctica. *Quaternary Research*, 31(2), 151–182.
- Grootes, P.M., E.J. Steig, and M. Stuiver. 1994. Taylor Ice Dome study 1993–1994: An ice core to bedrock. *Antarctic Journal of the U.S.*, 29(5), 79–81.
- Kellogg, D.E., and T.B. Kellogg. 1996. Diatoms in South Pole ice: Implications for eolian contamination of Sirius Group deposits. *Geology*, 24(2), 115–118.
- Kellogg, T.B., T. Hughes, and D.E. Kellogg. 1996. Late Pleistocene interactions of east and west antarctic ice flow regimes: Evidence from the McMurdo Ice Shelf. *Journal of Glaciology*, 42(142), 486–500.
- Parish, T.R., and D.H. Bromwich. 1987. The surface windfield over the antarctic ice sheets. *Nature*, 328, 51–54.
- Steig, E.J. 1996. 10-Beryllium in the Taylor Dome ice core: Applications to antarctic glaciology and paleoclimatology. (Ph.D. thesis, University of Washington, Seattle, Washington.)
- Stuiver, M., G.H. Denton, T.J. Hughes, and J.L. Fastook. 1981. History of the marine ice sheet in West Antarctica during the last glaciation: A working hypothesis. In G.H. Denton and T.J. Hughes (Eds.), *The last great ice sheets*. New York: Wiley-Interscience.

# Acquisition of borehole temperature measurements from Taylor Dome and the dry valleys for paleoclimate reconstruction

GARY D. CLOW, *Climate History Program, U.S. Geological Survey, Denver, Colorado 80225*  
EDWIN D. WADDINGTON, *Geophysics Program, University of Washington, Seattle, Washington 98195*

Subsurface temperature transients resulting from past climatic changes are often still present at depth within ice sheets and permafrost. Once measured in deep boreholes, these temperature transients can be used to reconstruct past climatic changes using geophysical inverse methods. This paleoclimate reconstruction technique, known as “borehole paleothermometry,” can provide the most accurate estimates of past temperatures on the Earth’s surface. Borehole temperature (BT) data can also be used to calibrate the isotopic oxygen-18 ( $\delta^{18}\text{O}$ ) proxy-temperature method for an ice core site as was recently done by Cuffey et al. (1995) for the Greenland Ice Sheet Project 2 (GISP2).

## Borehole temperatures

During the 1994–1995 and 1995–1996 field seasons, we acquired high-precision temperature measurements in the 554-meter (m) deep borehole (TD-D) recently drilled through the ice at Taylor Dome (77°50'S 159°00'E). This work is one component of the multifaceted Taylor Dome Ice Core project (see Grootes, Steig, and Stuiver 1994; Waddington, Morse, and Clow 1994). The BT data will be used to reconstruct paleoclimate through borehole paleothermometry and calibrate the  $\delta^{18}\text{O}$  paleothermometer for this site. During the last two field seasons, we also measured temperatures in boreholes on the Taylor Glacier and in Taylor Valley. The Taylor Dome/Taylor Valley transect lies in the climatic transition between the cold polar plateau and the maritime Ross Sea.

Temperatures below the firn/ice transition (74 m) were successfully measured in the TD-D borehole both before and after the installation of a “convective-damping” system; this system reduced the thermal noise associated with convective eddies in the borehole fluid to less than our system’s sensitivity, 0.14 millikelvins (mK). To obtain temperatures in the firn layer, we monitored temperatures at selected depths in the 130-m dry corehole (TD-C) located 50 m from TD-D. While monitoring at each depth, small temperature fluctuations (<30 mK) were detected that correlate very well with atmospheric pressure changes recorded on the surface (figure 1; Clow, Saltus, and Waddington in press). Since the TD-C corehole had been carefully sealed from air intrusion at the surface, the observed temperature fluctuations are due to the influence of atmospheric pressure variations on the firn layer. Temperature fluctuations in the 100-m corehole (TD-B) on the Taylor Glacier (77°38'S 159°39'E) are much smaller than at TD-C due to the reduced firn permeability at TD-B. The BT data indicate the present mean-annual surface temperature is  $-41.23^\circ\text{C}$  at Taylor Dome and  $-36.37^\circ\text{C}$  on the Taylor Glacier at TD-B.

During the early 1970s, several deep boreholes were drilled in the McMurdo Dry Valleys under the Dry Valleys Drilling Project (DVDP). Unfortunately, only one of the DVDP boreholes (11, near the Commonwealth Glacier) remains open below 75 m at this time. A comparison of our DVDP 11 temperature measurements with those obtained 20 years ago by Decker and Bucher (1977) shows that mean-annual temperatures in lower Taylor Valley have increased about 1 K over the last several decades (figure 2). This is consistent with the increase in summer temperatures suggested by rising lake levels in the McMurdo Dry Valleys (Wharton et al. 1992).

## Vertical strain rates at Taylor Dome

To interpret the BT data from Taylor Dome accurately in terms of past climatic changes, it is essential to understand the local ice dynamics. To measure the vertical component of the ice flow, metal bands were emplaced at 5-m intervals along the TD-C corehole. A down-hole video camera was then used to determine the position of the bands during January 1995 and January 1996. Vertical velocities and strain rates have been determined from the change in band positions during the intervening 12 months.

## Microclimate zones at Taylor Dome

The primary goal of the BT logging program is to determine past temperatures on the surface of Taylor Dome. Mean-annual surface temperatures presently vary by at least 5 K

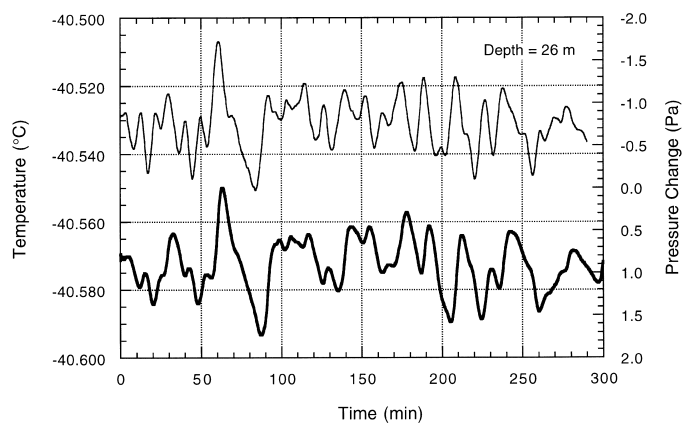


Figure 1. Temperatures recorded at 26 m while incrementally logging the 130-m TD-C corehole at Taylor Dome, Antarctica (lower curve). Atmospheric pressure changes (upper curve) were simultaneously recorded 10 centimeters below the surface of the snow adjacent to the borehole. The temperature fluctuations observed in the borehole correlate well with atmospheric pressure changes. (Pa denotes pascals).

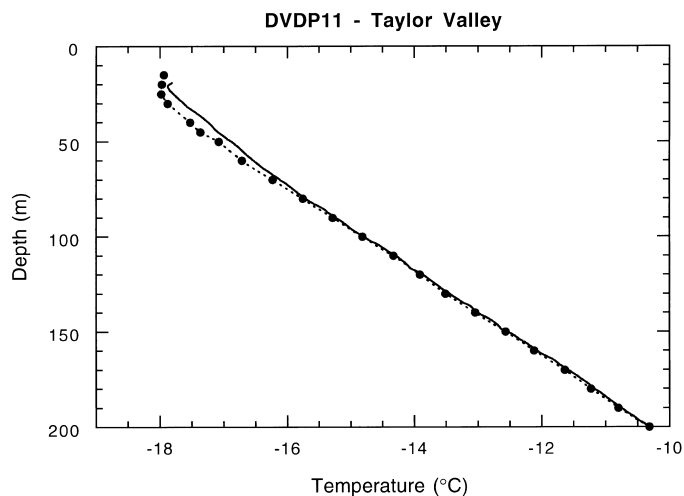


Figure 2. Temperatures recorded in the DVDP 11 borehole (Taylor Valley) during 1977 by Decker and Bucher (dots) and during December 1995 (solid line). The temperature increase in the upper 70 m of the hole since 1977 indicates mean-annual temperatures have increased about 1 K in lower Taylor Valley over the last several decades.

near Taylor Dome, however, because of microclimatic effects (Waddington and Morse 1994). This occurs between sites differing in elevation by only 65 m. Since 5 K represents 30 percent of the accepted ice-age/interglacial temperature change, it is essential to understand whether these microclimate zones are stable or whether they move over time. If the microclimate zones drift with time, they would leave a “trail” in the temperatures recorded in the boreholes, even though the shifts might not represent real shifts in regional climate.

We currently have four automatic weather stations recording wind speed, wind direction, and air and snow tem-

peratures at several levels. Preliminary data indicate that the temperature microclimates are associated with winter-time differences in the near-surface thermal inversion layer. We plan to examine advanced very-high-resolution radiometer (AVHRR) thermal infrared imagery to learn more about these microclimates and their possible impact on paleoclimate interpretations.

We thank many individuals in the U.S. Antarctic Program and also our invaluable field assistants, Jason Bailey, Susan Douglass, and Bob Hawley. This research was supported by National Science Foundation grant OPP 92-21261 and by the U.S. Geological Survey’s Climate History Program.

## References

- Clow, G.D., R.W. Saltus, and E.D. Waddington. In press. A new high-precision borehole temperature logging system used at GISP2, Greenland, and Taylor Dome, Antarctica. *Journal of Glaciology*.
- Cuffey, K.M., G.D. Clow, R.B. Alley, M. Stuiver, E.D. Waddington, and R.W. Saltus. 1995. Large arctic temperature change at the Wisconsin-Holocene glacial transition. *Science*, 270, 455–458.
- Decker, E.R., and G.J. Bucher. 1977. Geothermal studies in Antarctica. *Antarctic Journal of the U.S.*, 12(4), 102–104.
- Grootes, P.M., E.J. Steig, and M. Stuiver. 1994. Taylor Ice Dome study 1993–1994: An ice core to bedrock. *Antarctic Journal of the U.S.*, 29(5), 79–81.
- Waddington, E.D., and D.L. Morse. 1994. Spatial variations of local climate at Taylor Dome, Antarctica: Implications for paleoclimate from ice cores. *Annals of Glaciology*, 20, 219–225.
- Waddington, E.D., D.L. Morse, and G.D. Clow. 1994. Glacier geophysical studies at Taylor Dome: Year 4. *Antarctic Journal of the U.S.*, 29(5), 82–84.
- Wharton, R.A., Jr., C.P. McKay, G.D. Clow, D.T. Andersen, G.M. Simmons, Jr., and F.G. Love. 1992. Changes in ice cover thickness and lake level of Lake Hoare, Antarctica: Implications for local climatic change. *Journal of Geophysical Research*, 97, 3505–3513.

# Relation of ice face melting structures to oceanic characters using remotely operated vehicle observations, Mackay Glacier Tongue, Granite Harbor

JUNYU LIU and ROSS D. POWELL, *Department of Geology, Northern Illinois University, DeKalb, Illinois 60115*

The processes occurring between the base of ice shelves and the underlying ocean seem to play an important role in the formation of Antarctic Bottom Water and in the mass balance of large ice shelves in Antarctica (MacAyeal 1984; Jacobs et al. 1992). In an effort to help understand these processes, fieldwork was conducted at Mackay Glacier Tongue, Granite Harbor (76°58'S 162°24'E), during the austral summers of 1991, 1993, and 1994 using a submersible remotely operated vehicle (ROV) (figure 1).

Mackay Glacier Tongue is an outlet glacier that drains from the east antarctic ice sheet into the Ross Sea. Among the

instruments aboard the ROV are black-and-white and color video cameras and a conductivity-temperature-depth profiler. Oceanographic data were continuously measured and recorded every 5 seconds. Dives were conducted in the austral summers of 1991, 1993, and 1994, and this article reports our data from the 1991 and 1994 seasons.

Oceanographic data at all diving sites show an increasing trend in salinity and temperature with depth except site 1 of 1994 (figure 2), but some data collection in 1991 dives was unsuccessful. Temperature and salinity values define the water mass around Mackay Glacier Tongue as a deep core of

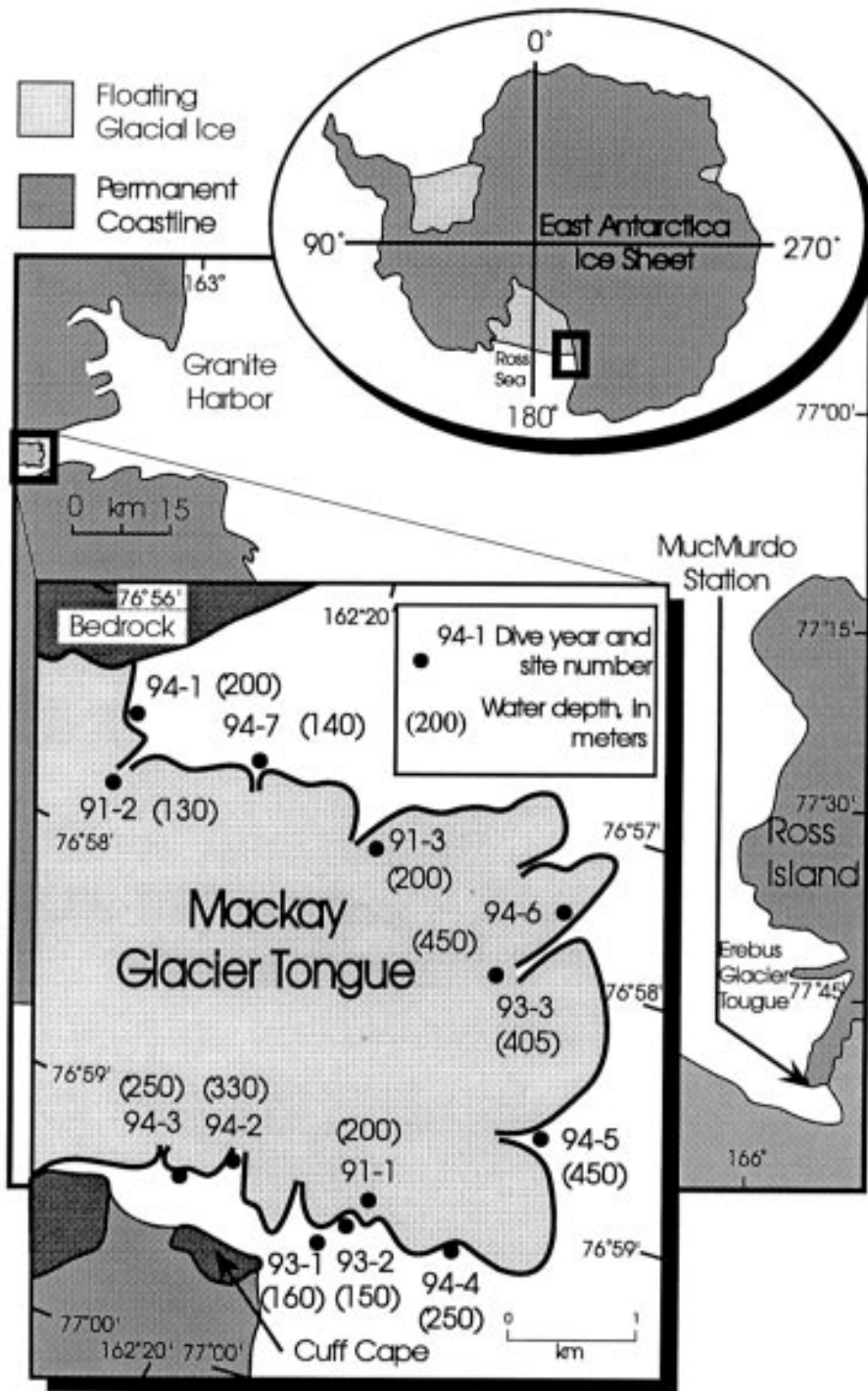


Figure 1. Location of Mackay Glacier Tongue and dive sites.

Ice Shelf Water (cf., Jacobs, Fairbanks, and Horibe 1985, pp. 59–85). Ice Shelf Water is the result of the formation of High Salinity Shelf Water during winter months and the subsequent significant melting of an ice shelf caused by the inflow of High Salinity Shelf Water under the ice shelf penetrating to the grounding line area (MacAyeal 1984; Jacobs et al. 1992). The melting water plume rises and incorporates ambient sea water gradually to form Ice Shelf Water. During the process, it may reach its freezing point and precipitate frazil ice. Frazil ice is visually observed at Mackay Glacier Tongue, and on

many dives, the upper part of the temperature profile has an inflection point above which temperature decreases when depth increases but below which temperature increases with depth (figure 2). This inflection point is explained by the heat release due to frazil ice precipitation. The depth of the colder node often coincides with the base of the frazil ice layer, which at Mackay Glacier Tongue varies from 20 to 40 meters.

Fine water-stratification features in the water column near Mackay Glacier Tongue were also present where steplike structures were observed on many temperature and salinity profiles of 1994 dives at Mackay Glacier Tongue (figure 2). Their thickness ranges from 10 to 50 meters, which is comparable to that found at Erebus Glacier Tongue (Jacobs et al. 1981). The magnitude of temperature and salinity changes that define the fine structures, however, are much lower than at Erebus Glacier Tongue. At Erebus Glacier Tongue, most of the significant fine structures occurred above a depth at which the *in situ* temperature is above the surface sea-water freezing point. Almost all dives at Mackay Glacier Tongue, however, have temperatures less than that (figure 2). Fine structures were not observed in 1991 dives.

Recent study of the melting behavior of ice in sea water shows that such fine steplike structures are produced in temperature and/or salinity profiles depicted by a local sea-water stratification (Jacobs et al. 1981). In this study, we have observed ice basal melting structures associated with these water column structures (figure 3). They vary in orientation and size, and most have well-rounded forms. Scalloped surfaces are the most common feature. Others include vertical runnels and horizontal ledges. Relief on scalloped surfaces can reach about 1 meter but usually is several centimeters

to 30 centimeters. Diameters of the scallops range from less than 10 centimeters to more than 1 meter. Runnels are better developed in deeper water tending to form in groups parallel to each other. They are usually a few to tens of meters long with a depth of several centimeters to tens of centimeters; wavelengths vary but usually are less than 50 centimeters. Ledges have greater relief than scalloped surfaces and runnels. They may extend out several meters from the vertical ice wall above them. Melting structures seen during 1991 dives were better developed than those of 1994. In some 1991 dives, with

increasing water depth, the dominant melting structures changed from scalloped surfaces to runnels and ridges. Conversely, scalloped surfaces were the main feature in 1994 dives, and they appeared to be smaller and their relief was less than their counterparts of 1991.

The observation of the melt structures on the ice face and fine structures in the water column at Mackay Glacier Tongue support the idea that the local oceanographic characteristics influence the melting behavior of glacier ice, and the ice melting, in turn, alters the details of water column stratification. Quantitative analysis is continuing, and we hope it will provide a better understanding of the interactive relation between glacier ice and the ocean.

This research was supported by National Science Foundation grant OPP 92-19048 to Ross D. Powell. Thanks to Steve Bograd, Mike Dawber, Lewis Hunter, Tom Hooyer, Jim McInnes, and John McNamee for their help as members of the field team; to the New Zealand Antarctic Programme (Alex Pyne and Peter Barrett) for helping with 1991 data collection; and to the National Science Foundation, Antarctic Support Associates, and U.S. Navy personnel for their valuable support.

### References

Jacobs, S.S., H.E. Huppert, G. Holdsworth, and D.J. Drewry. 1981. Thermohaline steps induced by melting of the Erebus Glacier Tongue. *Journal of Geophysical Research*, 86(C7), 6547-6555.

Jacobs, S.S., R.G. Fairbanks, and Y. Horibe. 1985. Origin and evolution of water masses near the antarctic continental margin: Evidence from  $H_2^{18}O/H_2^{16}O$  ratios in sea water. In S.S. Jacobs, *Oceanology of the antarctic Continental Shelf* (Antarctic Research Series, Vol. 43). Washington, D.C.: American Geophysical Union.

Jacobs, S.S., H.H. Hellmer, C.S.M. Doake, A. Jenkins, and R.M. Frolich. 1992. Melting of ice shelves and the mass balance of Antarctica. *Journal of Glaciology*, 38(130), 375-387.

MacAyeal, D.R. 1984. Thermohaline circulation below the Ross Ice Shelf: A consequence of tidally induced vertical mixing and basal melting. *Journal of Geophysical Research*, 89(C1), 597-606.

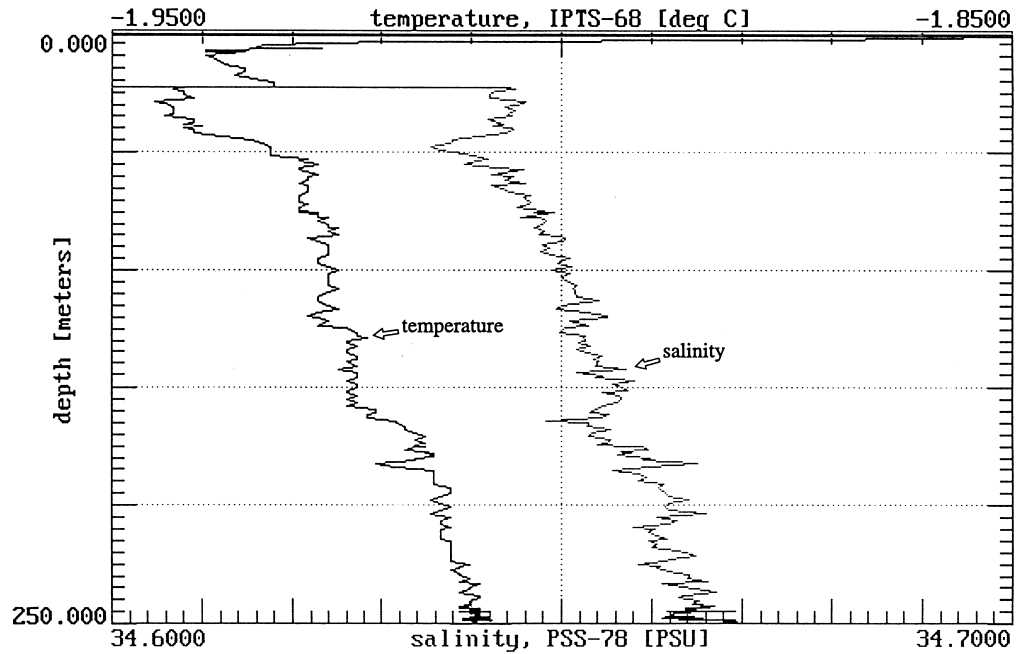


Figure 2. Temperature and salinity profiles of dive 7 at site 2, 1994. (IPTS-68 denotes International Practical Temperature Scale, 1968. PSS-78 denotes Practical Salinity Scale, 1978. PSU denotes practical salinity units.)

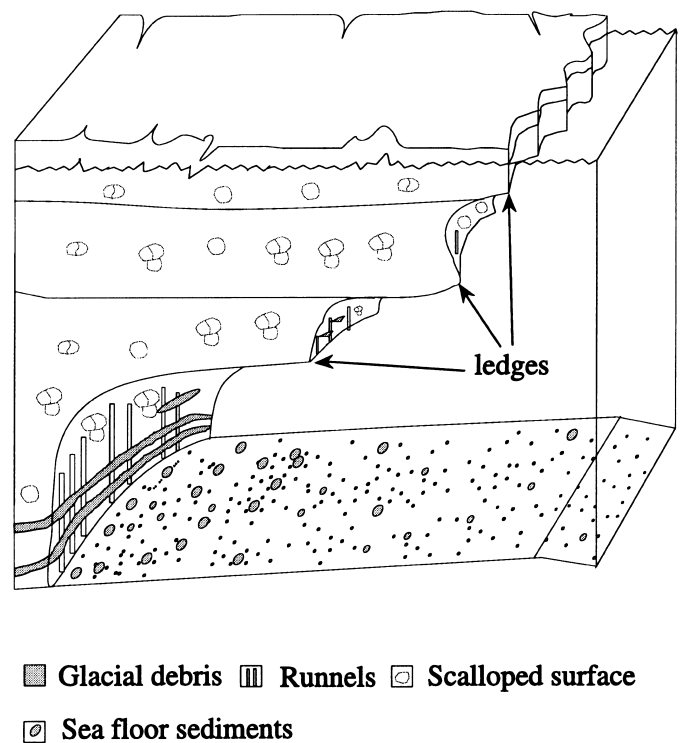


Figure 3. Three-dimensional sketch (not to scale) of Mackay Glacier Tongue showing major melt structures and their distribution.

# On the Mertz and Ninnis Glaciers, eastern Antarctica

GERD WENDLER, KRISTINA AHLNÄS, and CRAIG LINGLE, *Geophysical Institute, University of Alaska, Fairbanks, Alaska 99775*

In 1995, we participated in the cruise (USCGC *Polar Star*) from Australia to McMurdo, during which the coastal automatic weather stations were serviced in Adélie and King George Land. The main topic of our study is the katabatic wind and its interaction with sea ice. Wendler et al. (in preparation) reported on the winds in the coastal area; Wendler, Gilmore, and Curtis (in preparation) described their interaction with sea ice and the formation of coastal polynyas; and Hauser et al. (in preparation) discussed the surface energy budget of sea ice as function of meteorological parameters. Hence, instead of reporting in detail on one of the above topics, we concentrate here on two large glacier tongues that extend substantially across the coastline of King George Land. We were able to study these by remote sensing [synthetic aperture radar (SAR), JERS-1]. The tongue of the Mertz Glacier (figure 1) is in the state of advance, whereas the Ninnis Glacier tongue is retreating. Both glaciers display distinctive surface structure and the form of the glacier tongues indicates that they are floating.

The Mertz and Ninnis Glaciers are prominent features; the tongue of the Mertz Glacier, presently the larger of the two, extends some 95 kilometers (km) into the ocean and has an average width of about 40 km.

This area of Antarctica was first explored by Sir Douglas Mawson during his heroic trip between 1911 and 1914. Mawson established his main camp at Cape Denison (67.02°S 142.68°E) in Commonwealth Bay. Mawson's crew were also able to map the coastline and the outline of these two glaciers.

An Australian map (SQ55-56) of this area, issued in 1971, was based on aerial photography of 1961–1962 and again depicted the outline of these two glacier tongues.

In 1993, SAR imagery was obtained for the first time because, in contrast to ERS-1, JERS-1 has limited onboard tape-recording capabilities. Observations were carried out over eastern Antarctica, and the data were downloaded at the Geophysical Institute at the University of Alaska, Fairbanks. JERS-1 measures in the L-band, has a swath width of 75 km, and a pixel spacing of 12.5 meters in full resolution. Compared to more conventional satellite imagery, radar images are unaffected by weather and lighting conditions.

In figure 2, the outlines of the glacier tongues from these three sources were combined to obtain long-term changes in their aerial extent. The table lists the values found by measuring the size of the glacier tongues that extend out from the coastline.

The tongue of the Mertz Glacier has increased substantially in this century. It more than doubled its size, from about 3,830 km<sup>2</sup> in 1913 to about 8,100 km<sup>2</sup> presently. For the earlier part of the century, the glaci-

er tongue mostly broadened, but since 1962 the glacier tongue has advanced some 37 km as well.

The behavior of the Mertz Glacier tongue is in sharp contrast to the Ninnis Glacier tongue. Here, we observe an extraordinary retreat since 1913; during the 80-year period, the glacier tongue retreated 110 km, and its area was reduced to about one third of its original size. Most of the retreat was observed in the earlier part of the century. From 1913 to 1962, it retreated some 90 km, but even since then its size has been reduced substantially. Large decreases in size can be understood if a glacier tongue is freely floating, and large icebergs separate from it.

The sum of the area of the two glaciers (table) indicates that few losses or gains have occurred since 1913; the observed 3.6 percent increase in aerial extent is within the accuracy of the measurements. The behavior of these two glaciers, lying next to each other in the same climatic zone,



Figure 1. SAR (JERS-1) image of the tongue of the Mertz Glacier. Note the particular cellular structure on the glacier surface. North is 32° to the right.

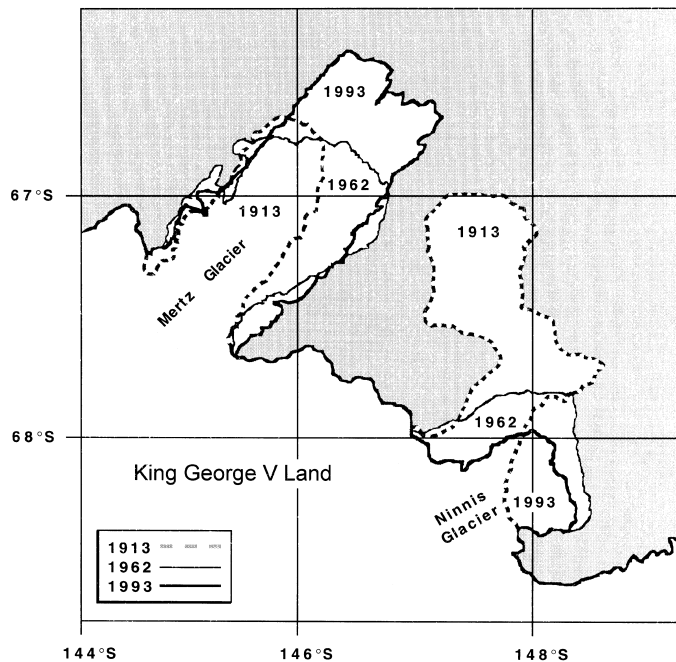


Figure 2. The position of the Mertz and Ninnis Glacier tongues in 1912–1913, 1962, and 1993.

shows again how difficult it is to relate the behavior of advances or retreats of floating glacier tongues to climatic change. A second SAR image of the Mertz glacier tongue some 18 months later enabled us to determine the velocity of the glacier tongue by electronically subtracting the two images from each other. The annual movement was determined as

#### Size<sup>a</sup> of the Mertz and Ninnis Glacier tongues

Glacier	1913		1962		1993	
	Size	Percent	Size	Percent	Size	Percent
Mertz	3,830	100.0	5,920	154.6	8,100	211.3
Ninnis	6,060	100.0	3,970	65.5	2,150	35.4
Both	9,890	100.0	9,890	100.0	10,250	103.6

<sup>a</sup>In square kilometers.

about 1.2 km. This is very close to the value of the advance of the tip of the tongue since 1963.

For more details, refer to Wendler, Ahlnäs, and Lingle (in press).

#### References

- Hauser, A., G. Wendler, U. Adolphs, and M. Jeffries. In preparation. Energy exchange in early spring over sea ice in the Pacific sector of the southern ocean. *Journal of Geophysical Research*.
- Wendler, G., K. Ahlnäs, and C. Lingle. In press. On the Mertz and Ninnis Glacier, eastern Antarctica. *Journal of Glaciology*.
- Wendler, G., D. Gilmore, and J. Curtis. In preparation. On the formation of coastal polynyas in the area of Commonwealth Bay, eastern Antarctica. *Atmospheric Research*.
- Wendler, G., C. Stearns, G. Weidner, G. Dargaud, and T. Parish. In preparation. On the extraordinary winds of Adélie Land. *Journal of Geophysical Research*.

## A dark line on the McMurdo Ice Shelf

IAN M. WHILLANS and GORDON S. HAMILTON, *Byrd Polar Research Center, Ohio State University, Columbus, Ohio 43210-1002*

A SPOT satellite image of the McMurdo region acquired in December 1994 reveals a dark line of the McMurdo Ice Shelf parallel to the calving front (figure).

A first thought was that this line is the trace of a crevasse and a precursor of a major calving event. The dark line does not appear on earlier images or photographs. The operational importance of the line arises because it crosses the road that connects McMurdo Station and Scott Base with Williams Field Skiway. A calving event along the line would make access to and from the skiway considerably more difficult.

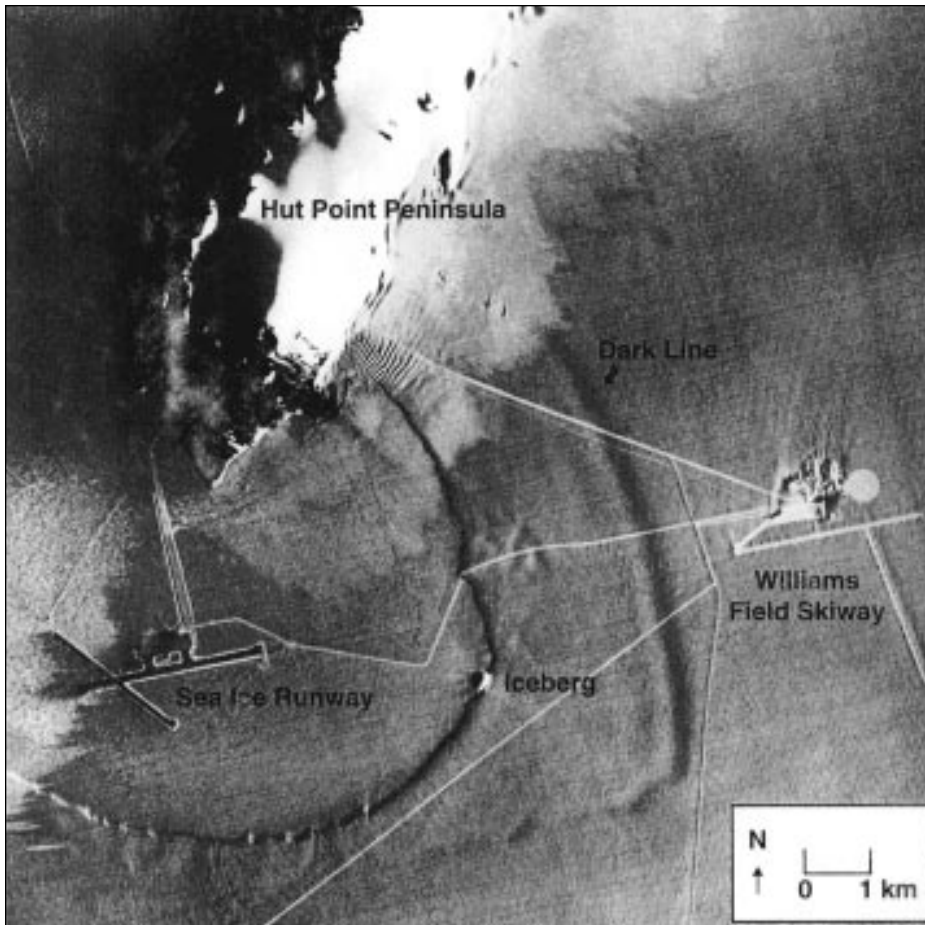
An alternative explanation is that the line may be a step in surface elevation due to a collapse of firn seaward of the line caused by brine infiltration (Kovacs et al. 1982). These types of fronts have been observed up to 15 kilometers (km) from the outer edge of the ice shelf (Morse and Waddington 1994). Perhaps the snow surface seaward of the dark line has

collapsed because of the weight of brine or because of weakening of the firn structure by percolating sea water.

Neither hypothesis can be tested from the imagery alone. A field program was undertaken in October and November 1995 to determine if a crevasse is opening at the site.

#### Field procedure

Strain grids were installed across the dark line and surveyed twice using global positioning system (GPS) methods. If the dark line is due to a sagging crevasse bridge, large strain rates are expected across the line. The dark line should be in the same position with respect to the ice edge as it appears in the image. Moreover, surface elevation profiles should show a depression. If the line is caused by infiltrating brine, surface elevations will show a step rather than a depression; horizontal strain rates will not be especially large at the line; and the



Annotated SPOT panchromatic image (ground resolution 10 meters) acquired 1 December 1994. The mysterious feature investigated is the dark line parallel to the ice shelf front.

position of the line will likely have migrated since the time of the image.

### Results

The methods and interpretation are described in Whillans, Merry, and Hamilton (in press). The results do not support the interpretation of the dark line as the trace of an opening crevasse. Strain rates across it are too small for an opening crevasse, and no sagging bridge is evident. Moreover, the feature is moving with respect to the ice. The concern raised by initial interpretations of the image can now be allayed.

Most of the observations fit the model of the line marking the limit of firn collapse due to brine infiltration. These observations include the shape of the surface, the migration of the feature and the simple pattern of horizontal strain rates.

Unresolved by this study is the cause of the bright line just seaward of the dark line observed on the image. This bright line was interpreted to be the far side of a sagging crevasse bridge, but elevation surveys show only a very minor reverse slope, which cannot account for the bright line on the image. We suggest that the reverse slope present in December 1994 is a transient feature that was no longer present in October 1995.

A new discovery is that major mechanical control on the ice shelf is compression originating at Dailey Islands. These islands lie some 40 km west of the study area. The ice shelf is losing contact with the islands; only two of the original six Dailey Islands now contribute to drag (Gow and Govoni 1994). The islands interact most directly with ice from Koettlitz Glacier, which in turn blocks the McMurdo Ice Shelf. It is important to continue to monitor the interaction of the ice shelf with Dailey Islands. Loss of contact with the islands could have major consequences to the skiway.

Fieldwork was conducted by Gordon Hamilton, Erik Venteris, and Ian Whillans, who received support from National Science Foundation grant OPP 95-28608.

### References

- Gow, A.J., and J.W. Govoni. 1994. An 80-year record of retreat of Koettlitz Ice Tongue, McMurdo Sound, Antarctica. *Annals of Glaciology*, 20, 249-253.
- Kovacs, A., A.J. Gow, J.H. Cragin, and R.M. Morey. 1982. *The brine zone in the McMurdo Ice Shelf, Antarctica* (CRREL Report 82-39). Hanover, N.H.: Cold Regions Research and Engineering Laboratory.
- Morse, D.L., and E.D. Waddington. 1994. Recent survey of brine infiltration in McMurdo Ice Shelf, Antarctica. *Annals of Glaciology*, 20, 215-218.
- Whillans, I.M., C.J. Merry, and G.S. Hamilton. In press. Investigation of a possible crevasse near the main airstrip on McMurdo Ice Shelf. *Annals of Glaciology*.

# Deglacial chronology of the western Ross Sea

BRENDA L. HALL, *Department of Geological Sciences, University of Maine, Orono, Maine 04469-5711*

GEORGE H. DENTON, *Department of Geological Sciences and Institute for Quaternary Studies, University of Maine, Orono, Maine 04469-5711*

During the last glacial maximum, a grounded ice sheet extended to (or close to) the edge of the continental shelf in the Ross Sea embayment (Stuiver et al. 1981; Anderson et al. 1992). Here we present several independent lines of geologic evidence suggesting that recession of the ice sheet from the western Ross Sea did not occur until 6,600–7,944 years ago as determined by carbon-14 ( $^{14}\text{C}$ ) dating.

A flow line of the ice sheet grounded on the Ross Sea floor extended westward around the northern tip of Ross Island and across McMurdo Sound (figure 1). This ice plugged the mouth of Taylor Valley, damming Glacial Lake Washburn. Blue-green algae that once lived in the lake are now preserved within moraines and deltas that formed in Glacial Lake Washburn. From radiocarbon dates of such algae, we have determined that thick grounded ice blocked the mouth of Taylor Valley between 8,340 and 23,800  $^{14}\text{C}$  years ago. Kenyte erratics in Taylor Valley drift dated at 9,300  $^{14}\text{C}$  years ago confirm the late existence of the flow line crossing McMurdo Sound from Ross Island.

During the last glaciation, extensive closed-basin lakes also existed in Wright and Victoria Valleys (figure 1). We argue that these lakes, along with Glacial Lake Washburn, owe their existence to a grounded ice sheet in the Ross Sea, not only because it physically dammed some lakes but also because its presence is linked to increased meltwater production in the dry valleys. Glacial meltwater production in the dry valleys is sensitive to local radiation, which is highest during clear weather. Beneath a thin ice layer on the surface of the glaciers, solar radiation causes melting along intercrystalline boundaries to a depth of up to 1 meter (Hendy et al. in preparation). A network of drainage channels fed by the intercrystalline meltwater forms on and

just below the glacier surface. This melt process accelerates with long stretches of clear weather because the intercrystalline meltwater does not freeze completely every evening (Hendy et al. in preparation). Today, open water in the adjacent Ross Sea is conducive to the formation of clouds, fog, and snow, which penetrate the dry valleys. Such conditions restrict meltwater production by reducing the length of clear, snowless weather, as well as by covering the glacier snouts with snow that shuts off the melt mechanism. For example, one heavy snowstorm in October 1977 terminated meltwater flow to Lake Vanda for an entire summer (Chinn 1981). The presence of grounded ice in the western Ross Sea would elim-

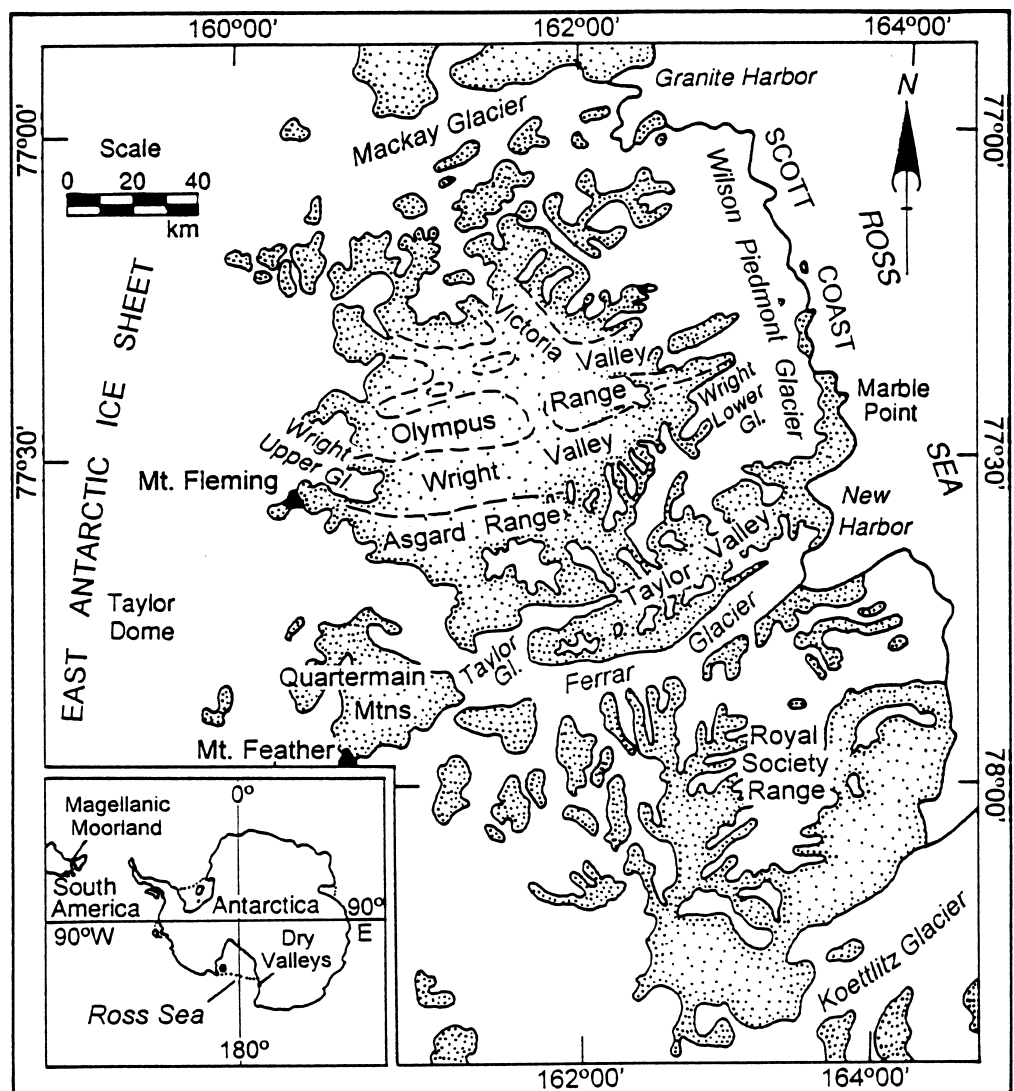


Figure 1. Index map of the dry valleys showing locations named in the text.

inate this local moisture source and thereby increase the length and frequency of clear, snowless weather in the dry valleys. In turn, this would boost radiation-induced meltwater production and, hence, raise lake levels. In this fashion, the high lake levels of late Wisconsin and early Holocene time imply increased aridity and radiative meltwater production tied to an extensive grounded ice sheet in the Ross Sea embayment. High lake levels were sustained 8,340–23,800 <sup>14</sup>C years ago in Taylor Valley; 7,944–25,697 <sup>14</sup>C years ago in Wright Valley; and 8,990–18,900 <sup>14</sup>C years ago in Victoria Valley. In Wright Valley, lake level dropped rapidly after 7,944 <sup>14</sup>C years ago, probably as a response to deglaciation in the western Ross Sea and the consequent penetration of moisture-bearing clouds into the dry valleys. Lakes in the dry valleys have fluctuated since 7,944 <sup>14</sup>C years ago, but they never have come close to attaining the high levels of late Wisconsin-early Holocene time.

Radiocarbon dates of marine shells, as well as of seal remains, afford close minimum ages for deglaciation of grounded ice in the western Ross Sea. The oldest individual shells and barnacles from McMurdo Sound date to 6,550–6,600 <sup>14</sup>C years ago (Stuiver et al. 1981; Kellogg, Kellogg, and Stuiver 1990; Gordon and Harkness 1992; Licht et al. 1996; all dates of marine material are corrected for an estimated 1,200-year marine reservoir effect). In addition, dates of shells from raised beaches and marine deposits along the Scott Coast are no older than 5,580 <sup>14</sup>C years ago (figure 2; Stuiver et al. 1981, pp. 319–436; Hall and Denton in preparation). Our preliminary relative sea-level curve indicates that recession of grounded ice occurred along the Scott Coast south of Cape Ross shortly before 6,400 <sup>14</sup>C years ago (Hall and Denton in preparation; figure 3). The oldest date of an *in situ* shell in raised marine sediments at Terra Nova Bay (350 kilometers north of McMurdo Sound) is 6,305 <sup>14</sup>C years old (Baroni and Orbelli 1991) and affords a minimum age for deglaciation of grounded ice.

In conclusion, we list independent lines of geological evidence from marine and terrestrial data that both suggest deglaciation of the western Ross Sea at 6,600–7,944 <sup>14</sup>C years ago. One implication of such late deglaciation is that the grounded ice sheet in the Ross Sea embayment was relatively impervious to most (76–88 percent) of the 105–121 meters of sea-level rise that accompanied the last

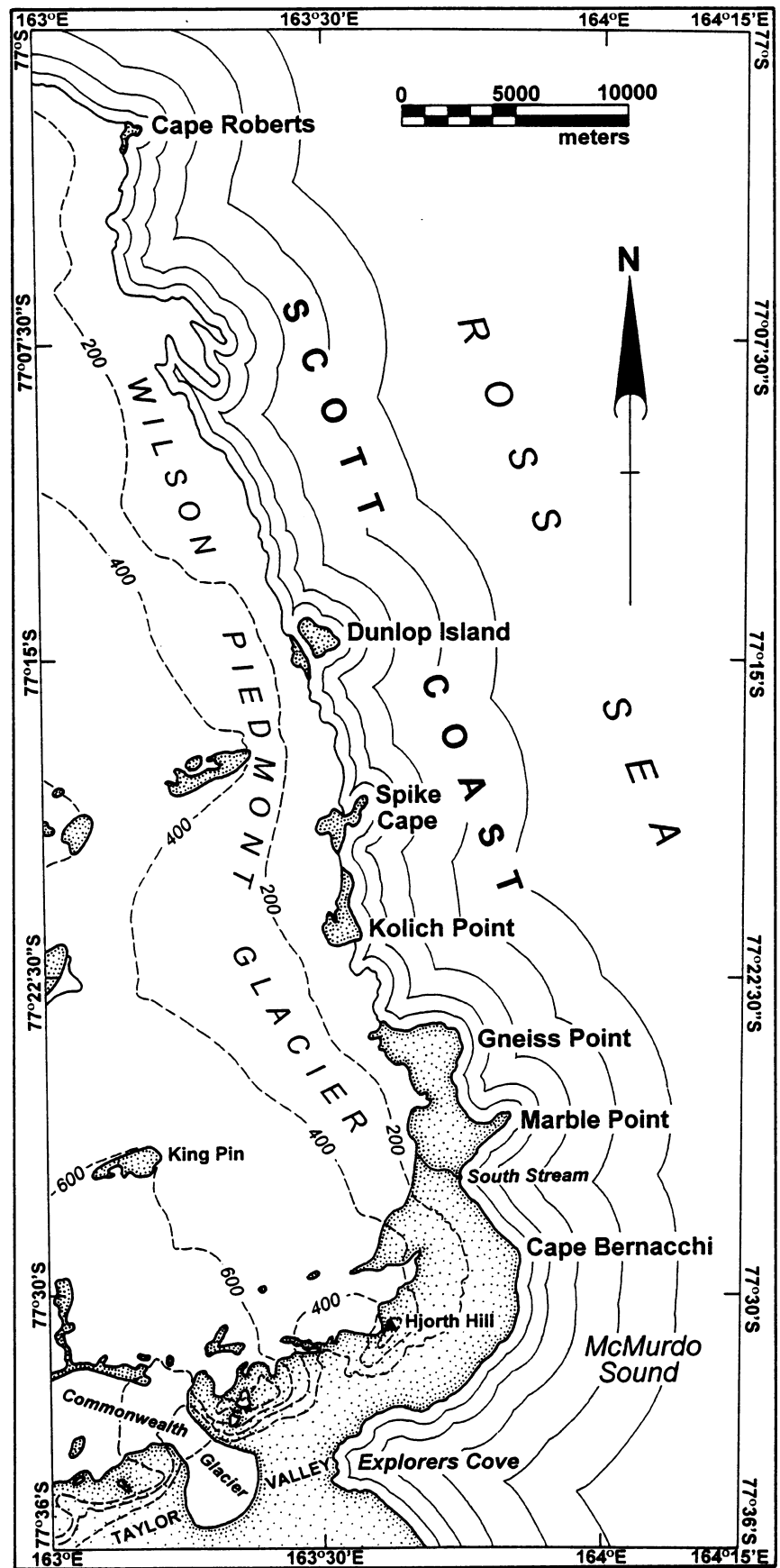


Figure 2. Index map of the Scott Coast showing locations where we obtained samples for the relative sea-level curve shown in figure 3.

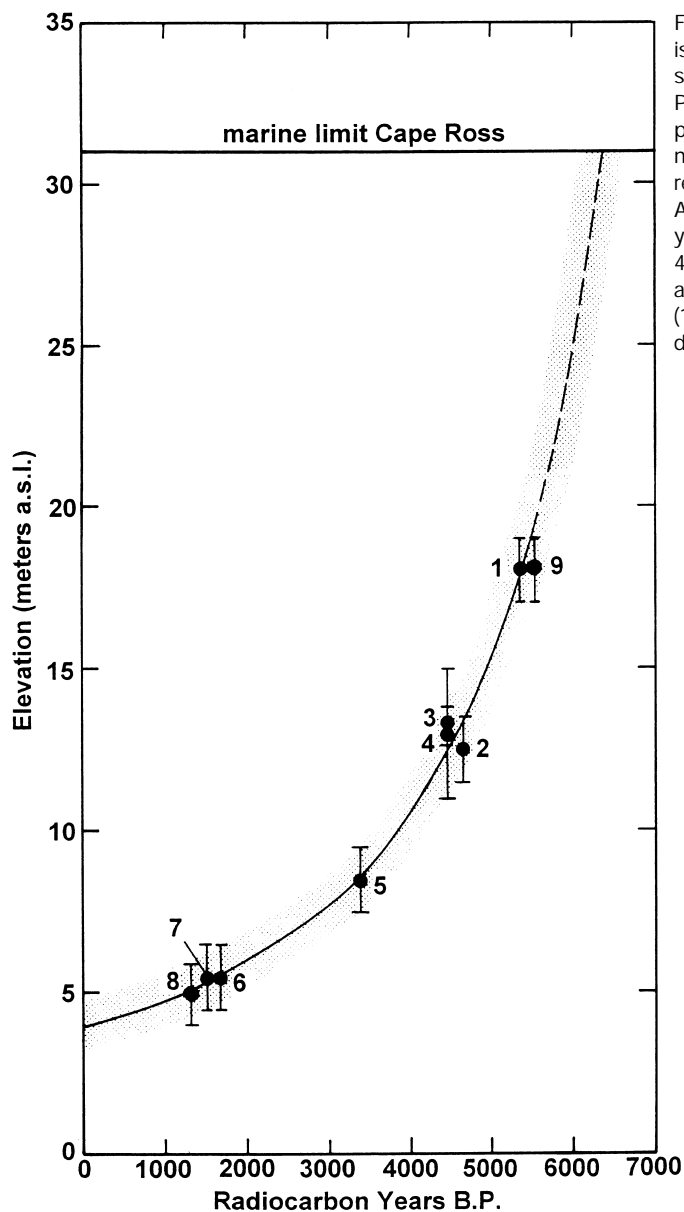


Figure 3. Preliminary relative sea-level curve for the Scott Coast. This curve is based on nine radiocarbon dates of *Adamussium colbecki* shells, seal skin, and elephant seal remains buried within raised beaches at Marble Point, Cape Roberts, Dunlop Island, and near South Stream. Sample 3 (elephant seal remains) was obtained by Nichols (1968), but the rest are from new localities. Dates in brackets are corrected for a 1,200-year marine reservoir effect. Samples: (1) AA-14039: 6,550±97 (5,350) <sup>14</sup>C years ago; (2) AA-14040: 5,864±96 (4,664) <sup>14</sup>C years ago; (3) L-627: 5,650±150 (4,450) <sup>14</sup>C years ago; (4) AA-17345: 5,649±59 (4,449) <sup>14</sup>C years ago; (5) AA-18215: 4,569±57 (3,369) <sup>14</sup>C years ago; (6) AA-18212: 2,820±56 (1,620) <sup>14</sup>C years ago; (7) AA-18213: 2,704±65 (1,504) <sup>14</sup>C years ago; (8) AA-18214: 2,487±51 (1,287) <sup>14</sup>C years ago; (9) AA-18912: 6,780±56 (5,580) <sup>14</sup>C years ago. (B.P. denotes before present; a.s.l. denotes above sea level.)

## References

- Anderson, J.B., S.S. Shipp, L.R. Bartek, and D.E. Reid. 1992. Evidence for a grounded ice sheet on the Ross Sea continental shelf during the late Pleistocene and preliminary paleodrainage reconstruction. In D. Elliot (Ed.), *Contributions to antarctic research III* (Antarctic Research Series, Vol. 57). Washington, D.C.: American Geophysical Union.
- Baroni, C., and G. Orombelli. 1991. Holocene raised beaches at Terra Nova Bay, Victoria Land, Antarctica. *Quaternary Research*, 36, 23–26.
- Chinn, T.J.H. 1981. Hydrology and climate in the Ross Sea area. *Journal of the Royal Society of New Zealand*, 11, 373–386.
- Fairbanks, R.G. 1989. A 17,000-year glacio-eustatic sea level record: Influence of glacial melting rates on the Younger Dryas event and deep-ocean circulation. *Nature*, 342, 637–642.
- Gordon, J.E., and D.D. Harkness. 1992. Magnitude and geographic variation of the radiocarbon content in antarctic marine life: Implications for reservoir corrections in radiocarbon dating. *Quaternary Science Reviews*, 11, 697–708.
- Hall, B.L., and G.H. Denton. In preparation. Holocene deglaciation of the western Ross Sea.
- Hendy, C.H., A.J. Sadler, G.H. Denton, and B.L. Hall. In preparation. Proglacial lake-ice conveyors: A new mechanism for deposition of glacial drift in polar environments.
- Kellogg, T.B., D.E. Kellogg, and M. Stuiver. 1990. Late Quaternary history of the southwestern Ross Sea: Evidence from debris bands on the McMurdo Ice Shelf, Antarctica. In C.R. Bentley (Ed.), *Contributions to antarctic research* (Antarctic Research Series, Vol. 50). Washington, D.C.: American Geophysical Union.
- Licht, K.J., A.E. Jennings, J.T. Andrews, and K.M. Williams. 1996. Chronology of late Wisconsin ice retreat from the western Ross Sea. *Geology*, 24, 223–226.
- Nichols, R.L. 1968. Coastal geomorphology, McMurdo Sound, Antarctica. *Journal of Glaciology*, 7, 449–478.
- Peltier, W.R. 1994. Paleotopography of glacial-age ice sheets. *Science*, 265, 195–201.
- Stuiver, M., G.H. Denton, T.J. Hughes, and J.L. Fastook. 1981. History of the marine ice sheet in West Antarctica during the last glaciation: A working hypothesis. In G.H. Denton and T.J. Hughes (Eds.), *The last great ice sheets*. New York: John Wiley and Sons.

glacial/interglacial transition (Fairbanks 1989; Peltier 1994). By our chronology, only the final pulse of sea-level rise in early Holocene time could have triggered ice retreat from the western Ross Sea. In this case, ice recession to the Siple Coast grounding line may have been due largely to dynamic processes internal to the ice sheet because deglacial sea-level rise was essentially accomplished by mid-Holocene time.

This work was supported by National Science Foundation grant OPP 91-18678. T. Cruikshank and B. Overturf assisted in the field. D. Kelly drafted the figures.

# Subglacial sediment transport and ice-stream behavior

RICHARD B. ALLEY and SRIDHAR ANANDAKRISHNAN, *Earth System Science Center and Department of Geosciences, Pennsylvania State University, University Park, Pennsylvania 16802*

KURT M. CUFFEY, *Department of Geological Sciences, University of Washington, Seattle, Washington 98195*

Ice flowing on a continuous, soft-sediment layer achieves high velocities despite low basal shear stress (e.g., Blankenship et al. 1987) through deformation of that sediment layer. Water-lubricated sliding over the substrate occurs whether or not that substrate is deforming; hence, bed deformation produces higher flow velocities than does sliding by itself. The Siple Coast ice streams of West Antarctica and the ice streams or lobes of the southern margin of the Laurentide ice sheet achieved high velocities with low basal shear stresses through the effects of soft subglacial sediments (e.g., Jenson et al. 1995). Ice streaming is possible although slowed if the soft sediment is locally discontinuous provided the bedrock "sticky spots" are water-lubricated (Rooney et al. 1987; Anandakrishnan and Alley 1994), but loss of that water may stop the rapid motion (Alley et al. 1994).

Continuous or nearly continuous soft-sediment glacier beds are most likely if ice advances over unconsolidated or poorly consolidated sediments. First, sediment generation clearly is easier from softer materials. The difference in abrasion rates between hard and soft materials may be two orders of magnitude (Cuffey and Alley 1996).

In addition, a thickening till layer on bedrock causes slowed abrasion but enhanced till export through deformation. If ice must act through intervening till on the clasts that abrade the bedrock, the abrading clasts can roll part of the time and abrasion is reduced by roughly an order of magnitude (Cuffey and Alley 1996). If a thickened till layer reduces or eliminates sliding of till over its substrate, a further order(s)-of-magnitude reduction in abrasion will result (Cuffey and Alley 1996). In general, abrasion rates beneath till are unlikely to produce till faster than 0.1 millimeter per year except on very soft or unconsolidated rocks (Cuffey and Alley 1996).

Several processes compete to remove subglacial sediment. Beneath warm glaciers with surface melt fed to the bed through moulins, subglacial stream transport can be exceptionally rapid because glaciers concentrate runoff in time and space and provide steep head gradients compared to subaerial streams, and sediment transport increases with head gradient and with runoff (see review by Alley et al. in press). Moulin-fed streams rising out of overdeepenings also can cause rapid sediment entrainment to the ice by freeze-on in response to the decreasing pressure-melting point along flow (Lawson et al. 1996; Strasser et al. 1996). These processes are unlikely to be significant, however, for most of the Antarctic unless storage and release of water in subglacial floods are important because in the absence of surface melt, not enough water is present to transport more than very fine sediment (e.g., Alley 1989).

Several other processes may remove sediment from beneath the antarctic ice sheet and other glaciers (reviewed by Alley et al. in press). One especially, regelation of ice into subglacial sediments, is important based on laboratory and model studies (Iverson and Semmens 1995). Entrainment rates are modeled to depend on basal water pressures, melt rates, and sediment grain size (Iverson and Semmens 1995). Export of sediment produced at a rate of 0.1–1.0 millimeters per year or even higher is likely, provided the sediments are not finer than fine silt (Alley et al. in press).

Thus, it is likely that material eroded from well-lithified bedrock will be entrained by the ice and transported away, rather than accumulating under the ice to form a thick, continuous deformable layer. In contrast, soft sediments can be eroded sufficiently rapidly to produce continuous or nearly continuous deforming layers. We thus expect to see a reasonably close correlation between ice streaming and the presence of sedimentary basins, as is observed (e.g. Rooney et al. 1991, pp. 261–265).

The general increase in continuity of subglacial soft sediment toward the ice margin may be involved in thermal surging, such that cooling may produce surges. Consider the common case of an ice sheet with a moderate surface slope over a thawed internal region, a steep surface slope in a marginal region frozen to bedrock (Weertman 1961), and a thick proglacial sediment accumulation. A cooling may trigger ice advance through sea-level fall or decreased marginal ablation or calving. As the ice thickens over the former margin, the bed there will warm and may thaw from the bedrock. At the same time, the advancing margin may tend to freeze to material over which it flows, maintaining the thawed-interior/frozen-margin pattern. In such a situation, the frozen margin will maintain a steep surface slope and high basal shear stress only if it freezes to bedrock. Otherwise, the sediment pile can deform below the freezing front, yielding the low surface slope of an ice stream.

A cooling-induced ice advance thus may cause a shift from a steep margin and moderate-slope interior to a low-slope margin and moderate-slope interior. This transition can cause mass loss from the ice sheet as a whole and might occur quite rapidly and appear surgelike. It is at least possible that this has relevance to former ice-sheet behavior, including the great discharges of debris in icebergs from the Laurentide ice sheet during Heinrich events, which appear to have occurred following oceanic coolings (Bond et al. 1992).

The coupled behavior of a deforming but slightly discontinuous subglacial till and of a water layer that lubricates sliding over the till and any sticky spots may be quite complex. Iverson et al. (1995) documented that a transient increase in

water pressure forced by moulin drainage through Storglaciaren, Sweden, a glacier with a discontinuous deforming bed, caused a transient decrease in the rate of bed deformation. Presumably, the water caused enhanced separation between ice and till and so faster sliding. The decreased deformation of the till then is explainable as a decreased basal shear stress on it, with force-balance for the glacier maintained by increased side drag or increased drag on sticky spots. Because of differences in roughness characteristics between till and bedrock, sliding over till may be more sensitive to water pressure than is sliding over bedrock (Alley 1989).

It has been hypothesized that ice stream C, West Antarctica, stopped recently because its basal meltwater was diverted to ice stream B (Anandakrishnan and Alley 1994; Alley et al. 1994). If so, and if the Iverson et al. (1995) observations are relevant to the longer times and larger size of the ice-stream situation, then ice stream B now has faster sliding between ice and subglacial till than before the meltwater diversion. The basal shear stress on the till beneath ice stream B then would be less today than before the water diversion because the higher ice velocity will have increased the drag from the ice-stream sides, may have increased the drag from subglacial sticky spots, and may have caused thinning or reduced surface slope and thus reduced driving stress for ice flow. If this decrease in basal shear stress on the till is more important than the softening of the till caused by the increased water supply, as on Storglaciaren, then the deforming layer beneath ice stream B is thinner or deforms more slowly and transports less sediment now than before the water diversion.

This research was supported by National Science Foundation grant number OPP 93-18677.

## References

Alley, R.B. 1989. Water-pressure coupling of sliding and bed deformation: I. Water system. *Journal of Glaciology*, 35(119), 108–118.  
 Alley, R.B., S. Anandakrishnan, C.R. Bentley, and N. Lord. 1994. A water-piracy hypothesis for the stagnation of ice stream C. *Annals of Glaciology*, 20, 187–194.

Alley, R.B., K.M. Cuffey, E.B. Evenson, J.C. Strasser, D.E. Lawson, and G.J. Larson. In press. How glaciers entrain and transport basal sediment: Physical constraints. *Quaternary Science Reviews*.  
 Anandakrishnan, S., and R.B. Alley. 1994. Ice stream C sticky spots detected by microearthquake monitoring. *Annals of Glaciology*, 20, 183–186.  
 Blankenship, D.D., C.R. Bentley, S.T. Rooney, and R.B. Alley. 1987. Till beneath ice stream B. 1. Properties derived from seismic travel times. *Journal of Geophysical Research*, 92(B9), 8903–8911.  
 Bond, G., H. Heinrich, W. Broecker, L. Labeyrie, J. McManus, J. Andrews, S. Huon, R. Jantschik, S. Clasen, C. Simet, K. Tedesco, M. Klas, G. Bonani, and S. Ivy. 1992. Evidence for massive discharges of icebergs into the North Atlantic ocean during the last glacial period. *Nature*, 360, 245–249.  
 Cuffey, K.M., and R.B. Alley. 1996. Erosion by deforming subglacial sediments: Is it significant? (Toward till continuity). *Annals of Glaciology*, 22, 17–24.  
 Iverson, N.R., B. Hanson, R. LeB. Hooke, and P. Jansson. 1995. Flow mechanism of glaciers on soft beds. *Science*, 267, 80–81.  
 Iverson, N.R., and D.J. Semmens. 1995. Intrusion of ice into porous media by regelation: A mechanism of sediment entrainment by glaciers. *Journal of Geophysical Research*, 100(B7), 10219–10230.  
 Jensen, J.W., P.U. Clark, D.R. MacAyeal, C. Ho, and J.C. Vela. 1995. Numerical modeling of advective transport of saturated deforming sediment beneath the Lake Michigan Lobe, Laurentide Ice Sheet. *Geomorphology*, 14, 157–166.  
 Lawson, D.E., E.B. Evenson, J.C. Strasser, R.B. Alley, and G.J. Larson. 1996. Subglacial supercooling, ice accretion, and sediment entrainment at the Matanuska Glacier, Alaska. *Abstracts with programs* (Vol. 28). Boulder, Colorado: Geological Society of America. [Abstract]  
 Rooney, S.T., D.D. Blankenship, R.B. Alley, and C.R. Bentley. 1987. Till beneath ice stream B. 2. Structure and continuity. *Journal of Geophysical Research*, 92B(B9), 8913–8920.  
 Rooney, S.T., D.D. Blankenship, R.B. Alley, and C.R. Bentley. 1991. Seismic reflection profiling of a sediment-filled graben beneath ice stream B, West Antarctica. In M.R.A. Thomson, J.A. Crame, and J.W. Thompson (Eds.), *Geological evolution of Antarctica*. Cambridge: Cambridge University Press.  
 Strasser, J.C., D.E. Lawson, G.J. Larson, E.B. Evenson, and R.B. Alley. 1996. Preliminary results of tritium analyses in basal ice, Matanuska Glacier, Alaska, U.S.A.: Evidence for subglacial ice accretion. *Annals of Glaciology*, 22, 126–133.  
 Weertman, J. 1961. Mechanism for the formation of inner moraines found near the edge of cold ice caps and ice sheets. *Journal of Glaciology*, 3(30), 965–978.

# Coring for microbial records of antarctic climate

GARY S. WILSON, PETER BRADDOCK, and STEVEN L. FORMAN\*, *Byrd Polar Research Center, Ohio State University, Columbus, Ohio 43210*

E. IMRE FRIEDMANN and ELISAVETA M. RIVKINA, *Polar Desert Research Center and Department of Biological Sciences, Florida State University, Tallahassee, Florida 32306*

JEFFREY P. CHANTON, *Department of Oceanography, Florida State University, Tallahassee, Florida 32306*

DAVID A. GILICHINSKY, DMITRY G. FYODOROV-DAVIDOV, VLADIMIR E. OSTROUMOV, and VICTOR SOROKOVIKOV, *Institute for Soil Science and Photosynthesis, Russian Academy of Sciences, Pushchino, Moscow Region, Russia*

MICHAEL C. WIZEVICH, *Department of Earth and Environmental Studies, Montclair State University, Upper Montclair, New Jersey 07043*

\*Present address: *Department of Geological Sciences, University of Illinois, Chicago, Illinois 60670*

Scientific understanding of the Cenozoic terrestrial glacial and climatic record of East Antarctica is limited by the near absence of Cenozoic strata cropping out on the antarctic craton (Wilson 1995). Because of this fact, much of the historical development of the antarctic cryosphere has been inferred from interpretations of proxy records in deep-sea sediments (e.g., Shackleton and Kennett 1975; Kennett 1977; and Kennett 1982). Although these proxy records afford certain constraints on the history of antarctic ice volume and paleoclimate, they are often ambiguous and interpretations depend on assumptions of certain geography, climate, and ice-sheet relationships (e.g., Wise et al. 1989; Kennett and Hodell 1993).

A decade ago, Webb et al. (1984) challenged the established interpretation of a progressive climatic deterioration of the Antarctic and a stable ice sheet, similar in form to that of the present day, blanketing and dominating the climate of the craton since middle Miocene times (Shackleton and Kennett 1975; Kennett 1977). From the presence of fossil marine floras and faunas reworked into the Sirius Group deposits high in the Transantarctic Mountains, Webb et al. (1984) deduced that the interior of the craton was episodically free of ice and flooded by marine seas, the latest ice sheet amelioration and marine incursion having occurred during the Pliocene. Long-standing work investigating the geomorphic development of the dry valleys region combined with new dating possibilities from *in situ* and reworked volcanic ashes appears to contradict the dynamic model and lends credence to the concept of ice sheet and particularly climatic stability of the region (Denton et al. 1984; Sugden, Marchant, and Denton 1993; Marchant et al. 1996). Apart from limited occurrences of *Nothofagus* remains within Sirius Group strata (Webb and Harwood 1993), however, neither method of investigation has provided a direct record of terrestrial climate variation throughout the Late Neogene (10–2 million years ago).

In the 1995–1996 antarctic field season, we carried out an independent pilot program to determine the feasibility of recovering and using ancient but viable terrestrial microbes to determine past climatic conditions in the McMurdo Dry Valleys. It was known from earlier investigations in the McMurdo Dry Valleys region that cryptoendolithic microorganisms colonize sandstone and granitic bedrock surfaces

(Nienow and Friedmann 1993). Friedmann, Druk, and McKay (1994) defined a climatic gradient, which delineated the degree of viability, versus fossilization of endolithic microbial communities, which indicated the retreat of colonization due to climatic deterioration. A by-product of bacterial colonization of bedrock is biogenic weathering and exfoliation of the rock surfaces they colonize. Because of the prevailing low temperatures, biologic processes in the rock are extremely slow, so that geological and biological timescales overlap. Our premise is that these climatically sensitive microbial communities can provide useful indications of past climates from the terrestrial realm, indications that are not directly available from other geologic or geomorphic records available in Antarctica. Ultimately, we hope to provide a direct record of Late Neogene and Pleistocene (10–0 million years ago) climatic evolution of the McMurdo Sound and wider antarctic regions.

It is well established that ancient Siberian and North American permafrost contain viable bacteria (Gilichinsky et al. 1992; Gilichinsky and Wagener 1994), but except for a short unconfirmed report (Cameron and Morelli 1974), little was known of the much colder antarctic permafrost. The studies of Nienow and Friedmann (1993) described the special conditions necessary for microbial life, and hence, we expected microbial occurrences to be very limited in their distribution. We expected, however, biogenously exfoliated particles to be transported and incorporated into local sedimentary basins carrying with them viable organisms. Thus, microorganisms would be introduced to sediment accumulations that are quickly frozen even if their growth was not favorable in the upper surface of the sedimentary pile. Their occurrences, both volumetrically and by species proportionality, should be representative of the favorability of climatic conditions through the time of colonization, erosion, and deposition in the sedimentary basin. Once accumulated in the sedimentary basin, their occurrences are part of the stratigraphic record, which can also yield environmental and chronologic information as well as allowing for correlation to other stratigraphic records.

To investigate this phenomenon, we transported a portable permafrost coring system from Russia to various localities in the dry valleys. The coring system was developed at the Institute of Soil Science and Photosynthesis of the Russian

Academy of Sciences, specifically for biologic studies of permafrost (figure 1A). The device uses no drilling fluid and relies on maintaining the frozen condition of the core for stratigraphic integrity and to prevent downhole contamination of the biogenic and sedimentologic characteristics of the core. Coring was carried out at a slow rate [approximately 3–5 meters (m) per day] to ensure integrity of the core. All core was lifted to the surface by hand and described, and samples were taken for initial microbial and ice-content studies. The core and subsequent samples were then sealed in sterilized plastic tubing for transportation to McMurdo Station and, from there, to the United States and Russia for laboratory studies. While in the field and during shipment, core and samples were kept at a constant  $-20^{\circ}\text{C}$  to prevent renewed microbial activity in uncontrolled settings. In the field and during shipment to McMurdo Station,  $-20^{\circ}\text{C}$  temperature was maintained by a solar powered, Peltier-effect freezer unit designed and built at Ohio State University (figure 1B). The freezer unit was operated by battery power or a gasoline generator during transportation and when climatic conditions prevented the use of solar energy.

During a 6-week field season, we established drilling camps at three locations in the dry valleys (figure 2). The first site was located toward the mouth of Taylor Valley, 3.2 kilometers from the Commonwealth Glacier face ( $77^{\circ}35'18.7''\text{S}$   $163^{\circ}24'27.5''\text{E}$ ; elevation, 50 m). The second site was located on the delta prograding into the western edge of Lake Miers in the Miers Valley ( $78^{\circ}05'49.4''\text{S}$   $163^{\circ}48'44.8''\text{E}$ ; elevation, 190 m). The third site was on the northeastern flank of Mount Feather above the head of Beacon Valley ( $77^{\circ}55'55.7''\text{S}$   $160^{\circ}26'05.3''\text{E}$ ; elevation, 2,570 m). In the Taylor Valley, we

recovered three cores from the same site, the deepest (COMRAC-3) penetrating to a depth of 17.30 m (downhole temperature,  $-18^{\circ}\text{C}$ ). It comprised alternating fluvial and eolian sediments that were coarse- to medium-grained, moderate- to well-sorted quartzofeldspathic sands and fine gravels with occasional small mudstone clasts often marking muddier horizons in the core. The sediment was ice cemented, and occasional subhorizontal-to-inclined ice lenses were observed. In the Miers Valley, coring penetrated to a maximum depth of 6.15 m (COMRAC-4; downhole temperature,  $-17^{\circ}\text{C}$ ) and recovered well-sorted coarse to medium-coarse ice-cemented quartzofeldspathic gravels and coarse sands, mostly of eolian and fluvial origin. From depth of 4.98 m to the base of the hole, we encountered ice that was clear and free of sediment (figure 3A).

On Mount Feather, we drilled four holes penetrating to a maximum depth of 3.20 m (COMRAC-8; downhole temperature,  $-27^{\circ}\text{C}$ ) into the Sirius Group till that infilled a depression beneath the Mount Feather peak. Coring encountered poorly sorted admixtures of quartzofeldspathic gravel, sand, and mud with abundant well-rounded, 5–15-centimeter-diameter quartz pebbles. At 0.66 m depth in COMRAC-8, we encountered a 0.5- to 1-m thick ice horizon that contained less than 20 percent sediment (figure 3B). Above this ice band, ice content was high (30–50 percent), and sediment coherency was maintained by ice cementation. Below the ice band, ice content was much lower (less than 10–20 percent), and sediment coherency was maintained by compaction.

Initial laboratory studies of core material have yielded the following results.

- Limited examination of the microbial content of the cores yielded results that were of substantial interest and that justified our expectations. Each core contained viable bacteria. The number of bacteria varied, up to  $10^2$ – $10^3$  per gram by plate counts and to  $10^5$  per gram by fluorescence. These numbers are comparable to, although somewhat less than, what were found previously in Siberian permafrost (Ting et al. in press). Most samples contained

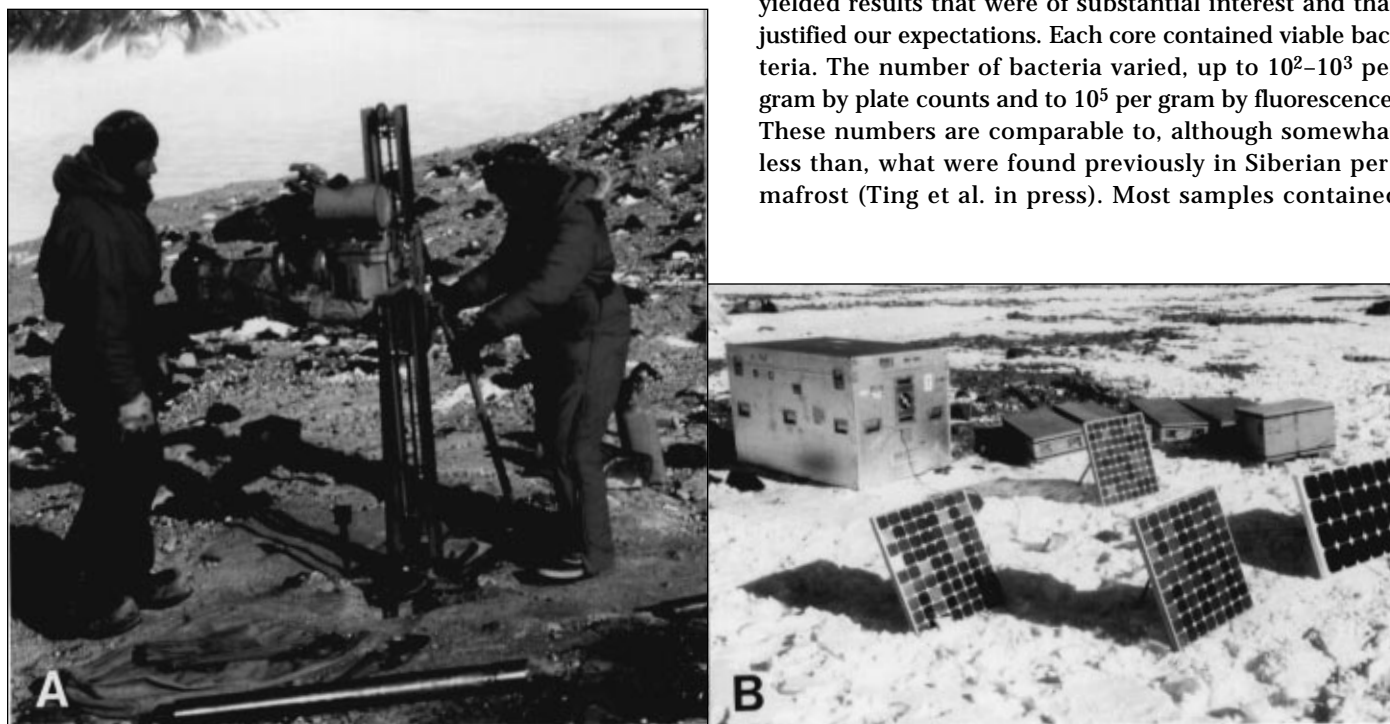


Figure 1. A. The portable permafrost coring system from the Institute for Soil Science and Photosynthesis of the Russian Academy of Sciences; pictured on the Sirius Group deposit, Mount Fleming, operated by David Gilichinsky (right) and Victor Sorokovikov (left). B. The solar-powered Peltier-effect freezer unit used to maintain core at  $-20^{\circ}\text{C}$  in the field and during transportation.

methane in quantities up to 2,000 parts per million. From the Miers Valley sites, we determined, based on its isotopic composition ( $\Delta^{13}\text{C} = 54.8\text{‰}$ ), that this methane is of biological origin, presumably from bacteria. We also found methane of mixed biological and abiogenic origin, as well as ethane and propane. Enzyme activity, also a sign of biological activity, was present in most samples.

- Preliminary chronostratigraphic studies demonstrate that sediments and bacteria recovered by coring in Taylor Valley are up to 150,000 years old, by correlation with the magnetostratigraphically dated DVDP-11 core from nearby (Elston and Bressler 1981). A new thermoluminescence age from 2.9 m depth in the COMRAC-4 core ( $20,500 \pm 2,500$  years) in the Miers Valley suggests an average sedimentation rate of 1.4 meters per thousand years. Sediments, microorganisms, and methane recovered from 4.9 m depth (immediately above the basal ice in the drillhole) are possibly older than 30,000 years and were deposited during the last interglacial cycle. Coring at Mount Feather recovered glaciogene Sirius Group sediments, and viable bacteria, of at least 2 million years in age (Webb and Harwood 1991) and possibly as old as 15 million years (Marchant et al. 1996).

We are currently analyzing additional samples to refine our chronology (using radiocarbon, thermoluminescence, and cosmogenic dating methods) and to define further the microbial content of the antarctic permafrost in the McMurdo Dry Valleys.

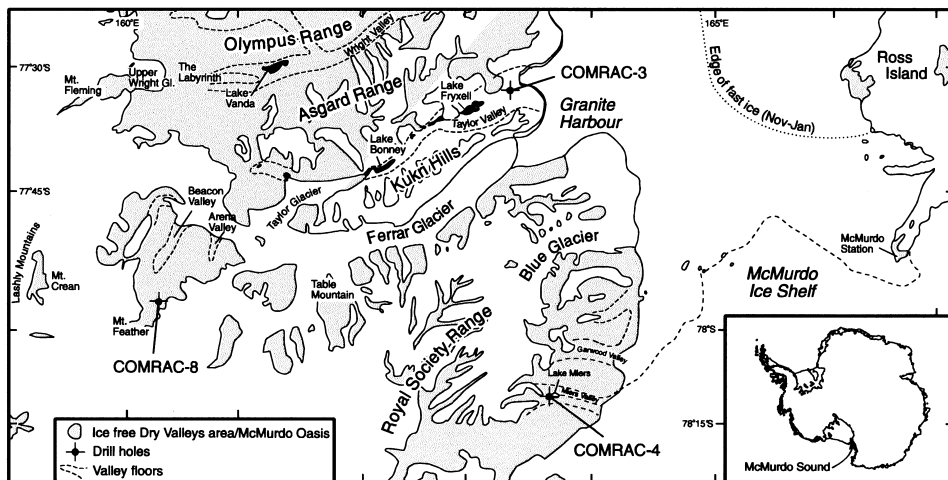


Figure 2. Map of the dry valleys area showing locations of the three sites where cores were recovered; only the deepest drill-hole at each site is labeled.

The permafrost has the potential to hold an older and more complete record of paleoclimate than other geologic reservoirs on several counts.

- Cameron and Morelli (1974) reported viable bacteria from a depth of 86 m in the DVDP-8 core (approximately 2.1 million years old, also from lower Taylor Valley), although unfortunately DVDP coring used a drilling fluid and, hence, contamination cannot be ruled out. If the report was correct, however, it should be possible to recover a complete Plio-Pleistocene (5–0-million-year) bacterial record from the permafrost infilling the floors of the dry valleys.
- The paleoclimate record is deduced from bacterial paleoecology, which is more direct than previous approaches.
- The permafrost is more long-lived and stable than the ice sheet itself, affording a more continuous record that continues back in geologic time and records both glaciated and deglaciated periods in the past. The coastal permafrost

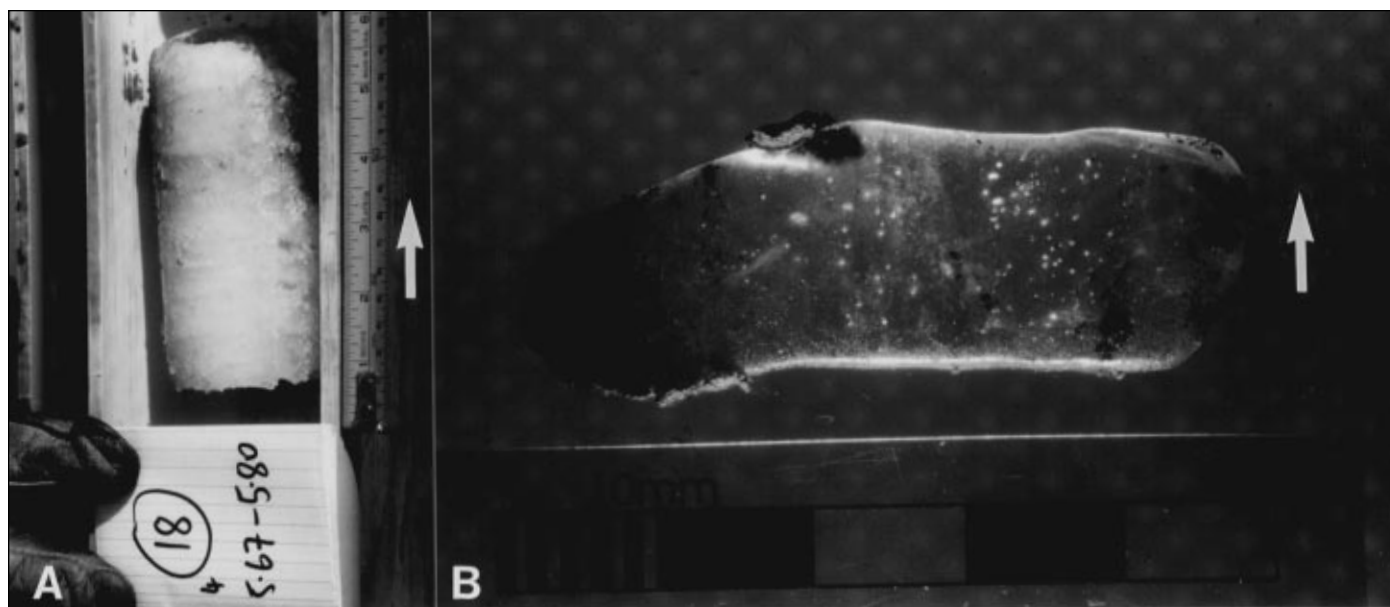


Figure 3. A. Ice core recovered from 5.67–5.80 m depth in the COMRAC-4 core, from the lacustrine delta of Lake Miers. B. A thin section of ice and sediment from 0.5–0.52 m depth in the COMRAC-8 core, from the Sirius Group deposit on Mount Feather.

record is also well placed to provide a vital link between ice-core records of recent paleoclimate and marine records responding to these climate changes.

This research was supported by National Science Foundation grants OPP 94-20227 (to E. Imre Friedmann) and OPP 94-20260 (to Gary S. Wilson). Field personnel during the 1995–1996 field season were Gary Wilson, David Gilichinsky, Peter Braddock, Dmitry Fyodorov-Davidov, Vladimir Ostroumov, Victor Sorokovikov, and Michael Wizevich. We thank Antarctic Support Associates field support staff, VXE-6, and the Royal New Zealand Air Force for successfully supporting a very demanding logistical program and Frank Huffman for building the Peltier-effect freezer.

## References

- Cameron, R.E., and F.A. Morelli. 1974. Viable microorganisms from ancient Ross Island and Taylor Valley drill core. *Antarctic Journal of the U.S.*, 9(5), 113–116.
- Denton, G.H., M.L. Prentice, D.E. Kellogg, and T.B. Kellog. 1984. Late Tertiary history of the antarctic ice sheet: Evidence from the dry valleys. *Geology*, 12(5), 263–267.
- Elston, D.P., and S.L. Bressler. 1981. Magnetic stratigraphy of DVDP drill cores and Late Cenozoic history of Taylor Valley, Transantarctic Mountains, Antarctica. In L.D. McGinnis (Ed.), *Dry Valley Drilling Project* (Antarctic Research Series, Vol. 33). Washington, D.C.: American Geophysical Union.
- Friedmann, E.I., A.Y. Druk, and C.P. McKay. 1994. Limits of life and microbial extinction in the antarctic desert. *Antarctic Journal of the U.S.*, 29(5), 176–179.
- Gilichinsky, D.A., E.A. Voroyoba, L.G. Erokhina, D.G. Fyodorov-Davidov, and N.R. Chaikovskaya. 1992. Long term preservation of microbial ecosystems in permafrost. *Advances in Space Research*, 12(4), 255–263.
- Gilichinsky, D.A., and S. Wagener. 1994. Microbial life in permafrost. In D.A. Gilichinsky (Ed.), *Viable microorganisms in permafrost*. Pushchino: Russian Academy of Sciences, Pushchino.
- Kennett, J.P. 1977. Cenozoic evolution of antarctic glaciation, the Circum-Antarctic Ocean, and their impact on global paleoceanography. *Journal of Geophysical Research*, 82, 3843–3860.
- Kennett, J.P. 1982. *Marine geology*. New Jersey: Prentice-Hall.
- Kennett, J.P., and D.A. Hodell. 1993. Evidence for relative climatic stability of Antarctica during the early Pliocene: A marine perspective. *Geografiska Annaler*, 75A(4), 205–220.
- Marchant, D.R., G.H. Denton, C.C. Swisher, III, and N. Potter, Jr. 1996. Late Cenozoic antarctic paleoclimate reconstructed from volcanic ashes in the dry valleys region of southern Victoria Land. *Geological Society of America Bulletin*, 108(2), 181–194.
- Nienow, J.A., and E.I. Friedmann. 1993. Terrestrial lithophytic (rock) communities. In E.I. Friedmann (Ed.), *Antarctic microbiology*. New York: John Wiley and Sons.
- Shackleton, N.J., and J.P. Kennett. 1975. Paleotemperature history of the Cainozoic and the initiation of antarctic glaciation: Oxygen and carbon analysis in DSDP sites 277, 279 and 281. In J.P. Kennett and R. Houtz (Eds.), *Initial reports of the deep sea drilling project* (Vol. 29). Washington, D.C.: U.S. Government Printing Office.
- Sugden, D.E., D.R. Marchant, and G.H. Denton (Eds.). 1993. The case for a stable east antarctic ice sheet. *Geografiska Annaler*, 75A(4), 151–331.
- Ting, S., R.H. Reeves, D.A. Gilichinsky, and E.I. Friedmann. In press. Characterization of viable bacteria from Siberian permafrost by 16S rDNA sequencing. *Microbial Ecology*.
- Webb, P.-N., and D.M. Harwood. 1991. Late Cenozoic glacial history of the Ross embayment, Antarctica. *Quaternary Science Reviews*, 10(2–3), 215–223.
- Webb, P.-N., and D.M. Harwood. 1993. Pliocene fossil *Nothofagus* (southern beech) from Antarctica: Phytogeography, dispersal strategies, and survival in high latitude glacial-deglacial environments. In J. Alden, S. Odum, and J.L. Mastrantonio (Eds.), *Forest development in cold regions*. New York: Plenum Press.
- Webb, P.-N., D.M. Harwood, B.C. McKelvey, J.H. Mercer, and L.D. Stott. 1984. Cenozoic marine sedimentation and ice volume on the east antarctic craton. *Geology*, 12(5), 287–291.
- Wilson, G.S. 1995. The Neogene antarctic ice sheet: A dynamic or stable feature? *Quaternary Science Reviews*, 14(2), 101–123.
- Wise, S.W., Jr., J.R. Breza, D.M. Harwood, and W. Wei. 1989. Paleogene glacial history of Antarctica. In D.W. Muller, J.A. McKenzie, and H. Weissart (Eds.), *Controversies in modern geology*. London: Academic Press.

---

# Global positioning system measurements of ice-sheet mass balance using the “coffee-can” method

GORDON S. HAMILTON and IAN M. WHILLANS, *Byrd Polar Research Center, Ohio State University, Columbus, Ohio 43210-1002*

The mass balances of the antarctic ice sheets are poorly known. The reason for this lack of measurements has been the considerable difficulty involved in obtaining them. Traditionally, the work involves large, intensive field programs (e.g., Whillans and Bindschadler 1988). Recent developments in global positioning system (GPS) technology and processing offer the possibility of making precise determinations of local rates of ice-sheet thickening or thinning, without the need for intensive field campaigns. During the 1995–1996 field season, we carried out GPS measurements for mass balance at four sites in Antarctica (figure 1).

The method entails comparing measurements of the vertical component of velocity of the near-surface of the ice sheet and the long-term accumulation rate (Hulbe and Whillans 1994a).

Vertical velocities are obtained from repeat GPS surveys of suites of markers anchored in the firn [typically 10–20 meters (m) deep]. Prototype markers were coffee cans. Now, smaller steel rods are used.

Accumulation rate is from firn cores. Where the accumulation rate is not otherwise available, we collect cores for gross beta measurements. Horizons of gross beta-radioactivity cor-

responding to atmospheric nuclear tests carried out in the mid-1950s and mid-1960s are detected in samples from known depths and of measured densities. These markers give 30- and 40-year average accumulation rates.

Minor adjustments need to be made for motion arising from firn densification and down-slope flow. Depth-density profiles enable firn densification below the markers to be quantified, and markers placed at different depths allow this to be checked. The contribution of down-slope flow is obtained from the local surface slope and horizontal velocity. Topographic maps are produced for an approximately 5-kilometer (km) by 5-km box around each site by conducting continuous kinematic GPS surveys from a snowmobile.

**South Pole**

Measurements are being conducted at three sites at South Pole (figure 2). One site, called the “farfield site,” approximately 8 km from the dome, was installed during the 1991–1992 field season. Another marker, called “dome,” was installed in a 90-m-deep hole under the station dome in December 1993. Its position is tied to the permanent GPS tracker located on top of the Skylab building by optical leveling. Both existing sites were resurveyed this season. Two new markers were installed this season in holes 120 m and 130 m deep approximately 2 km from the dome. These holes were drilled by the Polar Ice Coring Office for T. Sowers and M. Bender to recover cores during the 1994–1995 season. The advantage of using deeper holes, such as these, is that the markers are anchored to ice rather than firn. Their vertical velocity will not need to be corrected for firn compaction. Results from these three sites will allow the assessment of short-scale spatial variations in ice-sheet mass balance.

Results from relative surveys of the “dome” marker show that Skylab is sinking into the firn, at a rate of about 20 centimeters per year (cm a<sup>-1</sup>). Problems with data quality from the permanent GPS tracker at south pole have so far precluded the calculation of absolute velocities.

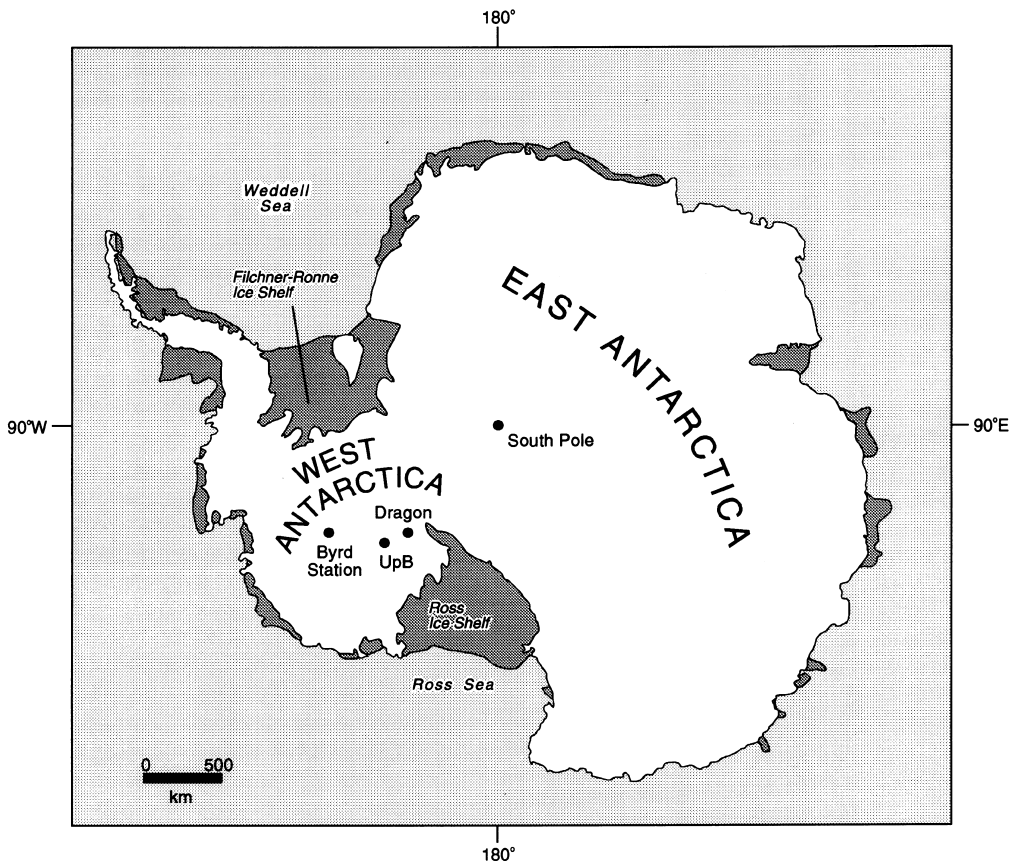


Figure 1. Location of “coffee-can” sites in Antarctica. (UpB denotes Upstream B camp.)

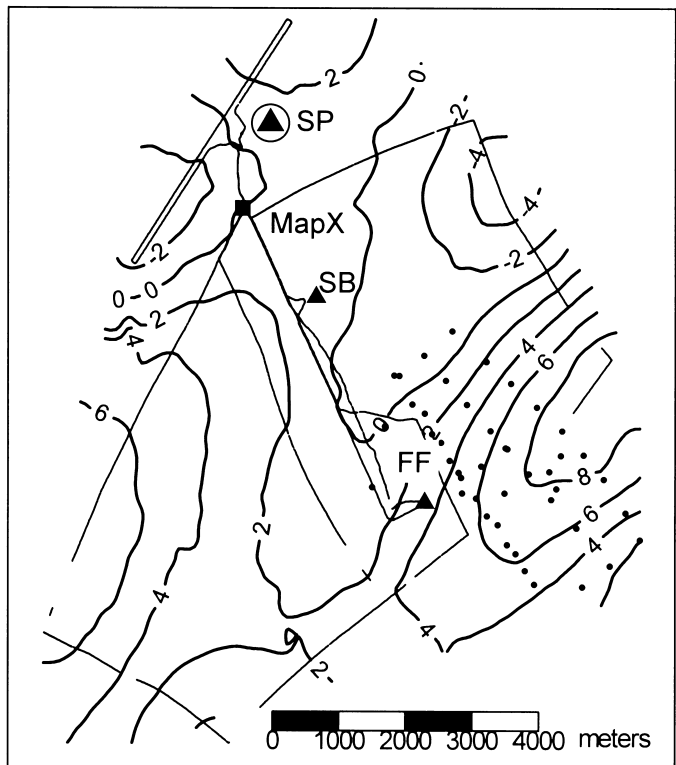


Figure 2. Topographic map of the region around Amundsen–Scott South Pole Station (SP) showing the location of marker sites (SB and FF) and the skiway. GPS data are from 1993 (dots) and 1995 (continuous tracks). Datum for elevation is defined to be zero at MapX. Contour interval is 2 m.

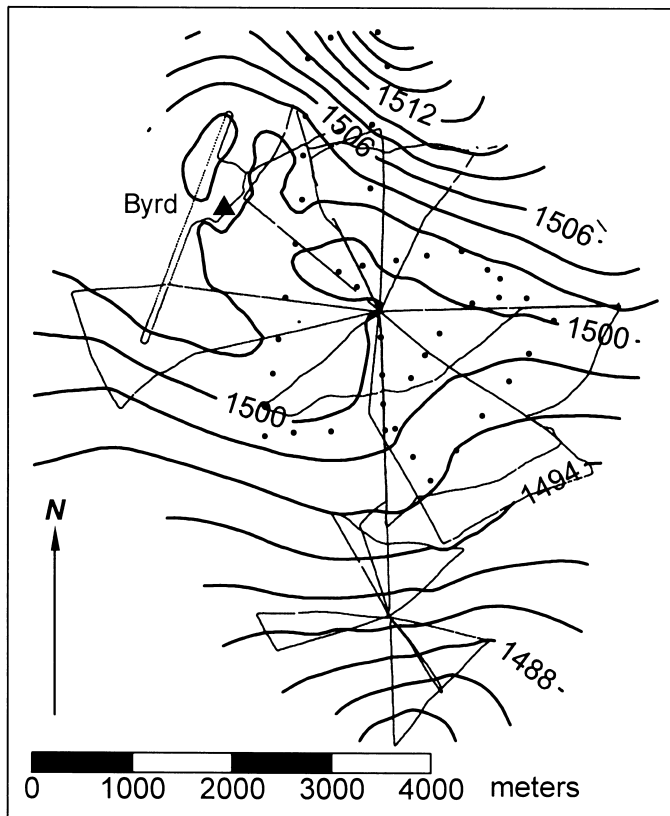


Figure 3. Topographic map of Byrd Surface Camp vicinity obtained from GPS data in 1993 (dots) and 1995 (continuous tracks). The skiway is outlined next to camp (triangle). Center of long radial tracks is "near-by" site where datum for elevation is defined to be 1,500 m. "Farfield" marker site is in the lower portion of the map. Contour interval is 2 m.

### Byrd Surface Camp

Byrd Station lies just within the latitudinal limits of space-borne altimeters. Coffee-can results will be compared with results from repeat satellite altimetry, which also measures changes in surface elevation. The new results can also be compared with earlier mass-balance estimates; for example, Whillans (1977) calculated that the ice sheet is thinning at  $0.03 \text{ m a}^{-1}$ .

Two marker sites are near Byrd Station (figure 3). One site, "nearby," 2 km true east of the station buildings, has been operational since November 1993. A second site, "farfield," was established during the 1995–1996 season, 3 km southeast of the original site. This second site provides a check for spatial consistency in results.

### Dragon

A site is located on an interstream ridge approximately 1 km outboard from the Dragon, the southern shear margin to ice stream B. This site has two epochs of remeasurement (December 1992 and December 1993). These measurements indicated a thinning rate of  $0.07 \text{ m a}^{-1}$ , with an uncertainty of  $0.05 \text{ m a}^{-1}$ . The new measurements will be used to confirm the accuracy of this result and reduce the uncertainty.

### Upstream B

A new suite of markers was installed at the relocated Upstream B camp on ice stream B. It is located at coordinates (km 2, km -8) of the strain grid of Hulbe and Whillans (1994b). Results from this site will be used to test whether the changes observed at the Dragon are also occurring in the trunk of the ice stream.

The work was undertaken by G.S. Hamilton, E.R. Venteris, and I.M. Whillans, who were supported by National Science Foundation grant OPP 94-19396.

### References

- Hulbe, C.L., and I.M. Whillans. 1994a. A method for determining ice-thickness change at remote locations using GPS. *Annals of Glaciology*, 20, 263–268.
- Hulbe, C.L., and I.M. Whillans. 1994b. Evaluation of strain rates in ice stream B, Antarctica, obtained using GPS phase measurements. *Annals of Glaciology*, 20, 254–262.
- Whillans, I.M. 1977. The equation of continuity and its application to the flow of the ice sheet near "Byrd" station, Antarctica. *Journal of Glaciology*, 18(80), 359–371.
- Whillans, I.M., and R.A. Bindschadler. 1988. Mass balance of ice stream B, West Antarctica. *Annals of Glaciology*, 11, 187–193.